CHAPTER 4

SYNTHESIS, SPECTROSCOPIC CHARACTERIZATION, FLUORESCENCE AND BIOCIDAL PROPERTIES OF SOME DIORGANOTIN(IV) COMPLEXES OF SALICYLALDEHYDE THIOSEMICARBAZONE AND RELATED LIGANDS

4.1 Introduction to organotin(IV) complexes of Schiff bases

The organotin complexes have been the subject of great interest for some time because of their versatile bonding modes [1,2] as well as their biomedical, commercial [3] and agricultural applications [4, 5, 6]. An important class of organotin(IV) complexes are those derived from Schiff bases. Over the recent decades, investigations on coordination of Schiff bases with organotin(IV) moieties have received considerable attention with respect to their potential applications in medicinal chemistry and biotechnology and their structural variety [7-13].These type of compounds have also found application in homogeneous catalysis [14]. Increasing attention has also been devoted to these classes of compounds in view of their special antitumour activities [13, 15-22]. Schiff bases in neutral and deprotonated forms react with organotin(IV) moieties and the complexes that are formed exhibit variable stoichiometry and different modes of coordination [23-25].

The condensation (Eq.1) of aliphatic or aromatic primary amines with aldehydes and ketones give products known as imines which contain a C=N bond. These compounds rapidly decompose or polymerize unless at least one among R, R' or R" is an aromatic organic group. The latter imines are called Schiff bases, since their synthesis was first reported by Schiff [26].

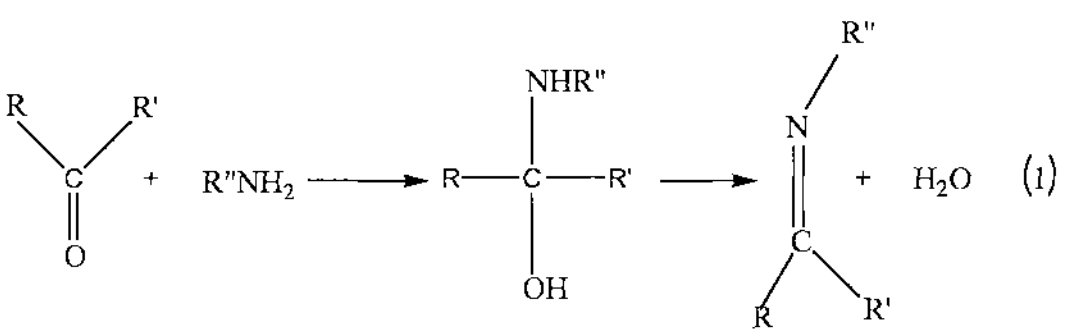

Aldehyde or Ketone | Primary amine | α-hydroxyamine | Schiff base

Dayagi and Degani [27] have reviewed the other methods of synthesis of the Schiff bases in the past.

4.1.1 Interactions of organotin(IV)$^{n+}$ with Schiff bases and their derivatives

The Schiff base complexes of organotin(IV) moieties have widely been investigated [28-33] and the subject was reviewed in 1984 [34].

Organotin(IV) Schiff base complexes of the type (L)SnR_2 [where R= CH_3, C_6H_5 or $CH_2CH_2CO_2CH_3$], (LH)$Sn(C_6H_5)_3$ and (L)$SnCl(CH_2CH_2CO_2CH_3)$ [where ligand, H_2L=2-*N*-salicylideneimino-2-methyl-1-propanol, derived from the condensation of salicylaldehyde and 2-amino-2-methyl-1-propanol] have been prepared and characterized on the basis of their elemental analyses, IR, ^1H, ^{13}C and ^{119}Sn NMR studies [35]. In these mononuclear complexes the Schiff base acts either as a dianionic tridentate or as a monobasic bidentate moiety by coordinating through an alkoxy group, an azomethine nitrogen and a phenoxide ion to tin. Sulphur dioxide inserts in the tin-methyl/-phenyl bond in the above Schiff base complexes to give tin-*O*-sulphinates of formulae (L)$RSn(SO_2R)$ and (LH)$(C_6H_5)_2Sn(SO_2C_6H_5)$. In a similar type of Sn-C bond cleavage reactions we have obtained di-μ_2-methoxo-bis[benzyl{5-chloro-2-oxido-benzaldehyde thiosemicarbazonato} tin(IV)] from the attempted recrystallization of an sample of $(PhCH_2)_2SnL$, where ligand LH_2 is *p*-chlorosalicylaldehyde thiosemicarbazone, from a methanol solution [36].

Equimolar reactions of Bu_2SnO with Schiff bases derived from amino acids led to the formation of a new series of dibutyltin(IV) complexes of general formula, Bu_2SnL (L=dianion of tridentate Schiff bases derived from the condensation of 2-hydroxy-1-naphthaldehyde or acetyl acetone with glycine, L-β-alanine, DL-valine, DL-4-aminobutyric acid, L-methionine, L-leucine and phenylglycine). The central Sn(IV) ions in all these complexes are penta-coordinated with a monodentate carboxylic group. The complexes have been tested against various bacteria and exhibited moderate activity. The cytotoxicities of these complexes were tested *in vitro* against several human tumour cell lines, namely, MCF-7, EVSA-T, WiDr, IGROV, M19 MEL, A498 and H226. The activities found experimentally were higher than those observed for cisplatin and carboplatin [37].

From the reactions of $SnCl_4$ with organotin(IV) chlorides ($RSnCl_3$, R_2SnCl_2 and R_3SnCl, where R = Bu, Me and Ph) with *N*-(2-hydroxybenzaldehyde)-1-amino-2-phenyleneimine, *N*-(2-hydroxyl-1-naphthaldehyde)-1-amino-2-phenyleneimine, *N*, *N'*-bis(2-hydroxybenzaldehyde)-1,2-phenylenediimine and *N*,*N'*-bis(2-hydroxy-1-naphthaldehyde)-1,2-phenylenediimine, a series of complexes have been synthesized and characterized, respectively, by microanalytical, IR, and ^1H NMR spectroscopic methods [38]. The Ph_2SnCl_2 reacted with *N*-(2-hydroxy-1-naphthaldehyde)-1-amino-2-phenyleneimine giving Ph_2Sn(NAPPDI) [where NAPPDI = deprotonated *N*, *N'*-bis(2-hydroxy-1-naphthaldehyde)-1,2-phenylenediimine], wherein the former Schiff base exhibited a facile intramolecular C=N bond cleavage and intermolecular C=N bond formation.

Diphenyltin(IV) complexes of *N*-(3,5-dibromosalicylidene)-α-amino acid, $Ph_2Sn[3,5\text{-}Br_2\text{-}2\text{-}OC_6H_2CH{=}NCH(R)COO]$ (where R=H, Me, *i*-Pr, Bz), and their 1:1 adducts with diphenyltin dichloride, $Ph_2Sn[3,5\text{-}Br_2\text{-}2\text{-}OC_6H_2CH{=}NCH(R)COO].Ph_2SnCl_2$, have been synthesized by Tian *et al.*[39].The crystal structure of $Ph_2Sn[3,5\text{-}Br_2\text{-}2\text{-}OC_6H_2CH{=}NCH(i\text{-}Pr)COO]$ shows a distorted trigonal bipyramidal geometry with axial locations occupied by a carboxylate-oxygen and a phenolic-oxygen atom of the ligand, and that of $Ph_2Sn[3,5\text{-}Br_2\text{-}2\text{-}OC_6H_2CH{=}NCH(i\text{-}Pr)COO].Ph_2SnCl_2$ reveals that the two tin atoms are joined via the carbonyl atom of the ligand to form a mixed organotin binuclear complex. Bioassay indicates that the compounds possess better cytotoxicity against three human tumour cell lines (HeLa, Col.o205 and MCF-7) than cisplatin and moderate antibacterial activity against two bacteria(*E.coli* and *S.aureus*).

Investigations on organotin(IV) amino acid and 2-amino-2-methyl-1-propanol Schiff base complexes were reported in literature [40,41].

Four tin(IV) complexes of tridentate dithiocarbazate Schiff bases have been synthesized and characterized by their elemental analyses, UV, ^1H NMR, Mössbauer spectroscopies and X-ray powder diffraction. The reactions of tin tetraacetate with the ligand LH_2 (Fig. 4.1) proceed smoothly but slowly with the elimination of acetic acid, which was removed azeotropically with toluene. Complexes having general formulae, $Sn(OCOCH_3)_2L$, where L= dianion of *S*-benzyl-*β*-*N*-(2-hydroxyphenyl)methylene and methyl dithiocarbazate (Fig. 4.1), are five-coordinated in distorted trigonal

bipyramidal geometry, whereas complexes of the type SnL_2 show hexa-coordination about the tin atom which is arranged in a distorted octahedral geometry with an orthorhombic lattice [42].

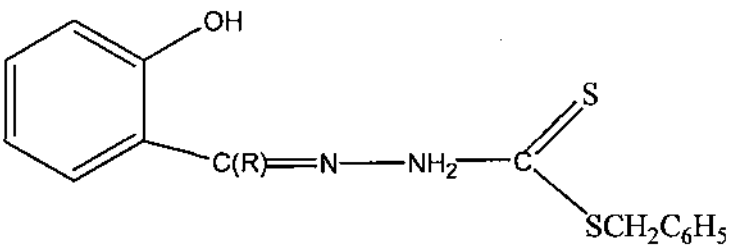

Fig.4.1 Structure of ligand LH_2 [42].

The schiff bases [H_2SBSaD], [H_2SBVD] and [H_2SBND], derived by the condensation of *S*-benzyldithiocarbazate and salicylaldehyde, 2-hydroxy-3-methoxybenzaldehyde and 2-hydroxy-1-naphthaldehyde respectively, react with diestertin dichlorides, R_2SnCl_2 [R= $-CH_2CH_2CO_2CH_3$, $-CH_2CH_2CO_2C_2H_5$ or $-CH_2CH_2CO_2C_4H_9$] in 1:1 molar ratio to yield complexes of the type R_2Sn(Schiff base), the base being tridentate [43]. The ^{13}C and ^{119}Sn NMR and the tin-carbon coupling constant data reveal the structures of the complexes to be octahedral with *trans* ester grouping, and bidentate ester linkages. The penta-coordinated complex, Me_2Sn(SBSaD) was prepared by the reaction of dimethyltin oxide with H_2SBSaD in equimolar proportions.

Diorganotin(IV)$^{2+}$ complexes with general formula R_2SnL (R= Ph, n-Bu, Me) were recently prepared by reacting R_2SnCl_2 and tetradentate Schiff bases (H_2L) containing N_2O_2 donor atoms in the presence of triethylamine (as base) in benzene. In the $Bu_2Sn(IV)^{2+}$ complexes formed with 3-methoxysalicylaldehyde derivatives, the Sn atom has a distorted octahedral structure, where the donor atoms of the Schiff base ligand occupy the four equatorial positions and the organo moieties are in *trans* axial positions [23].

Liu *et al.* [44] used the reaction of substituted benzoyl salicylahydrazone (Fig.4.2) (A= 2-phenyl, X=O, Y=H) with $[Cp(CO)_2Fe]_2SnCl_2$ and Ph_2SnCl_2 to synthesize complexes (Fig. 4.3 : B=$Fe(CO)_2Cp$ or Ph) and determined their molecular features.

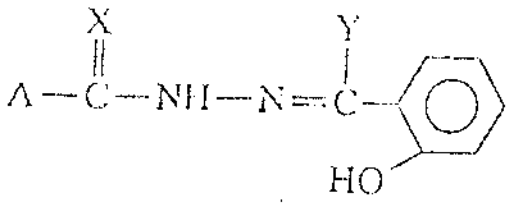

Fig. 4.2 Structure of substituted benzoyl salicylahydrazone.

In a similar work, the n-Bu_2[$(MeO)_3C_6H_2C(O)N_2CHC_6H_4O$]Sn complex (Fig. 4.3) was synthesized in the reaction of di-n-butyltin(IV) oxide with 3,4,5-trimethoxy-benzoyl salicylahydrazone (Fig. 4.2: A= 3,4,5-trimethoxyphenyl, X=O, Y=H) in dry benzene with azeotropic removal of water using a Dean-Stark trap [45].The complex was characterized by ^{1}H, ^{13}C and ^{119}Sn NMR and IR spectra. A single crystal X-ray diffraction study confirmed its molecular structure and revealed that 3,4,5-trimethoxy-benzoyl salicylahydrazone was a tridentate and approximately planar ligand. The tin atom had a distorted trigonal bipyramidal coordination (Fig.4.3: A= 3,4,5-trimethoxyphenyl , B= n-Bu).Two chain carbon atoms and the chelating nitrogen atom occupied the basal plane. The skeleton of two erect oxygen atoms and the tin atom was bent. In the complex, the ligand existed in the enol form.

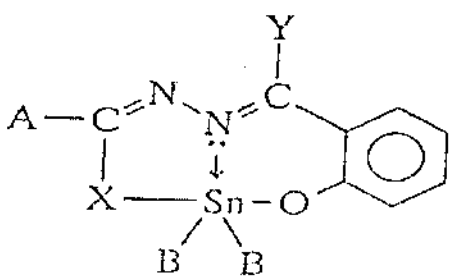

Fig.4.3 Structure of the organotin(IV) complex of substituted benzoyl salicylahydrazone.

2-Furanthiocarboxyhydrazide (Hfth), 4-hydroxyphenylthiocarboxyhydrazide (Hoth) and salicylaldehyde-2-furanthiocarboxyhydrazone (H_2L) form stable complexes of the compositions Ph_2SnCl_2·Hfth, $R_2Sn(LH)_2$ (where R = Ph or Bu and L = Hfth or Hoth), Ph_2SnCl_2·H_2L, $Ph_2Sn(HL)Cl$ and Bu_2SnL which have been characterized by elemental analysis and spectroscopic studies [46]. All the complexes were of octahedral geometry.

The ligating behaviour of di-2-pyridylketone-2-aminobenzoylhydrazone (HDPA), and phenyl(2-pyridyl)ketone 2-aminobenzoylhydrazone towards organotin derivatives was investigated [47]. The synthesis, IR and ^{119}Sn NMR spectroscopic characterization of the compounds were reported, together with the X-ray crystal structures of HDPA and $Sn(C_6H_5)_3Cl(OH_2)\cdot$HDPA, which were discussed and compared. The *in vitro* evaluation of antimicrobial properties revealed the strong activity of $Sn(C_6H_5)_2$(HDPA)Cl_2 and $Sn(C_6H_5)_3Cl(OH_2)\cdot$HDPA complexes. None of the compounds showed genotoxicity in the *Bacillus subtilis rec*-assay and in the *Salmonella*-microsome test.

Further results on organotin complexes with Schiff bases derived from hydrazones or substituted hydrazones were reported in [48-50].

Two compounds with the formula $[R_2Sn(OC_{10}H_6CH{=}NCH_2CH_2COO)]_2$ where R = CH_3 or n-C_4H_9, have been synthesized by Goh *et al.* [51]. The crystal structure of the dimethyltin compound is reported along with ^{1}H, ^{13}C and IR spectroscopic data for both compounds. The centrosymmetric dimethyltin complex exhibited octahedral coordination for each tin atom. The tridentate ligand chelate meridionally via the phenolate oxygen, the imino nitrogen and one carboxylate oxygen atom. Two further *trans* positions in the tin coordination sphere are taken up by the two methyl groups while the apical (sixth) position is filled by a shared carboxylate oxygen atom from the other organotin unit.

The reaction of 1-[3'-methoxyphenylimino)methyl]-2-naphthol with dimethyltin(IV) dichloride yielded an addition compound having 2:1 stoichiometry (ligand : organotin). The complex formed was characterized by elemental analysis, (^{1}H- and ^{13}C-) NMR, IR spectroscopy and X-ray analysis [52]. The coordination of the Schiff base to the metal occurred via the phenolic oxygen atom. This preferred mode of bonding was associated with the shift of the phenolic proton towards the azomethine atom resulting in a zwitter-ionic configuration for the ligand.

The crystal and molecular structure of the triphenyltin complex of 1-[4'-methylphen-ylimino)-methyl]-2-naphthol was reported. The complex adopted a five-coordinate trigonal bipyramidal geometry, with the phenyl groups taking up the equatorial positions around the tin atom. The ligand which existed in the form of a zwitter-ion

in the complex, binded to the tin via the phenolic oxygen atom. Free ligand cocrystallized with the complex in the ratio of one free ligand molecule to every two of the organotin complex units. The free ligand molecules pack in parallel strings in the crystal, between the organotin complex moieties, which are arranged as pairs of centrosymmetrically-related dimers [53].

Several Schiff bases derived from salicylaldehyde and aminopyridines were found to coordinate with Me_2SnCl_2 in 1:1 or 1:2 (tin:base) molar ratio in diethyl ether, depending on the nature of the Schiff base used, to form complexes of the general formula $Me_2SnCl_2.L$ or $Me_2SnCl_2.2L$ respectively [54].These Schiff bases coordinated with Ph_2SnCl_2 in similar manner, but if the reaction was carried out in chloroform or if the product formed was either dissolved in chloroform then colorless to pale yellow crystals were deposited. The latter were analyzed and found to be due to the ionic compounds $[H_2NpyN\text{-}H^+]_2[Ph_2SnCl_4]^{2-}$ which were formed as a result of an unusual cleavage of the C=N bond of the Schiff bases. The Schiff bases, their Me_2SnCl_2 complexes and the ionic compounds were analyzed physicochemically and spectroscopically. The crystal structures of two of the ionic compounds showed that the cation $[H_2NpyN\text{-}H^+]$ binds with the anion $[Ph_2SnCl_4]^{2-}$ via hydrogen bonds. The Schiff bases, their Me_2SnCl_2 complexes and the ionic compounds were screened against the three tumour cell lines, L_{929}, K_{562} and HeLa, and the results were compared with those of the anticancer drugs, cisplatin and carboplatin.

A series of organotin(IV) complexes with Schiff base ligand pyruvic acid-3-hydroxy-2-naphthoylhydrazone $[R_2SnLY]_2$, L=3-OH-$C_{10}H_6$-2-CON HN=C(CH_3) -COOH, R=n-C_4H_9, Y=CH_3OH(**1**), R=n-C_4H_9, Y= N (**2**), R=$PhCH_2$ (**3**), R=Ph, Y=CH_3OH(**4**), R=Me(**5**) and $[R_3SnLY]$, L=3-OH-C_{10}H6-2-CONHN=C(CH_3)-COOH, R= n-C_4H_9, Y=H_2O, (**6**), R= Ph (**7**), R= Me (**8**) were synthesized by the reaction of the Schiff base and trialkyltin in 1:1 stoichiometry [55]. By determination of the crystal structure of complex **1** it was noted that crystal containing two n-butyl and one oxygen atom from methanol coordinate to the tin atom. In the complexes **6-8** the Schiff base ligand coordinated to the Sn atom as a unidentate and the oxygen atom from the carboxylate participate to the coordination. Though strong bases were used in the reaction of complexes **1-5**

Fig.4.5 Structure of Schiff base salopH_2 [63].

(Fig. 4.4) and mild base in the complexes **6-8** (Fig. 4.4), the enolization was observed in all complexes. The reaction were carried out in methanol at refluxing temperature, however, these complexes could also be prepared in methanol at room temperature, but the reaction time should be prolonged for 24 hours. Different substitutes on n-butyl didn't cause obvious variation in the yield of the reaction.

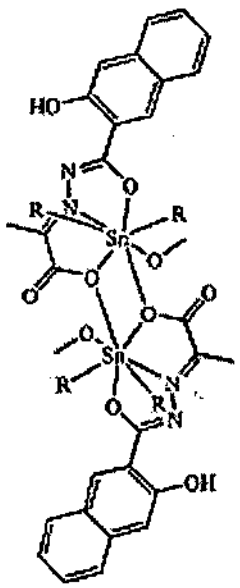

R= n-C_4H_9 (**1**)

R= Ph (**4**)

R= Me (**5**)

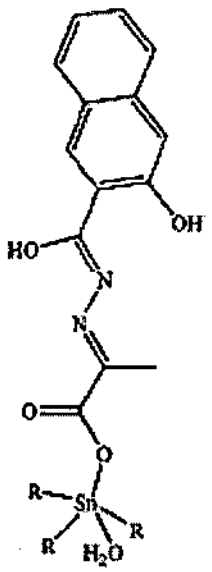

R= n-C_4H_9 (**6**)

R= Ph (**7**)

R= Me (**8**)

Fig. 4.4 Structure of organotin(IV) complexes of Schiff base ligand pyruvic acid 3-hydroxy-2-naphthoylhydrazone [55].

2- {[(2-Hydroxyhenyl)imino]methyl}phenol (salopH_2) (Fig. 4.5) is a typical potentially tridentate Schiff base ligand forming stable complexes with many transition and post- transition metal ions [56, 57]. Literature on metal-salopH_2 complexes of the group 14 elements is rather sparse [58, 59], only three tin (IV) complexes structurally characterized being reported, i.e. [$SnMe_2$(salop)] [60], [$SnPh_2$(salop)] [61] and [Sn(salop)]$_2$ [62].

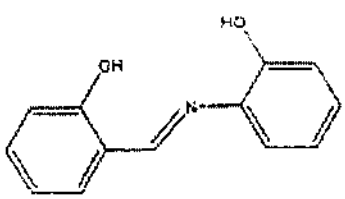

Fig.4.5 Structure of Schiff base salopH_2 [63].

From the reaction of SnR_2Cl_2 acceptors with an equimolar amount of 2- {[(2-hydroxyhenyl)imino]methyl}phenol ($salopH_2$) in methanol in the presence of bases (KOH, MeONa or NEt_3) the complexes [SnR_2(salop)] (R=Me, Ph, Vin, n-Bu and t-Bu) (Fig. 4.6 a) containing the donor in the dianionic tridentate form, have been obtained. The X-ray diffraction study of [$SnVin_2$(salop)] showed the metal to be five-coordinated in a distorted square pyramidal environment. The whole structure consisted of molecular units connected by intermolecular Sn-O interactions [63].

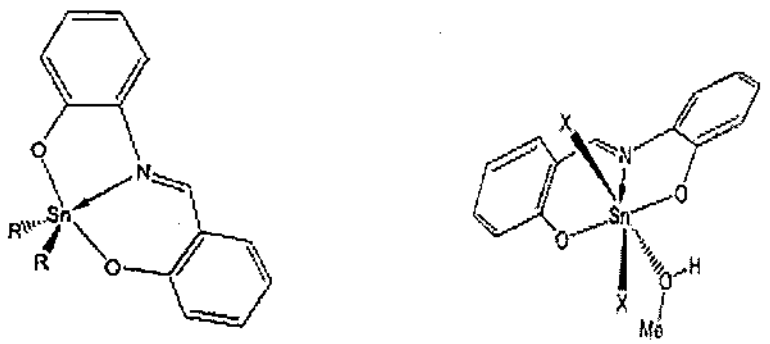

(a) (b)

Fig. 4.6 Structure proposed for (a) the diorganotin(IV) salop derivatives (b) mono- and dihalotin(IV) salop derivatives [63].

When $SnRX_3$ or SnX_4 acceptors were employed in the same reaction conditions, the complexes [SnX_2(salop)(S)] (X=Cl, Br,I ; R=Me, Ph, n-Bu; S=H_2O, MeOH) were obtained. Although these reactions seemed instantaneous when all reactants were mixed, refluxing for approximately 24 hours was carried out to ensure complete reaction. In the complexes [SnX_2 (salop)(CH_3OH)].CH_3OH (X= Cl or Br), the tin atom was found in a strongly distorted octahedral environment (Fig.4.6 b). All the [SnR_2(salop)] and [SnRX(salop)(solvent)] were fluxional in solution. On the other hand the reaction of SnX_4 with 2 mol of $salopH_2$ and 4 mol of base afforded the complex [Sn(salop)$_2$] in which all halide groups were substituted by two dianionic Schiff bases [63].

The synthesis and characterization of five organotin compounds containing the Schiff base ligands, LH_2 [L= Salophen(t-Bu), Salophen(t-Bu) = *N*, *N*'-phenylene-bis(3,5-di-*tert*-butylsalicylidenciminc) ; L= Salomphen(t-Bu), Salomphen(t-Bu) = *N*,*N*'-(4,5-dimethyl)phenylene-bis(3,5-di-*tert*-butylsalicylidenciminc)] and LH_3 [L= Phensal(t-Bu) [Phensal(t-Bu) = 3,5-di-*tert*-butylsalicylidenc(1-aminophenylene-

2-amine)] were described by Yearwood *et al.* [64]. The compounds of the ligand of the type LH_2 were prepared by combining $SnCl_4$ with LH_2 (compounds **1** and **2**) in the presence of triethylamine. Synthesis of compounds **1** and **2,** along with the compounds **3** and **4,** could also be achieved by combining n-$BuSnCl_3$ with LH_2 in presence of triethylamine (see Scheme 4.1). This lead to a mixture of L(n-Bu)SnCl and $LSnCl_2$. The formation of $LSnCl_2$ might be due to a disproportionation reaction (Eq.2) or a redistribution (Eq.3) occurring in solution.

$$2L(n\text{-}Bu)SnCl \longrightarrow LSnCl_2 + (n\text{-}Bu)_2SnL \quad \ldots\ldots\ldots (2)$$

$$L(n\text{-}Bu)SnCl + (n\text{-}Bu)SnCl_3 \longrightarrow LSnCl_2 + (n\text{-}Bu)_2SnCl_2 \quad \ldots\ldots\ldots (3)$$

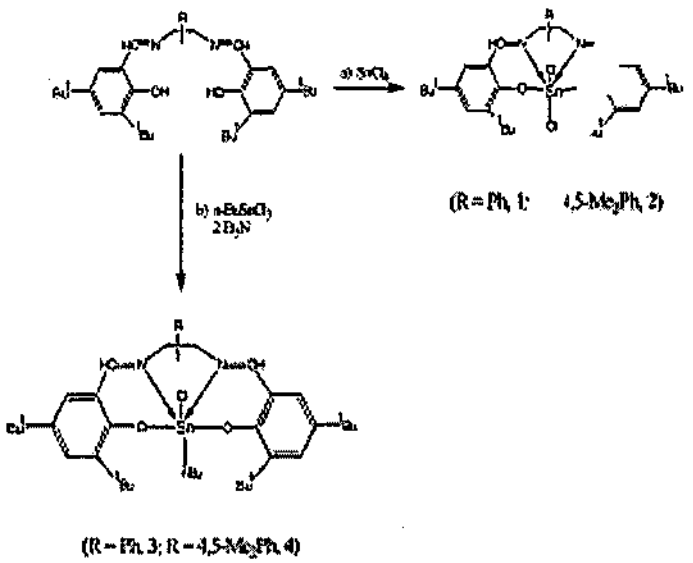

(a)

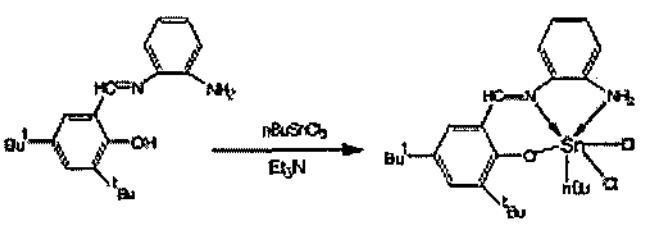

(b)

Scheme 4.1 (a) General Syntheses of compounds **1** – **4** (b) General Syntheses of compound **5** [64].

The organotin complex **5** of the ligand LH_3 was prepared by the reaction of the tridentate ligand (LH_3) with n-$BuSnCl_3$ in the presence of Et_3N.

Several investigations have shown that the salicylaldimine complexes with X=H are effective ligands for both inorganic and organotin(IV) species. Replacement of X by a methoxy group radically altered the nature of the metal salicylaldimine complexes as ligands, transforming them from bidentate to extremely effective tetradentate ligands. Much more surprising, however, was the finding that the behaviour of the complexes as ligands was markedly and dramatically influenced by the nature of the bridging group B (Fig. 4.7 a). When the number of 'C' atoms linking the imine 'N' atoms was increased beyond three, the effectiveness of the metal salicylaldimines as ligands was greatly reduced. For example, practically no organotin(IV) Lewis acids react with the complex of *N*, *N*-bis(3-methoxysalicylidene)pentane-1,5-diamine [65,66].

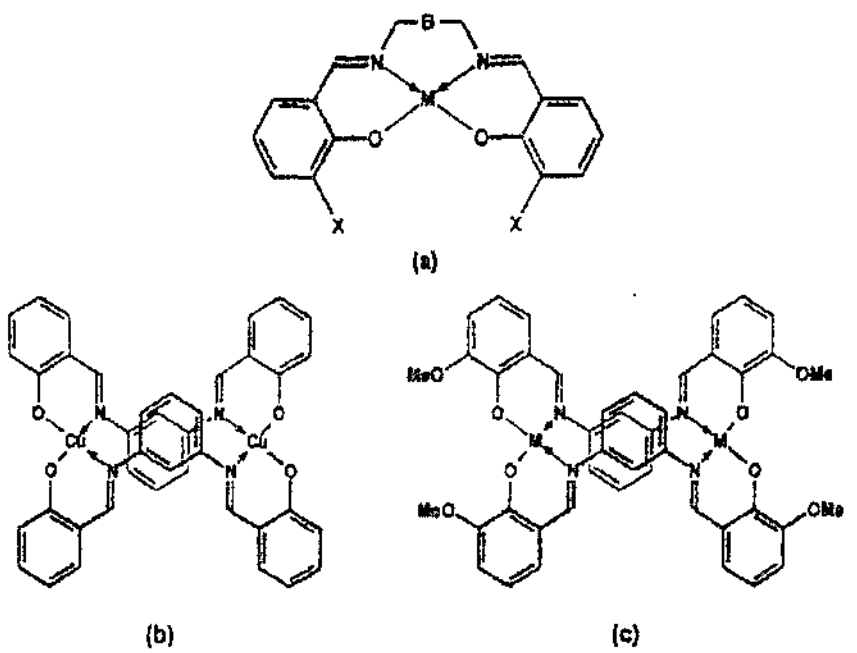

Fig. 4.7 Structures of metal salicylaldimine complexes [65, 66].

The dibutyltin complex of the Schiff base ligand 2, 9-diformylphenanthroline bis-acylhydrazone (H_2L) (Fig.4.8 a) was synthesized by refluxing the methanolic solution of the ligand with methanolic solution of dibutyltin diacetate for 2 hours, to give $[(C_4H_9)_2SnL]$ in good yield. The IR spectrum suggests a complete deprotonation

of the ligand and the coordination of the hydrazonic C=O groups, in fact the ν(N-H) and ν(C=O) bands disappear. These data are confirmed by the ^1H spectrum, where the N-H proton disappears and the aldehyde proton undergo an upfield shift in the complex. The crystal structure of $[(C_4H_9)_2SnL]$ (Fig. 4.8 b) confirmed that the ligand was deprotonated, in accord with the spectroscopic data. Based on the crystallographic data the authors have preferably described the coordination geometry around the metal in terms of a distorted hexagonal bipyramid with the ligand in the equatorial plane and the organic groups in the apical positions; it is noteworthy that this geometry is unusual, particularly for tin that results in eight-coordinated geometry [67].

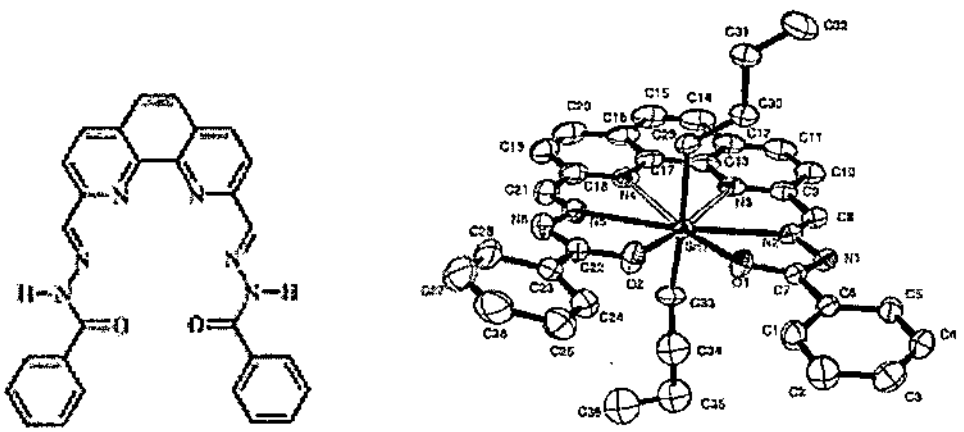

(a) (b)

Fig.4.8 (a) Schiff base ligand 2,9-diformylphenanthroline bis-acylhydrazone (H_2L)
(b) Perspective view of the crystal structure of $[(C_4H_9)_2SnL]$ [67].

The synthesis and characterization of new organotin(IV) complexes containing a potentially tetradentate NN'OS Schiff base ligand, methyl 2-[2(salicylideneamino)-ethylamino]cyclopent-1-ene-1-dithiocarboxylate (H_2cdsalen) was reported recently by T. Sedaghat and S. Menati [68]. This is an interesting Schiff base forming stable complexes with transition metal ions in deprotonated form as both tetradentate and bidentate ligand [69, 70]. H_2cdsalen (Fig.4.9 a) is conformationally flexible and contains hard and soft donor atoms.

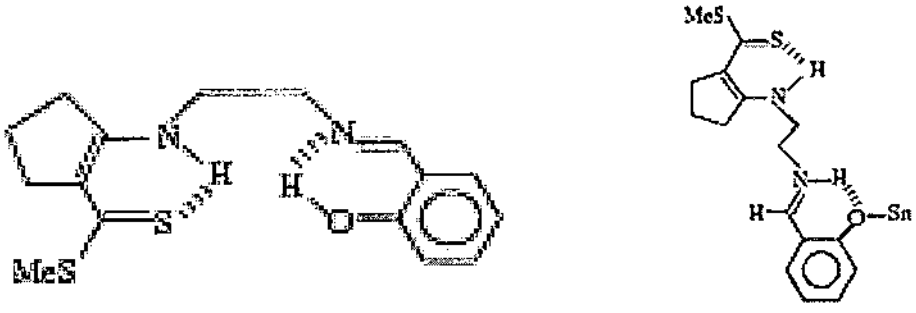

(a) (b)

Fig. 4.9 (a) Schiff base H_2cdsalen (b) Structure suggested for the coordination of Sn(IV) to H_2cdsalen [68].

The reactions in this study were performed by stirring SnR_2Cl_2 (where R=Me, Ph) with H_2cdsalen in benzene (or toluene) solution at room temperature and the new adducts [$SnMe_2Cl_2(H_2cdsalen)$] and [$SnPh_2Cl_2(H_2cdsalen)_2$] precipitated after 3 hours [68]. The new products were characterized by elemental analysis, IR, ^1H and ^{119}Sn NMR spectroscopies. Spectroscopic data suggested that in both complex the ligand was coordinated through oxygen. The phenolic hydrogen within the free ligand was transferred to the imine nitrogen atom due to the coordination of oxygen with tin after the complex formation (Fig.4.9 b).

Four new chiral organotin derivatives have been reported by Rivera *et al.* [71] with their crystal structures. They were synthesized by reaction of diphenyltin oxide and four different ligands obtained from the Schiff base condensation of 4-(diethylamino) salicylaldehyde and (1*R*, 2*S*) – (+) –norephedrine, (*R*) – (-) – phenylglycinol , (*R*) – (-) – 1-amino-2-propanol and (1*S*, 2*R*) – 2-amino-1,2-diphenylethanol. In the synthesis of the tin complex, equimolecular quantities of Schiff bases and diphenyltin oxide were reacted in acetonitrile for 3-6 h. The compounds were fully characterized by spectroscopic techniques.

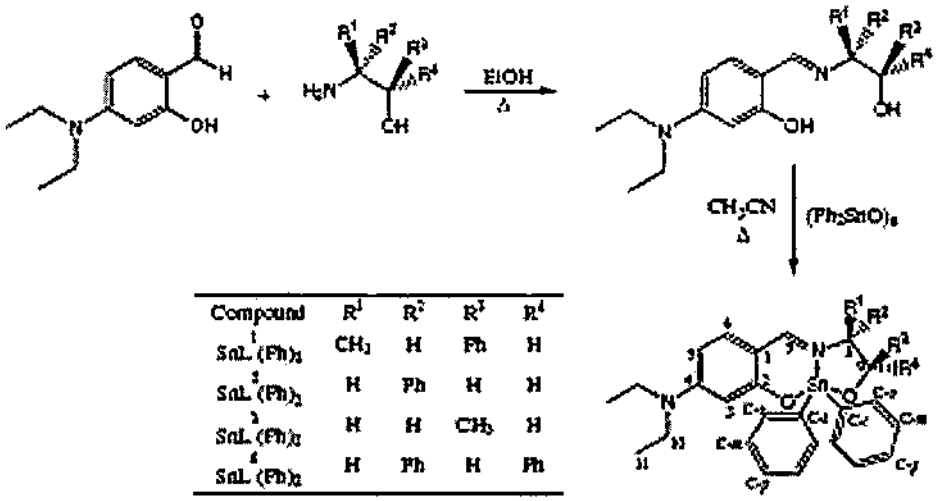

Compound	R^1	R^2	R^3	R^4
$SnL^1(Ph)_3$	CH_3	H	Ph	H
$SnL^2(Ph)_3$	H	Ph	H	H
$SnL^3(Ph)_3$	H	H	CH_3	H
$SnL^4(Ph)_3$	H	Ph	H	Ph

Scheme 4.2 Synthesis of chiral organotin derivatives [71].

The organotin complexes, namely $[(Bu_2Sn)_2O(EtO)(L1)]_2$ (**1**), $[(Bu_2Sn)_2O(EtO)(L2)]_2$ (**2**), $[(Bu_2Sn)_2O(EtO)(L3)]_2$ (**3**) were obtained by the reactions of n-dibutyltin oxide with 0.5 equivalent of 4-phenylideneamino-3-methyl-1,2,4-triazole-5-thione (HL1) , 4-furfuralideneamino-3-methyl-1,2,4-triazole-5-thione (HL2) , 4-(2-thienylideneamino-3-methyl-1,2,4-triazole-5-thione (HL3) in a mixed solvent of benzene and ethanol (2:1) , under reflux for eight hours. Complexes **1-3** showed similar structures containing a Sn_4O_4 ladder skeleton in which each of the *exo* tin atoms was bonded to the N atom of a corresponding thione-form deprotonated ligand. The compound $[Ph_3Sn(L4)].0.5H_2O$ (**4**) was obtained by the reaction of Ph_3SnOH with an equivalent amount of HL4 in benzene. The reaction system was refluxed for eight hours. Complex 4 showed a mononuclear structure in which the Sn atom of triphenyltin group was coordinated by the S atom of a thiol-form $L4^-$ anion [72].

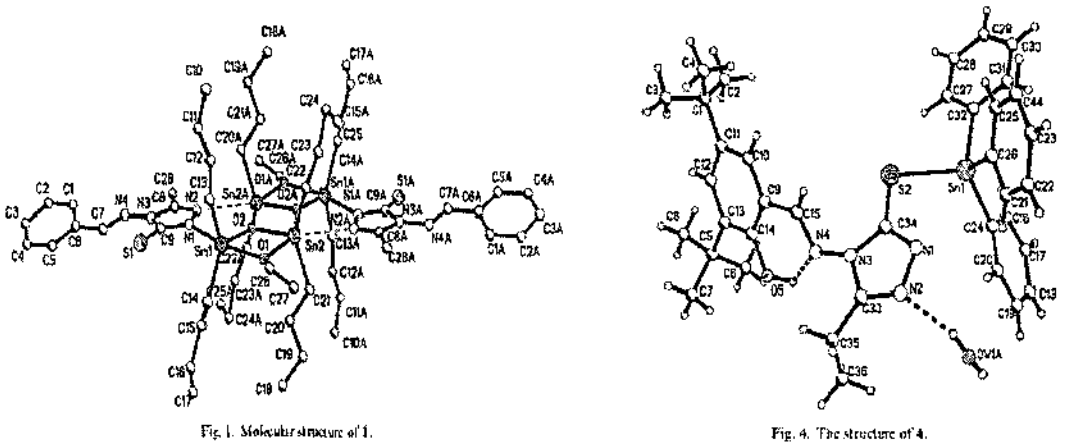

Fig. 4.10 (a) Molecular structure of **1** (b) Molecular structure of **4** [72].

The literature on organotin complexes of Schiff bases is vast and inexhaustive. The author has presented above a few selected examples to give a glimpse of the work done in the field of organotin Schiff bases. The organotin complexes of thiosemicarbazones are comparatively less studied than their transition metal analogues. At this point the author shall restrict her discussion on organotin(IV) complexes of Schiff bases derived from thiosemicarbazides, as they form one of the subject matter of the thesis.

4.1.2 Organotin(IV) complexes of thiosemicarbazones

Thiosemicarbazones and their metal complexes has been the subject of great interest of many researchers for a number of years. The statement is supported by the large number of papers and review articles [73-81]. Like majority of similar Schiff bases, thiosemicarbazones are obtained in good yield by the condensation of aqueous or alcoholic solutions of thiosemicarbazides with suitable aldehydes or ketones.

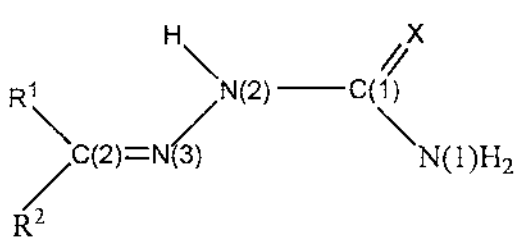

Fig.4.11 General formula of a thiosemicarbazone.

Thiosemicarbazones are versatile ligands in both neutral and anionic forms. They predominantly exist in thione form in the solid state but exist as an equilibrium mixture of thione and thiol forms in the solution state (Fig. 4.12).

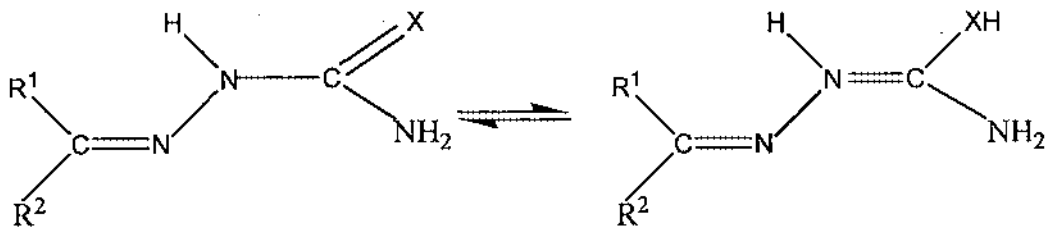

Fig.4.12 Thione-thiol tautomerism of thiosemicarbazones in solution.

These classes of compounds usually react with metallic cations giving complexes in which the thiosemicarbazones behave as chelating ligands. The coordination possibilities of thiosemicarbazones are increased if substituents R^1 and/or R^2 include additional donor atoms. In the canonical thiol form, there is an effective conjugation along the thiosemicarbazone skeleton resulting in an efficient electron delocalization along the thiosemicarbazone backbone. Presence of aromatic radicals bound to the azomethine carbon atom further enhances the delocalization of electron charge density [82].The coordination chemistry of thiosemicarbazones appeared to be very interesting from the point of view of both the number of metals forming the complexes with them and the diversity of the ligand systems themselves [83-85], i.e., their denticity, set of donor atoms, stabilization of various (less common) oxidation state of metals [86-89], reactions of coordinated ligands [85,90] etc.

S. Belwal and her coworkers [91] reported the synthesis of diorganotin(IV) derivatives of the type $R_2SnCl(TSCZ)$ and $R_2Sn(TSCZ)_2$ (where TSCZ is the anion of a thiosemicarbazone ligand, R=Ph or Me). The complexes were characterized by elemental analyses, molecular weight determinations and conductivity measurements. The mode of bonding was established on the basis of IR, ^1H, ^{13}C and ^{119}Sn NMR spectroscopic studies. Some of the complexes were also evaluated for their antimicrobial effects on different species of pathogenic fungi and bacteria *in vivo* as well as *in vitro*.

Three tin (IV) complexes of 2-benzoylpyridine *N*(4)-phenylthiosemicarbazone were prepared: $[Sn(L)Cl_3]$, $[n\text{-}BuSn(L)Cl_2]$ and $[(n\text{-}Bu)_2Sn(L)Cl]$, in which L stands for

the anionic ligand formed upon complexation with deprotonation and release of HCl. The complexes were characterized by a number of spectroscopic techniques. The crystal structure of $[(n\text{-}Bu)_2Sn(L)Cl]$ was determined. The molecules of this complex are associated by an intermolecular N4–H4---Cl bond. The Sn(IV) lies in the centre of a very distorted octahedron, formed by the carbon atoms of two n-Bu groups, one chloride and the anionic thiosemicarbazone coordinated through an N, N, S tridentate system [92].

2-Benzoylpyridine thiosemicarbazone (HL1), its *N*(4)- methyl (HL2) and *N*(4)-phenyl (HL3) derivatives with $SnCl_4$ and diphenyltin dichloride (Ph_2SnCl_2) gave $[Sn(L1)Cl_3]$ (**1**), $[Sn(L1)PhCl_2]$ (**2**), $[Sn(L2)Cl_3]$ (**3**), $[H_2L2]^+_2\,[Ph_2SnCl_4]^{2-}$(**4**) $[Sn(L3)PhCl_2]$ (**5**) and $[Sn(L3)Ph_2Cl]$ (6). IR, ^1H-, ^{13}C- and ^{119}Sn- NMR spectra of **1 – 3**, **5** and **6** are compatible with the presence of an anionic ligand attached to the metal through the N_{py}– N –S chelating system and formation of hexa-coordinated tin complexes. The crystal structures of **1 –3**, **5** and **6** showed that the geometry around the metal was a distorted octahedron. The crystal structure of **4** revealed the presence of *trans* $[Ph_2SnCl_4]^{2-}$ and $[H_2L2]^+_2$ [93].

The chelating behaviour of N, N, S-tridentate thiosemicarbazones derived from 2-formyl pyridine (HFPT) have been investigated and three different modes of coordination have been identified. 2-formyl pyridine thiosemicarbazone (HFPT) reacts with tin tetrahalides (X=Cl, Br, I) with abstraction of HX and the formation of hexa-coordinated species $[SnX_3(FPT)]$ (Fig. 4.13). In this complex the ligand acts as a mononegative N,N, S-tridentate ligand and coordinate to the metal through both nitrogen and the thiolate sulphur atoms [94]. A single crystal X-ray diffraction study of $[SnCl_3(FPT)]$ established *mer*-isomerism, the ligand coordinating through its N(3), S and pyridine 'N' atoms. The distorted octahedral coordination polyhedron of the tin atom is completed by three Cl atoms.

While in the corresponding dimethyltin(IV) complex $[Sn(CH_3)_2(FPT)Cl]$, the thiosemicarbazone anion acts as a bidentate ligand where the tin(IV) is coordinated to the azomethine nitrogen and deprotonated thiol sulphur while the pyridine nitrogen remains uncoordinated [95].

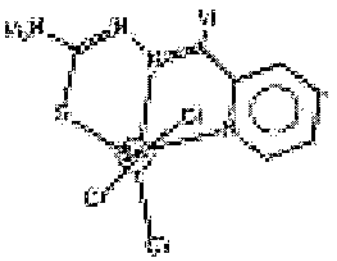

Fig. 4.13 Structure of $[SnCl_3(FPT)]$ [94].

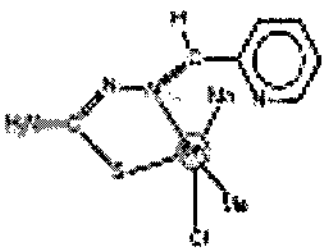

Fig. 4.14 Structure of $[Sn(CH_3)_2(FPT)Cl]$ [95].

The complex formation between organotin chlorides and 2-pyridinecarboxaldehyde thiosemicarbazone (PT) have been investigated. In only one case was a substitution reaction observed whereas in all other cases, 1:1 addition complexes were formed. The solid state configuration of the complexes was studied by ^{119m}Sn Mössbauer and far infrared spectroscopy. The chelating ligand (PT) functioned as a bidentate ligand towards diorganotin chlorides giving octahedral coordination geometry around the tin atom [96].

The synthesis, X-ray structure, behaviour in solution, and biological properties of the complex $[SnMe_2(PyTSC)(OAc)]$.HOAc (HPyTSC = pyridine-2-carbaldehydethiose -micarbazone) were reported. The complex was synthesized by refluxing a mixture of HPyTSC and $Sn_2Me_2(OAc)_2$ in dry methylene chloride [97]. The tin atom of this complex was coordinated to an N, N, S-tridentate PyTSC anion, to a monodentate acetate ion, and to the two methyl groups (in axial positions) in an approximately pentagonal bipyramidal environment with a vacant equatorial position. In this compound, the PyTSC ligand adopts Z- configuration and is planar. Although the

acetate anion was monodentate the non-coordinated 'O' atom probably played an important role in determining the geometry of the coordination polyhedron around the tin atom.

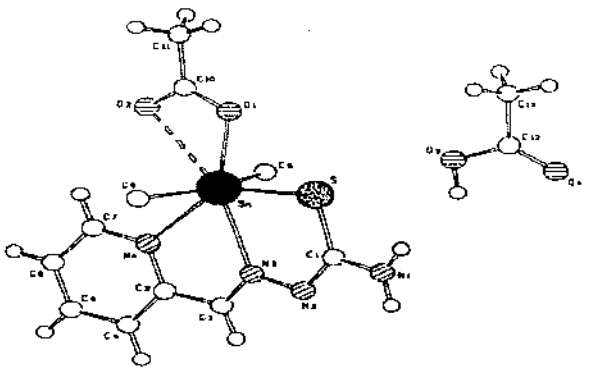

Fig. 4.15 Structure of $[SnMe_2(PyTSC)(OAc)].HOAc$ [97].

Investigations on the chelating properties of 2,6-diacetylpyridinebis(semicarbazone) (H_2DAPSC) and 2,6-diacetylpyridinebis(thiosemicarbazone) ($H_2DAPTSC$) have revealed that tin in these complexes attain a seven-coordinated geometry. Two tin complexes of H_2DAPSC and $H_2DAPTSC$ have been characterized. The planar pentadentate ligand 2,6-diacetylpyridinebis(semicarbazone), H_2DAPSC, was found to combine with $SnCl_3^-$ dissociated from $[Pt(SnCl_3)_5]^{3-}$ and formed a pentagonal bipyramidal complex of Sn(IV), $[SnCl_2(H_2DAPSC)]Cl_2{\cdot}2H_2O$ [98]. The complex was characterized by an X-ray crystal structure study. The cation, $[SnCl_2(H_2DAPSC)]^{2+}$ was a slightly distorted pentagonal bipyramid in which the H_2DAPSC ligand formed a pentagonal plane and two chloride ions occupied the axial positions. This is the first example of a metal oxidation taking place in the presence of H_2DAPSC and being stabilized by the ligand.

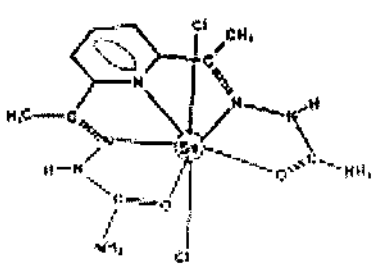

Fig. 4.16 Structure of $[SnCl_2(H_2DAPSC)]Cl_2{\cdot}2H_2O$ [98].

Two hepta-coordinated organotin complexes, [MeSnCl(HDAPTSC)]Cl·MeOH and [MeSnCl(H_2DAPSC)]Cl_2·$2H_2O$, have been prepared from the reaction between $MeSnCl_3$ and H_2DAPTSC or H_2DAPSC, respectively. Single crystal X-ray diffraction studies showed them to be approximately pentagonal bipyramidal (PBP), with the organic ligands lying in the equatorial plane. H_2DAPTSC and $SnCl_4$ formed a complex with the formula [ClSnCl(HDAPTSC)]Cl , which was presumed to have an analogous PBP structure. On the other hand, the complex obtained from H_2DAPSC and Me_2SnCl_2 was tentatively formulated as [(Me_2SnCl_2)$_2$(H_2DAPSC)] and ^{119}Sn Mössbauer spectroscopic evidence suggested an octahedral coordination for the two tin atoms [99].

The reaction of the title ligand (H_2DAPTSC) with SnR_2O (R=Me, Ph) in DMF afforded the complexes [SnR_2(DAPTSC)]. The phenyl derivative crystallized as [$SnPh_2$(DAPTSC)]·2DMF. The molecular complex was pentagonal bipyramidal with the five donor atoms of the ligand in the pentagonal plane and the two phenyl groups in the axial positions [100].

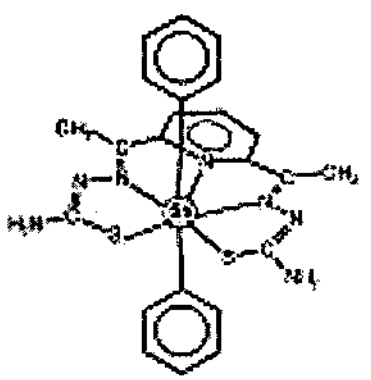

Fig. 4.17 Structure of [$SnPh_2$(DAPTSC)]·2DMF [100]

A comparative study based on the spectral properties (IR, Mössbauer and ^{1}H, ^{13}C and ^{119}Sn NMR spectroscopy) of the two complexes suggested a similar structure for [$SnMe_2$(DAPTSC)] [100].

[$SnPh_2$(HDAPTSC)]Cl was obtained by refluxing H_2DAPTSC.HCl and Ph_2SnCl_2 in methanol [101]. The Sn(IV) atom in this complex is hepta-coordinated and also had a pentagonal bipyramidal geometry, where only one of the H_2DAPTSC arms has undergone deprotonation. But, this does not significantly modify the bond lengths in

either of the thiosemicarbazone arms or in the coordination polyhedron, and the angles underwent only small changes.

S.W. Ng *et al.* [102] have prepared dibutyltin salicylaldehydethiosemicarbazonate [$SnBu_2$(STSC)] by melting together equimolar amounts of dibutyltin oxide and salicylaldehyde thiosemicarbazone. The ligand behaved as a (N, S, O)-tridentate ligand in Z- configuration and a *cis*-trigonal bipyramidal coordination polyhedron with the phenolic hydroxyl 'O' in one axial positions and the thiosemicarbazonate 'S' in the other.

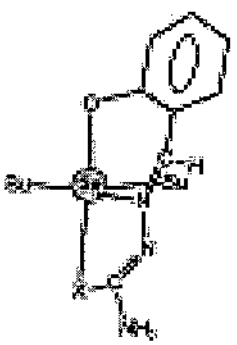

Fig.4.18 Structure of [Bu_2Sn(STSC)] [102].

Similar structures have been reported [103] for [$SnMe_2$(STSC)] and [$SnPh_2$(STSC)], the slight differences being due to the different organotin units. Both these compounds were obtained by refluxing $SnR_2(O)$ and salicylaldehyde thiosemicarbazone in benzene for five days and removing the resulting azeotropic benzene–water mixture by distillation in a Dean-Stark apparatus.

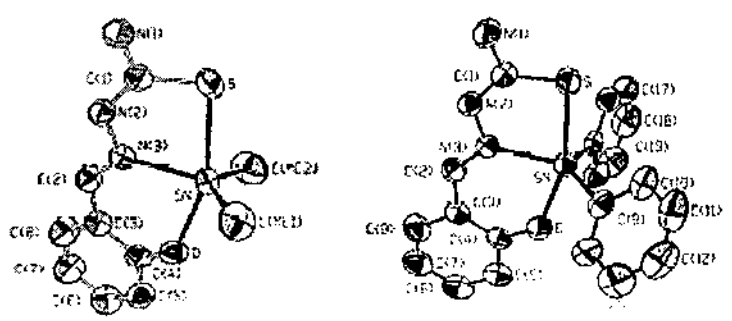

(a) (b)

Fig.4.19 Structure of (a) [Me_2Sn(STSC)] (b) [Ph_2Sn(STSC)] respectively with their atom numbering scheme [103].

The crystal structure of triphenyltin 1-amino-4-(2-hydroxyphenyl)-2, 3- diazapenta-(*E*)-1, (*E*)- 3- dienyl -1- thiolate was reported by Ng *et al.* [104]. The complex was obtained by slow evaporation of a solution of triphenyltin hydroxide and the thiosemicarbazone in 1 :1 molar ratio in ethanol. The tin atom was in a distorted tetrahedral environment, with the three carbon atoms of the phenyl groups and the thiosemicarbazone 'S' atom defining the tetrahedral polyhedron. In this compound, the *S*-coordinated thiosemicarbazonate group was twisted rather than planar. The phenolic proton in the thiosemicarbazonate and in the uncomplexed ligand was hydrogen -bonded to the N (3) atom.

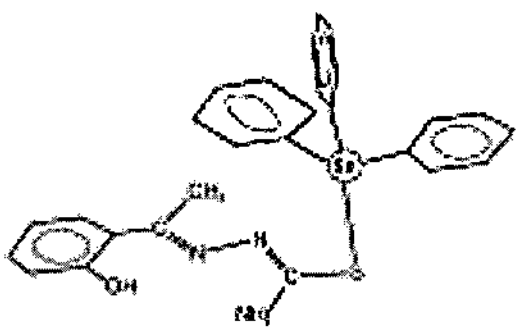

Fig. 4.20 Structure of triphenyltin 1-amino-4-(2-hydroxyphenyl)-2,3-diazapenta-(*E*)-1, (*E*)-3-dienyl-1-thiolate [104].

The reaction between Ph_2SnCl_2 and thiosemicarbazide using acetone-ethanol as solvent resulted in the formation of bis(acetone thiosemicarbazone-*S*) dichlorophenyltin(IV), $[SnPh_2Cl_2(ATSC)_2]$, acetone thiosemicarbazone (ATSC) having been derived *in situ* from the reaction of thiosemicarbazide and acetone [105]. The X-ray crystal structure of the bis(acetone thiosemicarbazone-*S*) dichlorophenyltin(IV) showed a distorted octahedron about tin atom which was coordinated to two phenyl, two chloride and two acetone thiosemicarbazone (ATSC) groups. Each of the ATSC ligand coordinated to the tin atom in a *trans* configuration and therefore behaved as a monodentate ligand bonding only through 'S' atom.

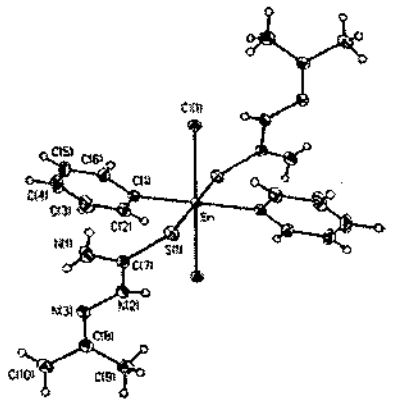

Fig.4.21 Structure of $[SnPh_2Cl_2(ATSC)_2]$ [105].

The reactivity of the polydentate ligands bis(2-acetylpyridine) carbonohydrazone (H_2APE) and 2-acetylpyridine semicarbazone (HAPS) as well as of their sulphur containing analogues bis(2-acetylpyridine) thiocarbonohydrazone (H_2APT) and 2-acetylpyridine thiosemicarbazone (HAPTS) was investigated towards organotin compounds [106]. An X-ray crystal structure determination carried out on $Ph_2Sn(HAPT)Cl.H_2O$ and $(n\text{-}Bu)_2Sn(APTS)(OAc)$ revealed that in both compounds the hydrazonic ligand was terdentate via sulphur atom and two nitrogen atoms. The tin atom was six-coordinated in $Ph_2Sn(HAPT)Cl.H_2O$ (Fig. 4.22) and seven-coordinated in the dibutyltin derivative $(n\text{-}Bu)_2Sn(APTS)(OAc)$. The similarities observed in the IR and ^1H NMR spectra were indicative of a similar behaviour of the ligand in all the complexes, thus suggesting a six-coordinated tin in the chloro derivatives and a seven-coordinated tin in the acetate ones. In $Ph_2Sn(HAPT)Cl.H_2O$, the hydrazone ligand was monodeprotonated and acted as a terdentate N_2S donor giving rise to two five-membered chelate rings, one of which (SnNCCN) was strictly planar, while the other (SnSCNN) showed a slight degree of puckering. The coordination sphere of the metal was completed to a highly distorted octahedral by a chlorine atom in the equatorial plane and two *trans*-positioned phenyl rings in the axial sites. The main distortion from the regular octahedral geometry came from the stereochemical constraint of HAPT. The water molecule was involved in an intermolecular O...Cl hydrogen bond [106].

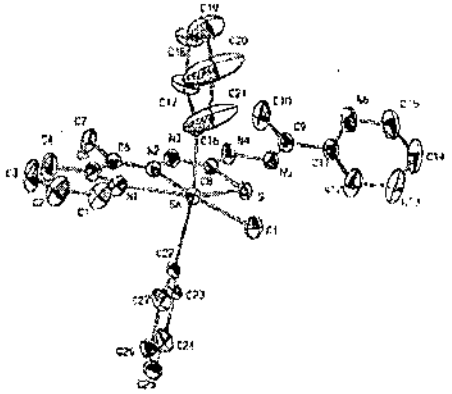

Fig. 4.22 Structure of $Ph_2Sn(HAPT)Cl.H_2O$ [106].

Treatment of 5-methoxy -5, 6- diphenyl -4, 5 – dihydro -2*H* - [1, 2, 4]triazine-3-thione (LH_2OCH_3) with compounds SnR_2X_2 (R = Me and Ph; X = Cl and NO_3) afforded, for the first time, metal derivatives of a cyclic thiosemicarbazone [107]. Treatment of LH_2OCH_3 with the appropriate diorganotin(IV) chloride in dichloromethane provided 1:1 complexes, but 1:2 derivatives were isolated when the nitrate salts in distilled water were used. The complexes were studied by mass spectrometry, IR and multinuclear (^1H, ^{13}C and ^{119}Sn) NMR in solution, and also by ^{119}Sn CP/MAS NMR spectroscopy and by X-ray diffraction in the solid state. In all the complexes, the thiosemicarbazone had been modified by formation of a new C=N bond. In addition, the ligand had lost a hydrogen atom, acting as an anion. The crystal structures of $[SnPh_2(C_{15}H_{10}N_3S)Cl]$ and $[SnMe_2(C_{15}H_{10}N_3S)_2]$ each consisted of discrete molecules with the tin atom bonded to the sulphur and amine nitrogen atoms to give a four-membered chelate ring with the [1,2,4]triazine modified. For phenyl derivative, the tin atom was in a trigonal bipyramidal environment with the phenyl rings in equatorial positions, and for the methyl derivative, it was in an octahedral arrangement, with the methyl groups in axial positions.

The synthesis and crystal structure of the $[Bu_2Sn(2,6Achexim)]$ was reported recently by G.F. de Sousa *et al.* The dianion of $H_2$2,6Achexim {where $H_2$2,6Achexim=2,6-diacetylpyridine bis(3-hexamethyleneiminylthiosemicarbazone) monohydrate} acted as a pentadentate ligand , 2, 6Achexim, in a planar conformation to a central tin(IV) ion. The tin(IV) was hepta-coordinated in a distorted pentagonal bipyramidal configuration , with five SNNNS donor atoms of 2,6Achexim in the pentagonal plane and the two n-butyl groups in the axial positions [108].

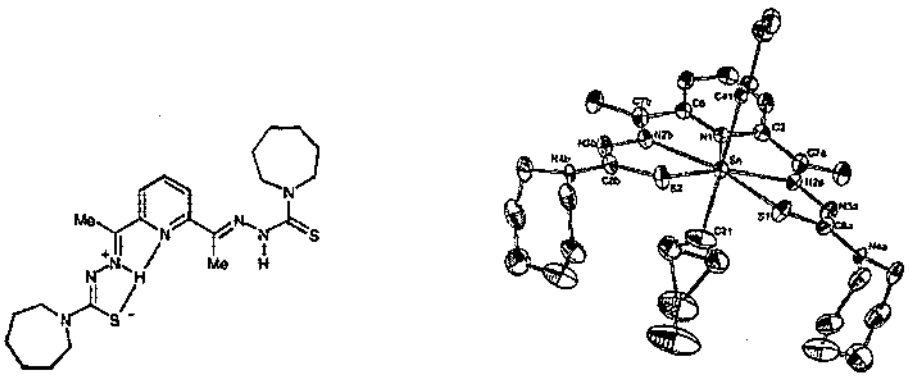

(a) (b)

Fig. 4.23 (a) $H_2$2,6 Achexim and (b) Structure of [Bu_2Sn(2,6Achexim)] [108].

4.1.3 Biological activity of thiosemicarbazones

Thiosemicarbazones are amongst the most important N, S donor ligands [74, 109] because of their highly interesting chemical, biological and medicinal properties [73, 74, 110].

One of the main reasons why the literature concerning thiosemicarbazones is rich and diverse is the higher biological activity of the same. Since the pioneering work of Domagk *et al.* [111] in 1946 on the antitubercular activity of *p*-acetamidobenzaldehyde thiosemicarbazone (trivial names Thiacetazone or Tibon) and *p*-methoxybenzaldehyde thiosemicarbazones, the number of papers concerning the pharmacological use of these compounds has dramatically expanded due to the wide spectrum of their biological activity found in recent years [76,112-115]. Some of the detected biological activities of thiosemicarbazones are antibacterial [116-122], antifungal [123,124], antimalarial [125], antiviral [126-129], antiamoebic [130], antitumour [131,132] and specially anti-HIV activity [133,134].Thiosemicarbazones have also been found to be active against influenza [135] and smallpox [136]. Genova *et al.* reported the toxic effects of bis(thiosemicarbazone) compounds and its Palladium (II) complexes on herpes simplex virus growth [137].It has been reported

by Gausman *et al.*[138] in 1953 that the activity of thiosemicarbazones is due to their property of forming chelates with metals.

In a recent study by Singh and his coworkers, they found two dimethyl silicon complexes of biologically active hetrocyclic thiosemicarbazones act as sterilizing agents by reducing the production of sperm in male mice, thus indicating their antifertility activity [79].

Many recent works report the antimicrobial (antibacterial and antifungal) activities of thiosemicarbazones[139-144].

It has been reported that the fungicidal activity of the thiosemicarbazones is due to their ability to chelate essential metals which the fungus needs for its metabolism [145,146]. On the basis of chelation theory the fungicidal activity of compounds containing an SH group adjacent to nitrogen have been well explained [147]. Also, metal complexes can act as antifungals by inhibiting enzymes, such as those involved in the biosynthesis of yeast cell walls [148].

S. Belwal *et al.* [91] synthesized diorganotin derivatives of the types $R_2SnCl(TSCZ)$ and $R_2Sn(TSCZ)_2$ (where TSCZ is the anion of a thiosemicarbazone ligand, R=Ph or Me) and evaluated their antimicrobial effects on different species of pathogenic fungi and bacteria *in vivo* as well as *in vitro*.

The antifungal activity of acetone thiosemicarbazone and its diphenyltin derivative was investigated by S.G.Teoh and his coworkers [105]. They found that the complex displayed marked fungitoxicity against the fungal strains tested and that the complex was more fungitoxic than acetone thiosemicarbazone and Ph_2SnCl_2.

Rebolledo *et al.* studied the antifungal activity of the 2-benzoylpyridine *N*-(4)-phenylthiosemicarbazone ligand and its tin(IV) complexes against *Candida albicans*. In this case, they found that the thiosemicarbazone proved to be more active than the tin(IV) complexes [92]. They proposed that the activity of thiosemicarbazone complexes depends upon two factors:

- Bulkiness of complexes: The bulkiness of complexes do not facilitate their permeation through the yeast cell membranes and hence decreases the activity.
- Lipophilicity of the complexes: Increase in lipophilicity leads to increased activity since the compounds can cross the cell membranes better.

Collins *et al.* have reported the correlation between structure and anti-mycobacterial activity in a series of 2-acetylpyridine thiosemicarbazones [149].

A study of novel pyrazoles and thiosemicarbazones by *Brown et al.* [150] have shown a definite correlation between compound structure and antibacterial activity. Those compounds having a lipophilic chain had greater antibacterial activity than compounds having less lipophilic structure such as the methoxy group. The hydrophilic core of the compound contributes to the movement of the compound into aqueous solution while the lipophilc characteristic enhances the ability to interact with the hydrophobic area of the membrane. Structural features that contributed to increased solubility and membrane interaction may greatly increase biological activity of compounds.

4.2 Scope and Objective

The Schiff bases obtained by the condensation of salicylaldehyde and substituted salicylaldehydes with thiosemicarbazide form a class of versatile O,N,S donor ligands. Many studies of these latter molecules as ligands have so far dealt with transition metal complexes of thiosemicarbazones of salicylaldehyde and substituted salicylaldehydes [81,151-153] whereby they stabilize unusual oxidation states and exhibit different coordination numbers in the complexes. Recently, an unusual coordination mode of salicylaldehyde thiosemicarbazone was observed in a group of $[M(PPh_3)_2(saltsc)_2]$ complexes, where R= Ru, Os and saltsc = anion of salicylaldehyde thiosemicarbazone [154,155]. Thiosemicarbazones and related ligands are reported to bind a metal ion as monoanionic bidentate ligand coordinating through N and S atoms forming a five-membered chelate ring [74,156]. This work was motivated by the desire to investigate the ligating behaviour of the versatile thiosemicarbazones towards the organotin(IV) moieties. Also, organotin compounds

are being used as agricultural biocides [157].Besides, the high fungicidal and bactericidal properties [158], various organotin compounds have been reported to possess antitumour activity with some derivatives being more active than cisplatin [159,160].The present work was also motivated by the desire to study the biocidal activity and cytotoxicty of these newly synthesized organotins. It is to be noted that during the progress of this work we became aware of reports of closely related studies [102,103,161] where some organotin(IV) complexes of semi- and thiosemicarbazones, along with the compounds (**1**) – (**3**) (Scheme 4.3) were described. These have been included herein to allow comparison of their biocidal properties with the corresponding Cl/Br-substituted ligands and because the compounds were synthesized via a different route, requiring shorter reaction times giving higher yields. Further, full details of their supramolecular structures are reported as well as a correlation of geometric parameters with those of the halide congeners.

4.3 Experimental

4.3.1 General comments

The solvents used in the reactions were of AR grade and were obtained from commercial sources (Merck, Germany). The solvents were dried using standard literature procedures. Petroleum ether and benzene were distilled from sodium whereas methanol was distilled after reacting it with magnesium. Proper health precautions were undertaken while working with benzene as a solvent.

4.3.2 Materials

Salicylaldehye (Fluka AG, Switzerland), 5-chlorosalicylaldehye (Lancaster, USA), 5-bromosalicylaldehyde (Lancaster, USA), thiosemicarbazide (Loba chemie, India), n-dibutyltinoxide (Alfa, USA), Me_2SnCl_2 (Fluka, Germany), Ph_2SnCl_2 (Aldrich, USA) and n-Bu_2SnCl_2 (Merck, Germany) were used as received from commercial sources. Bz_2SnCl_2 was prepared using the method of Sisido *et al.* [162]. Me_2SnO and Ph_2SnO were prepared by the alkaline hydrolysis of Me_2SnCl_2 and Ph_2SnCl_2 respectively in water/ether mixtures.

4.3.3 Measurements

IR spectra in the range 4000-250 cm $^{-1}$ were recorded on Pye-Unicam SP 300S spectrophotometer as Nujol mulls using CsI optics. ^{1}H and ^{13}C NMR spectra were obtained in $CDCl_3$ and C_6D_6 using TMS as an internal standard on a Bruker DPX 300 spectrometer. The solution ^{119}Sn NMR spectra were measured in $CDCl_3$ solution at 149.05 MHz using a Jeol Eclipse Plus 400 spectrometer and were referenced against $SnMe_4$. Tin was estimated gravimetrically as SnO_2 using standard procedures. Microanalyses were performed at RSIC, NEHU, Shillong, India. The electronic spectra were recorded on a Shimadzu UV 240 spectrophotometer with methanol as the solvent. Fluorescence studies were carried out on Elico SL174 spectrofluorometer. Melting points were determined using sulphuric acid bath and are uncorrected.

4.3.4 Synthetic procedures

The methods employed for the preparation of Schiff bases of salicylaldehyde/substituted salicylaldehyde from thiosemicarbazide are described in Section *4.3.4.1 – 4.3.4.4.* The synthesis of organotin(IV) complexes of the thiosemicarbazones are described in Sections *4.3.4.5 – 4.3.4.18.* Their characterization, analytical and spectroscopic data are given in Section 4.4.

4.3.4.1 Preparation of salicylaldehyde thiosemicarbazone (L^1H)

To a hot 1:1 ethanol-water solution (100 ml) of thiosemicarbazide (2.238 g, 24.56 mmol) was added dropwise an ethanolic solution (25 ml) of salicylaldehyde (3 g, 24.56 mmol) with continuous stirring. The stirring was continued for one hour at room temperature. The resultant solution was concentrated on a water bath and kept overnight. The pale yellow crystals were obtained the next day. The crystals were filtered and then thoroughly washed with ethanol to yield L^1H. The product was dried in vacuo.

L^1H : Yield: 4.26 g, 81.3 %., M.P.: 230 °C (dec.).

Elemental analysis (Calcd. for $C_8H_9N_3OS$):

Calcd.: C, 49.23 ; H, 4.61; N, 21.54 %.

Found: C, 49.20; H, 4.65; N, 21.43 %.

IR (cm^{-1}) : $\nu(NH_2)_{asym}$ 3442 cm^{-1}, $\nu(NH_2)_{sym}$ 3317 cm^{-1}, ν(C=N) 1612 cm^{-1}, ν(C=S) 777 cm^{-1}.

4.3.4.2 Preparation of 5-bromosalicylaldehyde thiosemicarbazone (L^2H)

A hot ethanolic solution (50 ml) of 5-bromosalicylaldehyde (4 g, 19.89 mmol) was added to a hot 1:1 ethanol-water solution (75 ml) of thiosemicarbazide (1.813 g, 19.89 mmol) with continuous stirring. The stirring was continued for two hours at hot conditions. The resultant solution was concentrated on a water bath and kept overnight. The cream coloured flaky crude product was obtained the next day. The product was filtered and then recrystallized from ethanol to yield L^2H. The product was dried in vacuo.

L^2H : Yield: 4.6 g, 79 %, M.P.: > 245 °C (dec.).

Elemental analysis (Calcd. for C_8H_8NOSBr):

Calcd.: C, 35.05 ; H, 2.92; N, 15.33 %.

Found: C, 35.10 ; H, 2.93; N, 15.26 %.

IR (cm^{-1}) : $\nu(NH_2)_{asym}$ 3412 cm^{-1}, $\nu(NH_2)_{sym}$ 3236 cm^{-1}, ν(C=N) 1611cm^{-1}, ν(C=S) 776 cm^{-1}.

4.3.4.3 Preparation of 5-chlorosalicylaldehyde thiosemicarbazone (L^3H)

A hot 1:1 ethanol-water solution (75 ml) of thiosemicarbazide (1.45 g, 15.96 mmol) was added dropwise to a hot ethanolic solution (50 ml) of 5-chlorosalicylaldehyde (2.5 g, 15.96 mmol) with continuous stirring. The stirring was continued for two hours at hot conditions. The pale yellow crystals were obtained upon concentration of the resultant mixture. The crystals were filtered and then thoroughly washed with ethanol to yield L^3H. The product was dried in vacuo.

L^3H : Yield: 3 g, 75.9 %., M.P.: 235 °C (dec.).

Elemental analysis (Calcd. for C_8H_8NOSCl) :

Calcd.: C, 41.83 ; H, 3.48 ; N, 18.30 %.

Found: C, 41.79; H, 3.52 ; N, 18. 41 %.

IR (cm^{-1}) : $\nu(NH_2)_{asym}$ 3406 cm^{-1}, $\nu(NH_2)_{sym}$ 3234 cm^{-1}, ν(C=N) 1610 cm^{-1}, ν(C=S) 777 cm^{-1}.

4.3.4.4 Preparation of napthaldehyde thiosemicarbazone (L^4H)

Naphthaldehyde (4 g, 23.23 mmol) in 100 ml of ethanol was added dropwise with continuous stirring to a hot 1:1 ethanol-water solution (75 ml) of thiosemicarbazide (2.11 g, 23.23 mmol). The reaction mixture was stirred at hot conditions for three hours. The brown coloured product was obtained upon concentration of the resultant mixture. The product was filtered and then thoroughly washed with ethanol to yield L^4H. The product was then dried in vacuo.

L^3H : Yield: 4.82 g, 78.8 %. M.P.: >245 °C (dec.).

Elemental analysis (Calcd. for $C_{10}H_7NOS$):

Calcd.: C, 58.77 ; H, 4.48 ; N, 17.14 %.

Found: C, 58.62 ; H, 4.45 ; N, 17.02 %.

IR (cm^{-1}) : $\nu(NH_2)_{asym}$ 3448 cm^{-1}, $\nu(NH_2)_{sym}$ 3240 cm^{-1}, ν(C=N) 1610 cm^{-1}, ν(C=S) 775 cm^{-1}.

4.3.4.5 Synthesis of dimethyltin(IV) salicylaldehyde thiosemicarbazonate, Me_2SnL^1 (1)

To a solution (45 ml) of salicylaldehyde thiosemicarbazone (0.650 g, 3.33 mmol) in methanol was added dropwise 0.1 N methanolic NaOH (74 ml, 0.266 g, 6.65 mmol) under stirring. The reaction system was stirred for 2 h and then a methanolic solution (40 ml) of Me_2SnCl_2 (0.732 g, 3.33 mmol) was added. The reaction mixture which turned fluorescent yellow was refluxed for 8 h under inert conditions. The volatiles were removed and the dry mass extracted with hot petroleum ether (60-80°C, 75 ml).The crude product obtained was recrystallized from benzene to yield yellow crystals of the desired product.

4.3.4.6 Synthesis of dibutyltin(IV) salicylaldehyde thiosemicarbazonate, $n\text{-}Bu_2SnL^1$ (2)

To a solution (45 ml) of salicylaldehyde thiosemicarbazone (0.500 g, 2.564 mmol) in methanol was added dropwise 0.1 N methanolic NaOH (57 ml, 0.205 g, 5.128 mmol) under stirring. The reaction system was stirred for 2 h and then a methanolic solution

(35 ml) of n-Bu_2SnCl_2 (0.779 g, 2.564 mmol) was added. The reaction mixture which turned fluorescent yellow was refluxed for 8 h under inert conditions. The volatiles were removed and the dry mass extracted with hot petroleum ether (60-80°C, 50 ml). Yellow needle- shaped crystals of the desired product were obtained immediately.

4.3.4.7 Synthesis of diphenyltin(IV) salicylaldehyde thiosemicarbazonate, Ph_2SnL^1 (3)

To a solution (50 ml) of salicylaldehyde thiosemicarbazone (0.500 g, 2.564 mmol) in methanol was added dropwise 0.1 N methanolic NaOH (57 ml, 0.205 g, 5.128 mmol) under stirring. The reaction system was stirred for 2 h and then a methanolic solution of Ph_2SnCl_2 (0.881 g, 2.562 mmol) was added. The fluorescent yellow reaction mixture was refluxed for 8 h under inert nitrogen gas condition. The volatiles were removed and the dry mass extracted with hot petroleum ether (60-80°C, 100 ml). Slow cooling yielded yellow crystals of the desired product.

4.3.4.8 Synthesis of dimethyltin(IV) 5-bromosalicylaldehydethiosemicarbazonate $Me_2SnL^2.H_2O$ (4)

A mixture of Me_2SnO (0.359g, 2.18 mmol) and 5-bromosalicylaldehyde thiosemicarbazone (0.597g, 2.18 mmol) in benzene (100 ml) was refluxed under inert nitrogen atmosphere conditions for 10 h, the water produced being removed azeotropically. The volatiles were removed from the fluorescent yellow reaction mixture and the dry mass extracted with hot petroleum ether (60-80°C, 50 ml). Yellow crystals of the desired product were obtained by cooling the solution.

4.3.4.9 Synthesis of dibutyltin(IV) 5-bromosalicylaldehyde thiosemicarbazonate n-Bu_2SnL^2 (5)

The compound **5** was prepared by refluxing a mixture of n-Bu_2SnO (0.500g, 2.01 mmol) and 5-bromosalicylaldehyde thiosemicarbazone (0.550g, 2.01 mmol) in benzene (100 ml) under inert conditions for 10 h, the water produced being removed

azeotropically. The volatiles were removed by distillation from the fluorescent yellow reaction mixture and the dry mass extracted with hot petroleum ether (60-80°C, 45 ml) to give a viscous deep yellow colour liquid as the product. The product was then dried in vaccum pump to exclude traces of any solvent and then stored in a dessicator.

4.3.4.10 Synthesis of diphenyltin(IV) 5-bromosalicylaldehyde thiosemicarbazonate Ph_2SnL^2 (6)

A mixture of Ph_2SnO (0.630 g, 2.18 mmol) and 5-bromosalicylaldehyde thiosemicarbazone (0.597g, 2.18 mmol) was suspended in benzene (100 ml) and refluxed under inert conditions for 10 h, the water produced being removed azeotropically. The volatiles were removed from the fluorescent yellow reaction mixture and the dry mass extracted with hot petroleum ether (60-80°C, 135 ml). Yellow crystals of the desired product were obtained by cooling the solution.

4.3.4.11 Synthesis of dimethyltin(IV) 5-chlorosalicylaldehydethiosemicarbazonate Me_2SnL^3 (7)

The compound 7 was synthesized by reacting 5-chlorosalicylaldehyde thiosemicarbazone (0.836g, 3.64 mmol) and Me_2SnO (0.600g, 3.64 mmol) in 125 ml anhydrous benzene in a 250 ml flask fitted with a Dean-Stark trap and water-cooled condenser. The reaction mixture was refluxed for 10 h, and filtered while hot. The filterate was collected and the volatiles were removed. The residue was extracted with hot petroleum ether (60-80°C, 80 ml). Yellow crystals of the desired product were obtained after two days from the petroleum ether extract of 7 kept at room temperature.

4.3.4.12 Synthesis of dibutyltin(IV) 5-chlorosalicylaldehydethiosemicarbazonate $n\text{-}Bu_2SnL^3$ (8)

A mixture of $n\text{-}Bu_2SnO$ (0.650g, 2.614 mmol) and 5-chlorosalicylaldehyde thiosemicarbazone (0.599 g, 2.614 mmol) in anhydrous benzene (100 ml) was

refluxed under inert conditions for 10 h, the water produced being removed azeotropically using a Dean-Stark trap. The volatiles were removed from the fluorescent yellow reaction mixture and the dry mass extracted with hot petroleum ether (60-80°C, 50 ml). The product obtained was a deep yellow viscous liquid which was pumped for 8 hours in a vaccum pump to exclude traces of solvent and subsequently stored in a dessicator.

4.3.4.13 Synthesis of diphenyltin(IV) 5-chlorosalicylaldehydethiosemicarbazonate Ph_2SnL^3 (9)

A mixture of Ph_2SnO (0.700g, 2.42 mmol) and 5-chlorosalicylaldehyde thiosemicarbazone (0.556g, 2.42 mmol) in benzene (135 ml) was refluxed under inert conditions for 10 h, the water produced was removed azeotropically using a Dean-Stark trap. The volatiles were removed from the fluorescent yellow reaction mixture and the dry mass extracted with hot petroleum ether (60-80°C, 150 ml). The petroleum ether solution was concentrated and left for crystallization at room temperature. Yellow crystals of the desired product were obtained after 2 days from the petroleum ether solution.

4.3.4.14 Synthesis of dimethyltin(IV) napthaldehydethiosemicarbazonate Me_2SnL^4 (10)

A mixture of Me_2SnO (0.650g, 3.94 mmol) and naphthaldehyde thiosemicarbazone (0.966 g, 3.94 mmol) was suspended in 135 ml anhydrous benzene and refluxed under inert conditions for 12 h, the water produced during the reaction was removed azeotropically using a Dean- Stark trap. The reaction mixture was filtered while hot. The volatiles were removed from the filterate to yield a dry mass. The dry mass was then extracted with hot petroleum ether (60-80 °C) in quantities of 4-5 ml for 20 times. The petroleum ether solution was concentrated and left for crystallization at room temperature. Reddish brown crystals of **10** were obtained after one day.

4.3.4.15 Synthesis of dibutyltin(IV) napthaldehydethiosemicarbazone, n-Bu_2SnL^4 (11)

A mixture of n-Bu_2SnO (0.600g, 2.41 mmol) and naphthaldehyde thiosemicarbazone (0.591g, 2.41 mmol) in benzene (150 ml) was refluxed under inert conditions for 12 h, the water produced being removed azeotropically. The volatiles were removed from the reaction mixture and the dry mass extracted with hot petroleum ether (60-80°C, 50 ml). A reddish brown coloured viscous liquid was obtained as the product. The product was dried in vacuo and then stored in a dessicator.

4.3.4.16 Synthesis of diphenyltin(IV) napthaldehydethiosemicarbazonate Ph_2SnL^4 (12)

The compound **12** was synthesized by reacting napthaldehydethiosemicarbazone (0.424g, 1.73 mmol) and Ph_2SnO (0.500g, 1.73 mmol) in 100 ml anhydrous benzene in a 250 ml flask fitted with a Dean-Stark trap and water-cooled condenser. The reaction mixture was heated under reflux for 12 h, and filtered while hot. The filterate was collected and the volatiles were removed. The residue was extracted with hot petroleum ether (60-80°C, 90 ml). Reddish brown crystals of the desired product were obtained after 48 h from the petroleum ether extract of **12** at room temperature.

4.3.4.17 Synthesis of dibenzyltin(IV) of salicylaldehyde thiosemicarbazonate, Bz_2SnL^1 (13)

To a solution of salicylaldehyde thiosemicarbazone (0.650 g, 3.33 mmol) in methanol was added dropwise 0.1 N methanolic NaOH (74 ml, 0.266 g, 6.65 mmol) under stirring. The reaction mixture was stirred for 2 h and then a methanolic solution (45 ml) of Bz_2SnCl_2 (0.732 g, 3.33 mmol) was added. The fluorescent yellow reaction mixture was refluxed for 6 h under inert conditions. The volatiles were removed and the dry mass extracted with hot petroleum ether (60-80°C, 75 ml). A yellow coloured solid product was obtained.

4.3.4.18 Synthesis of dibenzyltin(IV) derivative of 5-chlorosalicylaldehyde thiosemicarbazone, $[Sn(Bz)_2(C_8H_6ClN_3OS)_2(CH_3O)_2]$ (14)

A methanol solution (50 ml) of 5-chlorosalicylaldehyde thiosemicarbazone (0.500 g, 2.17 mmol) was stirred continuously in a 0.1 N methanolic NaOH solution (45.9 ml, 0.174g, 4.35 mmol) for 2 h. Bz_2SnCl_2 (0.809g, 2.17mmol) dissolved in 50 ml of methanol was then added to the reaction mixture which was refluxed for 6 h under an inert atmosphere. The volatiles were removed by distillation and the residue obtained was washed thoroughly with hot petroleum ether (b.p. 60-80°C) in quantities of 4-5 ml, extracted into benzene (50 ml) and filtered. The product obtained was then repeatedly recrystallized from methanol to give **14**.

4.3.5 Crystal structure determinations

4.3.5.1 Crystal structure determinations of 1, 3, 4, 6 and 9

Intensity data were measured for selected crystals of **1, 3, 4, 6** and **9** at 223 K on a Bruker AXS SMART CCD with graphite monochromatized Mo*K*α radiation (0.71069 Å) so that θ_{max} = 30.0/30.1°. Each structure was solved by heavy-atom methods [163] and refined [164] on F^2 with non-hydrogen atoms modelled with anisotropic displacement parameters, with hydrogen atoms in the riding model approximation and using a weighting scheme of the form $w = 1/[\sigma^2(F_o^2) + (aP)^2 + bP]$ where $P = (F_o^2 + 2F_c^2)/3$). In the refinement of **6**, rather large residual electron density peaks within 1 Å of the bromide atoms were noted. This is ascribed to the rather poor quality of the crystals and the possibility of pseudo symmetry -- the unit cell parameters roughly approximate a hexagonal unit cell. Otherwise, the final difference maps were relatively featureless. The crystallographic data and refinement details are given in Table 4.1- 4.5. The numbering schemes are shown in Section 4.4 and were drawn with ORTEP [165]. Diagrams of the supramolecular structures were generated with the aid of the DIAMOND [166] programme.

4.3.5.2 Crystal structure determination of 14

Intensity data were measured for selected crystals of **14** at 173 K on a Rigaku AFC12K/SATURN724 diffractometer with graphite monochromatized Mo$K\alpha$ radiation so that $\theta_{max} = 27.6°$. The structure was solved by heavy-atom methods [163] and refined [164] on F^2 with non-hydrogen atoms modelled with anisotropic displacement parameters, with hydrogen atoms in the riding model approximation and using a weighting scheme of the form $w = 1/[\sigma^2(F_o^2) + (aP)^2 + bP]$ where $P = (F_o^2 + 2F_c^2)/3$).Crystal data are given in Table 4.6. The numbering scheme is shown in Fig. 4.34 and was drawn with ORTEP [165]. Diagrams of the supramolecular structures were generated with the aid of the DIAMOND [166] programme.

4.3.6 Biological studies

4.3.6.1 Antibacterial activity

4.3.6.1.1 Bacterial strains and determination of antibacterial properties of organotin complexes

The organotin compounds studied were dissolved in 0.3 % DMSO-water. The solutions were always prepared fresh and the pH adjusted to 7.4. The bacterial strains used in the study were *Aeromonas hydrophila* strain 646 (MTCC, India, Gram-negative pathogenic), *Salmonella typhi* strain 737 (NICED, India, Gram-negative pathogenic), *Salmonella typhimurium* strain 3099 (NICED, India, Gram-negative pathogenic), *Salmonella flexnri* strain NK 2226 (NICED, India,Gram-negative pathogenic), *Escheria coli* strain 25922 (NICED, India, Gram-negative pathogenic), *Salmonella aureus* (kind gift from M. Saha, National Institute for Cholera and Enteric Diseases, Kolkata, India, Gram-negative pathogenic), *Bacillus subtilis* strain 6633 (ATCC, India, Gram-positive non-pathogenic) and *Lactobacillus rhamnosus* strain 1408 (ATCC, India, Gram-positive non-pathogenic). Bacteria were maintained in nutrient agar slant at 4°C and for experimental need they were grown in specific medium to log phase at optimal temperature.

The antibacterial properties of the organotins were evaluated by the disc-diffusion method [167]. Bacteria were grown to mid-log phase and spread on nutrient agar plates. Sterile filter discs containing different concentrations of the organotins in 20-40 µl were applied on the bacterial plates and incubated at optimal temperature for 24 h. The inhibition zones appearing around each disc were measured and the sensitivity determined from the zone diameters appearing on the plates based on NCCLS charts. When the bacteria gave a zone with diameter less than 13 mm in the presence of an organotin, it was interpreted as resistant (R), when the zone had a diameter of 15-16 mm, the bacteria were considered to have intermediate sensitivity (I) and a clear zone with diameter of 17 mm or more indicated a high degree of sensitivity towards the compound (S).

4.3.6.1.2 Role of 2 on bacterial disease

Aeromonas hydrophila is a known fish pathogen responsible for E.U.S (Epizootic Ulcerative Syndrome). 1 x 10^{10} bacteria were incubated with **2** overnight at 30 °C in BHI containing ampicillin (100 µg/ml). Following incubation the bacteria were washed repeatedly with sterile saline water (0.9%) and introduced by intramuscular route into healthy fish in 100 µl saline. Control fish were injected with untreated bacteria. The development of redness and ulcer formation were checked in both group of animals. Healthy fish were also injected with untreated bacteria (1 x 10^{10}/100 µl saline). 72 hours after **2** was locally injected at the site of infection, at 24 hours interval for three consecutive days, the development of disease phenotype was checked. Control fish were injected with 0.3% DMSO solution or saline [167].

4.3.6.2 Antifungal activity

The fungal strains used were gifts from The Department of Botany, University of North Bengal. The strains were *Curvularia eragrostidis* (a pathogen of tea, *Camellia sineusis*), *Alternaria porri* (a pathogen of niger, *Guizotia abyssinica*), *Dreschlerea oryzae* (a pathogen of rice, *Oryzae sativa)* and *Macrophomina phaseolina* (a pathogen of brinjal, *Solanum melongena*). These strains were grown on potato-dextrose-agar (PDA, HiMedia, India) medium at 28 ±1 °C.

The fungicidal activities were determined following spore germination bioassay as described by Rouxel *et al.* [168]. Purified eluents (10 µl) were placed on two spots 3 cm apart on a clean, grease-free slide and the solvent was allowed to evaporate. One drop of spore suspension (20 µl), prepared from 15 day-old cultures of the fungi, was added to the treated spots. The slides were incubated at 27±1 °C for 24 h under humid conditions in Petri plates. Finally, after proper incubation period, one drop of a Cotton Blue-Lactophenol mixture was added to each spot to fix the germinated spores. The number of spores germinated compared with the germinated spores of control (where no chemicals were used) was calculated using an average of 300 spores per treatment. The minimum inhibitory concentration required for complete inhibition was recorded in units of µg/ml.

4.3.6.3 Phytotoxic effects

Oryzae sativa (IR-8, ICAR, India), *Lens culinaris,* and *Cicer aurantinum* were collected from the University Agricultural Research Institute, Visva-Bharati, and the phytotoxic effects of different organotins determined [169]. Briefly, seeds of different species were incubated with different concentration of organotins for different time periods. Following incubation the seeds were washed with distilled water and incubated in aerated moist chambers for 96 h at 28 °C. The percentage of seed germination was calculated and compared with the results obtained with seeds dipped in DMSO-water as well as with those incubated in water only.

4.3.7 Crystallographic data and refinement details for **1**, **3**, **4**, **6**, **9**, & **14**

Table 4.1 Crystallographic data and refinement details for $[Me_2SnL^1]$ (**1**)

	1
Formula	$C_{10}H_{13}N_3OSSn$
Formula weight	341.98
Crystal system	Monoclinic
Space group	$P2_1/n$
a (Å)	9.4175(6)
b (Å)	13.4230(9)
c (Å)	10.5187(7)
α (°)	90
β (°)	100.266(1)
γ (°)	90
V (Å^3)	1308.39(15)
Z	4
D_c (g cm^{-3})	1.736
μ (Mo$K\alpha$, mm^{-1})	2.096
Measured data	10789
Unique data	3792
Observed data	
[$I \geq 2.0\sigma(I)$]	3291
R, obs. data; all data	0.030; 0.036
a; b in weighting scheme	0.038; 0.431
R_w, obs. data; all data	0.075; 0.079
Largest residual (e Å^{-3})	0.85
CCDC deposition no.	638421

Table 4.2 Crystallographic data and refinement details for $[Ph_2SnL^1]$ (**3**)

	3
Formula	$C_{20}H_{17}N_3OSSn$
Formula weight	466.12
Crystal system	Monoclinic
Space group	$P2_1/c$
a (Å)	15.5284(8)
b (Å)	10.0604(5)
c (Å)	13.3743(7)
α (°)	90
β (°)	113.673(2)
γ (°)	90
V (Å^3)	1913.54(17)
Z	4
D_c (g cm^{-3})	1.618
μ (Mo$K\alpha$, mm^{-1})	1.458
Measured data	15651
Unique data	5538
Observed data	
$[I \geq 2.0\sigma(I)]$	4188
R, obs. data; all data	0.035; 0.052
a; b in weighting scheme	0.040; 0
R_w, obs. data; all data	0.080; 0.087
Largest residual (e Å^{-3})	0.86
CCDC deposition no.	638422

Table 4.3 Crystallographic data and refinement details for $[Me_2SnL^2].H_2O$ (**4**)

	4
Formula	$C_{10}H_{14}BrN_3O_2SSn$
Formula weight	438.90
Crystal system	monoclinic
Space group	*C*2/*c*
a (Å)	15.5788(8)
b (Å)	13.6076(7)
c (Å)	13.9124(7)
α (°)	90
β (°)	93.936(2)
γ (°)	90
V (Å^3)	2942.3(3)
Z	8
D_c (g cm^{-3})	1.982
μ (Mo*K*α, mm^{-1})	4.592
Measured data	12167
Unique data	4300
Observed data	
[$I \geq 2.0\sigma(I)$]	3384
R, obs. data; all data	0.038; 0.054
a; *b* in weighting scheme	0.035; 0
R_w, obs. data; all data	0.080; 0.085
Largest residual (e Å^{-3})	1.13
CCDC deposition no.	638423

Table 4.4 Crystallographic data and refinement details for $[Ph_2SnL^2]$ (**6**)

	6
Formula	$C_{20}H_{16}BrN_3OSSn$
Formula weight	545.02
Crystal system	triclinic
Space group	*P*-1
a (Å)	12.7793(5)
b (Å)	12.8645(5)
c (Å)	13.5952(5)
α (°)	93.877(2)
β (°)	93.640(2)
γ (°)	118.031(2)
V (Å^3)	1956.79(13)
Z	4
D_c (g cm^{-3})	1.850
μ (Mo*K*α, mm^{-1})	3.470
Measured data	16439
Unique data	11161
Observed data	
[$I \geq 2.0\sigma(I)$]	8228
R, obs. data; all data	0.053; 0.075
a; *b* in weighting scheme	0.077; 0.429
R_w, obs. data; all data	0.131; 0.142
Largest residual (e Å^{-3})	4.78
CCDC deposition no.	638424

Table 4.5 Crystallographic data and refinement details for $[Ph_2SnL^3]$ (**9**)

	9
Formula	$C_{20}H_{16}ClN_3OSSn$
Formula weight	500.56
Crystal system	triclinic
Space group	*P*-1
a (Å)	8.8596(6)
b (Å)	9.9809(7)
c (Å)	12.7142(8)
α (°)	111.759(1)
β (°)	109.741(1)
γ (°)	91.927(1)
V (Å^3)	966.44(11)
Z	2
D_c (g cm^{-3})	1.720
μ (Mo*K*α, mm^{-1})	1.583
Measured data	8204
Unique data	5504
Observed data	
[$I \geq 2.0\sigma(I)$]	4898
R, obs. data; all data	0.045; 0.051
a; *b* in weighting scheme	0.055; 0.497
R_w, obs. data; all data	0.103; 0.107
Largest residual (e Å^{-3})	1.45
CCDC deposition no.	638425

Table 4.6 Crystallographic data and refinement details for **14**

	14
Formula	$[Sn_2(C_7H_7)_2(C_8H_6ClN_3OS)_2.(CH_3O)_2]$
Formula weight	937.04
Crystal system	Monoclinic
Space group	$P2_1/c$
a (Å)	11.617(7)
b (Å)	13.484(4)
c (Å)	12.430(4)
β (°)	117.367(5)
V (Å^3)	1729.1(13)
Z	2
D_c (g cm^{-3})	1.800
μ (Mo$K\alpha$, mm^{-1})	1.77
Measured data	44284
Unique data	3906
Observed data	
[$I \geq 2.0\sigma(I)$]	3887
R, obs. data; θ_{max}	0.051; 27.6°
a; b in weighting scheme	0.0396; 5.0883
R_w, obs. data; all data	0.050; 0.117
Largest residual (e Å^{-3})	0.99

4.4 Results and Discussion

4.4.1 Synthesis of Schiff base of salicylaldehyde, substituted salicylaldehyde and naphthaldehyde from thiosemicarbazide

The ligands used here are Schiff bases derived either from salicylaldehyde or substituted salicylaldehyde (5-bromosalicylaldehyde, 5-chlorosalicylaldehyde) or naphthaldehyde with thiosemicarbazide. The thiosemicarbazones were obtained in good yield (> 75%) by reacting equimolar amounts of thiosemicarbazides and respective salicylaldehyde/ substituted salicylaldehydes/ naphthaldehyde in 1:1 ethanol-water mixture [155]. The products were recrystallized from ethanol. The formulae of the ligands and the abbreviations of the complexes are presented in Scheme 4.3.

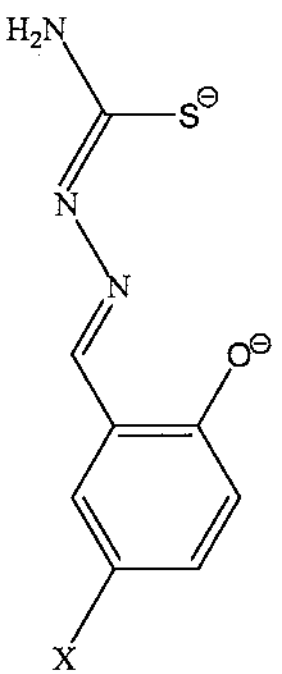

L^1: X =H ; L^2: X = Br ; L^3: X = Cl ; L^4: X = C_6H_4 .

1: Me_2SnL^1; **2**: n-Bu_2SnL^1; **3**: Ph_2SnL^1; **4**: $Me_2SnL^2.H_2O$; **5**: n-Bu_2SnL^2;
6: Ph_2SnL^2, **7**: Me_2SnL^3; **8**: n-Bu_2SnL^3; **9**: Ph_2SnL^3 ; **10**: Me_2SnL^4;
11: n-Bu_2SnL^4;**12**: Ph_2SnL^4.

Scheme 4.3

The Schiff bases synthesized are soluble in ethanol, methanol but insoluble in petroleum ether (b.p. 60-80 °C), benzene and carbon tetrachloride. They are all high and sharp melting compounds. The synthetic details and characterization data for $L^1H - L^4H$ are described in section 4.3.

4.4.2 Synthesis of diorganotin(IV) complexes of salicylaldehyde/ substituted salicylaldehyde/naphthaldehyde thiosemicarbazones

In this section the synthesis, characterization and crystal structures of new organotin derivatives of thiosemicarbazones are presented. Two different methods for the synthesis were adopted for the diorganotin(IV) complexes of the Schiff bases reported here. The objective was to compare the yields obtained by following two different synthetic routes. The synthetic conveniences, though, primarily led to the choice of a suitable procedure and have been described in detail in section 4.3.

4.4.2.1 Synthesis of diorganotin(IV) complexes of salicylaldehyde thiosemicarbazo - ne (L^1HH')

The diorganotin(IV) derivatives of salicylaldehyde thiosemicarbazone (R=Me, n-Bu, Ph) were obtained in moderate yields by the equimolar reaction of diorganotin(IV) dichlorides with the sodium salt of the ligand in methanol as solvent at reflux temperature (Scheme 4.4). The sodium salt of the ligand was generated *in situ* by the addition of methanolic solution of NaOH to the hot methanolic solution of salicylaldehyde thiosemicarbazone.

$$L^1HH' + 2NaOH \longrightarrow L^1Na_2 + 2H_2O \quad \ldots\ldots\ldots (4)$$

$$L^1Na_2 + R_2SnCl_2 \longrightarrow R_2SnL^1 + 2NaCl \quad \ldots\ldots\ldots (5)$$

The reactions were completed in 8 hours time. The reaction mixture was evaporated to dryness and then subsequently extracted with hot petroleum ether (b.p. 60- 80 °C) in quantities of 2-3 ml for 10 –15 times. A comparatively large amount of petroleum ether (100 ml) was needed to extract the diphenyltin analogue as the solubility was found to be poor in petroleum ether (b.p. 60- 80 °C).The synthetic methodology is

described in Scheme 4.4. The exact synthetic details for the above complexes along with their characterization data are listed in Table 4.7.

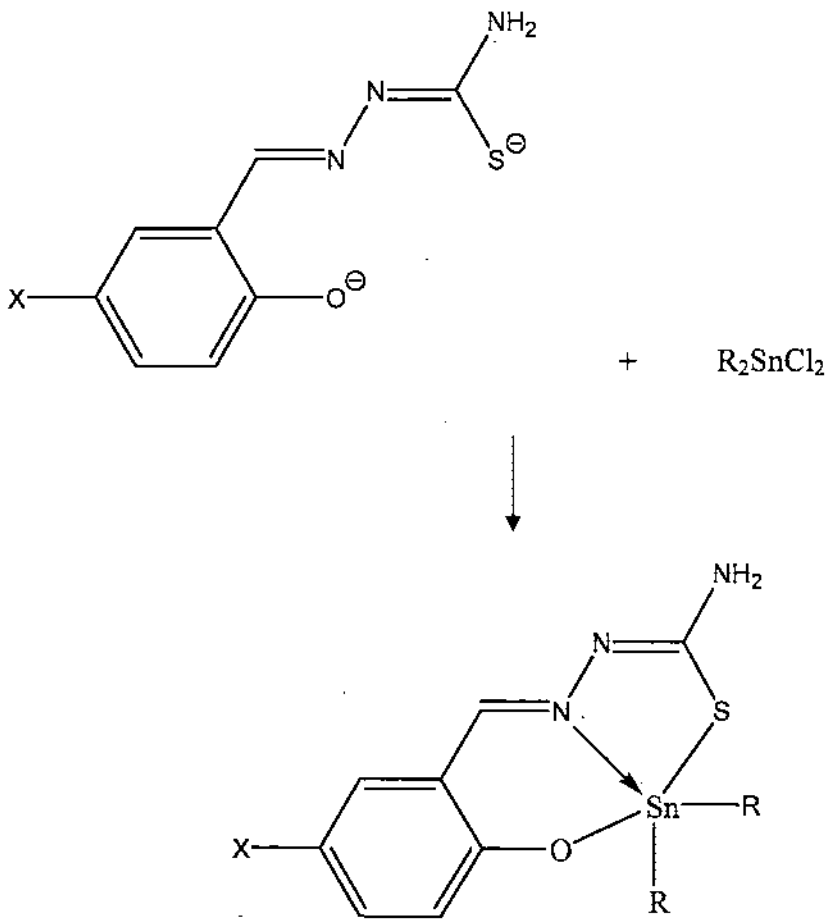

1: R= Me ; **2**: R= n-Bu ; **3**: R= Ph.

Scheme 4.4

The dibenzyltin(IV) complexes of salicylaldehyde thiosemicarbazones were synthesized analogously. These complexes are discussed separately in Section 4.4.4.

4.4.2.2 Synthesis of diorganotin(IV) complexes of substituted salicylaldehyde/ naphthaldehyde thiosemicarbazones (L^2HH'- L^4HH')

The diorganotin(IV) complexes of substituted salicylaldehyde/ naphthaldehyde thiosemicarbazones were synthesized by the reaction of the diorganotin(IV) oxides

with the respective ligand in 1:1 molar ratio in benzene as the solvent at reflux temperature. Since the Schiff bases were insoluble in benzene, the reaction mixture turned out to be heterogeneous and greater reaction times were usually required for the completion of the reaction. The water produced during the reaction was removed using a Dean-Stark trap to facilitate faster completion of the reactions. The compounds were obtained in moderate to good yields. The reaction system in all cases were evaporated to dryness and then extracted with hot petroleum ether (b.p.60-80 °C). The solubility for the diphenyltin analogues was generally poor when compared to the other complexes. Therefore, large quantities of petroleum ether (b.p. 60-80 °C) was required to extract the diphenyltin(IV) complexes, however the other diorganotin(IV) complexes were extracted readily using petroleum ether. The compound **4** was isolated as a monohydrate. The compounds are relatively stable in moist air and can be recrystallized from suitable organic solvents. The synthetic methodology is described in Scheme 4.5. Synthetic details along with the physical data are summarized in Table 4.7. All the complexes are soluble in chloroform, methanol, acetone, n-hexane and benzene.

$$LH_2 + R_2SnO \longrightarrow R_2SnL + H_2O \quad \text{..... (6)}$$

4 : R= Me, L= L^2; **5** : R= n-Bu, L= L^2; **6** : R= Ph, L= L^2
7 : R= Me, L= L^3; **8** : R= n-Bu, L= L^3; **9** : R= Ph, L= L^3
10 : R= Me, L= L^4; **11** : R= n-Bu, L= L^4; **12** : R= Ph, L= L^4

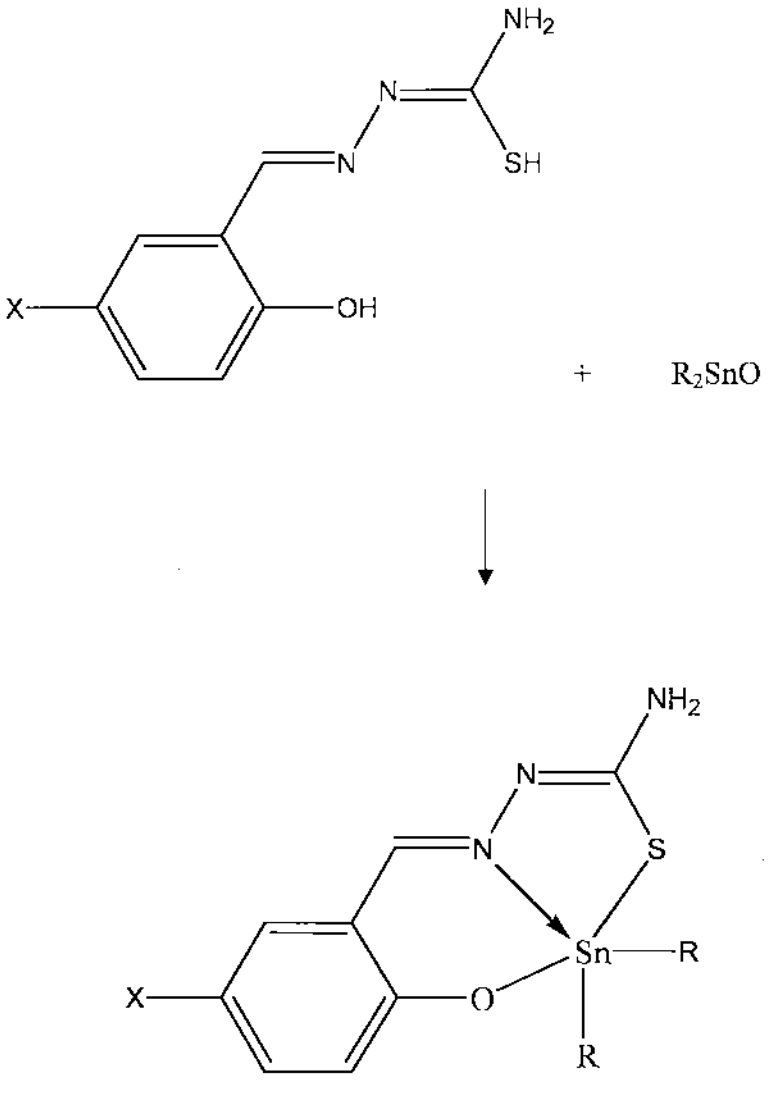

Scheme 4.5

Table 4.7 Characterization and analytical data for the diorganotin(IV) complexes[a]

Complex	Reaction time (h)	Crystallization solvent	Colour	Yield (%)	M.p. (°C)	Elemental composition: Found (Calc.) (%)			
						C	H	N	Sn
1	8[b]	Benzene	Yellow	85	152	34.59 (35.12)	3.78 (3.80)	12.27 (12.29)	34.60 (34.73)
2	8[b]	Petroleum ether[d]	Yellow	80	93-94	45.01 (45.10)	5.85 (5.87)	9.79 (9.87)	27.69 (27.88)
3	8[b]	Petroleum ether[d]	Yellow	70	131	51.45 (51.53)	3.61 (3.65)	9.00 (9.02)	25.40 (25.49)
4	10[c]	Petroleum ether[d]	Yellow	75	111-113	27.29 (27.36)	3.12 (3.19)	9.55 (9.57)	26.99 (27.06)
5	10[c]	Petroleum ether[d]	Yellow	69	-	37.98 (38.04)	4.73 (4.75)	8.30 (8.32)	23.49 (23.52)
6	10[c]	Petroleum ether[d]	Yellow	67	161-163	44.01 (44.06)	2.91 (2.93)	7.68 (7.71)	21.65 (21.79)
7	10[c]	Petroleum ether[d]	Yellow	45	105-106	31.88 (31.90)	3.18 (3.19)	11.15 (11.16)	31.48 (31.55)
8	10[c]	Petroleum ether[d]	Yellow	65	-	41.05 (41.72)	5.18 (5.21)	9.10 (9.13)	25.69 (25.79)
9	10[c]	Petroleum ether[d]	Yellow	48	169-171	47.90 (47.98)	3.18 (3.20)	8.38 (8.39)	23.61 (23.73)
10	12[c]	Petroleum ether[d]	Reddish brown	49	165-167	42.81 (42.89)	3.84 (3.82)	10.70 (10.72)	30.27 (30.30)
11	12[c]	Petroleum ether[d]	Reddish brown	56	-	50.43 (50.45)	5.65 (5.67)	8.82 (8.83)	24.90 (24.95)
12	12[c]	Petroleum ether[d]	Reddish brown	42	194-195	55.85 (55.84)	3.67 (3.68)	8.09 (8.14)	23.02 (23.01)

[a]Sticky liquid.

[b] Method: reflux in methanol ; [c] Method: reflux in benzene.

[d] Petroleum ether (b.p. 60-80 °C).

4.4.3 Spectroscopic characterization and X-ray crystallography of diorganotin(IV) complexes

4.4.3.1 Spectroscopic characterization and X-ray structure determination of diorganotin(IV) complexes, R_2SnL ($L=L^1$ to L^4; R=Me, n-Bu, Ph)

The complexes were characterized by UV, IR, NMR (^1H, ^{13}C and ^{119} Sn) and elemental analyses. In general, the X-ray crystallographic data of the complexes supports the observed spectral data. Fluoresence spectra of some complexes of distinctly different types to study the fluorescence properties of these newly synthesised compounds were also recorded.

4.4.3.1.1 IR Spectra

Selected IR bands and their assignments for the diorganotin complexes have been presented in Table 4.8. The infrared spectral data together with the stoichiometric composition of these organotin(IV) complexes suggested that the salicylaldehyde thiosemicarbazones and the naphthaldehyde thiosemicarbazone act as dinegative O,N,S tridentate ligands, with the central tin (IV) coordinated to the deprotonated phenolic 'O', azomethine 'N' and the deprotonated thiocarbonyl/thiol 'S' atom. This mode of chelation was confirmed by X-ray crystallographic structure of the organotin(IV) complexes of salicylaldehyde thiosemicarbazones in this study. The $\nu(NH_2)$, $\nu(C{=}N{-}N{=}C)$ and $\nu(Sn{-}C)$ bands were identified based on literatures values [170,171]. The $\nu(NH_2)_{asym}$ and $\nu(NH_2)_{sym}$ stretching vibrations of the ligands appear in the range 3234-3442 cm^{-1}. These bands did not shift significantly upon complex formation in the diphenyltin derivatives of the ligands indicating that the amino nitrogen atom is not involved in coordination with tin. In the dimethyltin and dibutyltin derivatives of these ligands, the $\nu(NH_2)_{asym}$ and $\nu(NH_2)_{sym}$ stretching vibrations are shifted to smaller wave numbers than in the free ligand spectrum. These shifts are probably due to the hydrogen bond in which the NH_2 group is involved being stronger than in the phenyl derivatives [13,103].The $\nu(C{=}S)$ vibration in free salicylaldehyde thiosemicarbazones and naphthaldehyde thiosemicarbazone occurring

around 777 cm^{-1} was shifted towards lower frequency to 740 ±10 cm^{-1} in complexes suggesting coordination of thiocarbonyl 'S' to the metal ion. The spectra showed medium to strong absorptions within the range of 1600-1651 cm^{-1} due to ν(C=N–N=C) [171]. The $\nu(Sn–C)_{asym}$ and $\nu(Sn–C)_{sym}$ bands appear at 520-540 cm^{-1} and 460-480 cm^{-1} respectively. In the spectrum of **4**, a broad band in the range 3290-3410 cm^{-1} was observed which indicated the presence of both OH stretching vibrations and the NH_2 stretching vibrations, consistent with **4** crystallizing as a hydrate [13]. The new bands which appeared at 340-350 cm^{-1} have been assigned to ν(Sn-S) stretching bands.

Table 4.8 IR spectral data (cm^{-1}) for **1-12**[a]

Complex	$\nu(NH_2)_{asym}$	$\nu(NH_2)_{sym}$	ν(C=N-N=C)	ν(Sn-C)	ν(Sn-S)
1	3300(w)	3124(w)	1651(s)	536(m),478(w)	340(m)
2	3307(w)	3151(w)	1645(m)	532(w), 461(s)	342(m)
3	3446(w)	3340(w)	1604(m)	530(w),475(w)	342(m)
4	3290-3410(b,w)	-	1633(m)	521(w),475(w)	347(m)
5	3302(w)	3158(m)	1620(m)	525(w).470(w)	345(m)
6	3452(w)	3292(w)	1622(m)	535(w),480(w)	342(m)
7	3433(m)	3280(w)	1606(m)	520(w),475(w)	338(m)
8	3300(s)	3168(s)	1600(s)	538(w),480(w)	350(m)
9	3452(w)	3292(w)	1624(m)	540(w),485(w)	345(m)
10	3374(w)	3200(w)	1634(s)	535(m),474(m)	341(m)
11	3380(w)	3290(w)	1600(s)	539(w),480(m)	349(m)
12	3443(w)	3238(m)	1609(s)	541(w),486(w)	346(m)

[a] s, strong; m, medium; w, weak; b, broad.

4.4.3.1.2 NMR Spectra

The ^1H NMR data for the diorganotin(IV) complexes of salicylaldehyde thiosemicarbazones are presented in Table 4.9 while the ^1H NMR data for the

diorganotin(IV) complexes of naphthaldehyde thiosemicarbazones are presented in Table 4.10 respectively. The observed resonances were assigned on the basis of their integration and multiplicity patterns. The ligand and tin-bound organic group protons gave signals in the expected ranges [103,172,173].

The spectrum of the diphenyltin compounds **3, 6** and **9** show complex patterns for the aromatic protons (both ligand and Sn-Ph). In compound **3,** the C–H and aromatic protons appeared as complex multiplets in the range 8.40-6.50 ppm. In **3**, the C–H proton of CH=N has been identified at 8.24 ppm. Spin-spin coupling between the tin nucleus and the azomethine-proton, ^{3}J (SnN=CH), were detected in all spectra thereby confirming the presence of nitrogen-tin coordination. In addition, the values of the coupling constants for ^{3}J(SnN=CH), i.e. 33-45 Hz, ^{2}J($SnCH_3$), i.e. 69-74 Hz, are within the ranges reported for penta-coordinated organotin(IV) complexes with ONO and ONS tridentate Schiff bases [174].

Solution ^{13}C NMR data of the diorganotin(IV) complexes of salicylaldehyde thiosemicarbazones are presented in Table 4.11 while the ^{13}C NMR data for the diorganotin(IV) complexes of naphthaldehyde thiosemicarbazone presented in Table 4.12 respectively. The number of ^{13}C signals found corresponded with the number of magnetically non-equivalent carbon atoms in the complexes. Contrary to the literature [103,161] the author was inclined to propose C-2 signal (attached to a phenyl group and a =N-N= moiety) to be the most deshielded carbon atom followed by C-1 (attached to two N atoms and a –S-Sn moiety) and then the C-4 carbon of the phenyl ring of the ligand. In author's opinion, the satellites attached here with the C-4 carbon atom should be associated with $^{2}J(^{119}Sn–O-^{13}C)$ [175] rather than the $^{2}J(^{119}Sn –N-^{13}C)$ as proposed by Casas and his coworkers [103].The dimethyltin complexes **1, 4, 7, 10** exhibited $^{1}J(^{119}Sn-^{13}C)$ coupling values in the range 592-596 Hz. The $^{1}J(^{119}Sn-^{13}C)$ coupling values in all the complexes were indicative of penta-coordination around the tin atom [176] and were in accordance with the X-ray crystal structures [13] and previous literature reports [103,161]. The di-*n*-butyltin(IV) complexes exhibited $^{1}J(^{119}Sn-^{13}C)$ coupling values in the range 557-564 Hz.

Table 4.9 ^{1}H NMR chemical shifts (ppm) and coupling data (Hz) for **1-9**[a]

	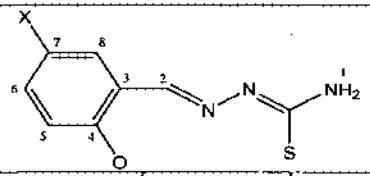						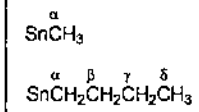		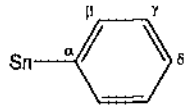	
	H-1	**H-2**	**H-5**	**H-6**	**H-7**	**H-8**	**H-α**	**H-β**	**H-γ**	**H-δ**
1	5.10 (s, 2H)	8.49 (s, 1H) [40][c]	6.78-6.76 (d, 1H)	7.29 (m, 1H)	6.72 (t, 1H)	7.12-7.09 (d, 1H)	0.87 (s, 6H) [72][d]	-	-	-
2	4.97 (s, 2H)	8.48 (s, 1H) [37.5][c]	6.78-6.75 (d, 1H)	7.29 (m, 1H)	6.69 (t, 1H)	7.10-7.08 (d, 1H)	1.82-1.61 (m, 4H)	1.55-1.42 (m, 4H)	1.34 (m, 4H)	0.87 (t, 6H)
3	4.47 (s, 2H)	8.24 (s, 1H)	6.63-6.61 (d, 1H)	7.23 (m, 1H)	6.52 (m, 1H)	7.28 (d, 1H)	-	8.27 (m, 4H)	7.23 (m, 4H)	7.23 (m, 2H)
4	5.02 (s, 2H)	8.40 (s, 1H) [39][c]	6.68-6.65 (d, 1H)	7.35-7.31 (d, 1H)	-	7.21-7.20 (s, 1H)	0.87 (s, 6H) [73/70][d]	-	-	-
5	5.18 (s, 2H)	8.37 (s, 1H) [39][c]	6.67-6.64 (d, 1H)	7.30 (d, 1H)	-	7.18-7.17 (s, 1H)	1.69-1.57 (m, 4H)	1.55-1.49 (m, 4H)	1.42-1.25 (m, 4H)	0.87 (t, 6H)
6	4.33 (s, 2H)	7.96 (s, 1H) [n.d.][b]	6.66-6.65 (d, 1H)	6.83-6.80 (d, 1H)	-	7.31-7.17 (s, 1H)	-	8.33-8.03 (m, 4H)	7.31-7.17 (m, 4H)	7.31-7.17 (m, 2H)
7	5.14 (s, 2H)	8.39 (s, 1H) [38][c]	6.72-6.70 (d, 1H)	7.26-7.19 (d, 1H)	-	7.07-7.06 (s, 1H)	0.87 (s, 6H) [74/71][d]	-	-	-
8	5.00 (s, 2H)	8.39 (s, 1H) [34][c]	6.72-6.69 (d, 1H)	7.22-7.18 (d, 1H)	-	7.05-7.04 (s, 1H)	1.69-1.59 (m, 4H)	1.55-1.44 (m, 4H)	1.42-1.26 (m, 4H)	0.87 (t, 6H)
9	5.10 (s, 2H)	8.41 (s, 1H) [44][c]	7.05-6.97 (d, 1H)	7.05-6.97 (d, 1H)	-	7.44-7.24 (s, 1H)	-	8.01-7.65 (m, 4H)	7.44-7.24 (m, 4H)	7.44-7.24 (m, 2H)

[a] Spectra recorded in $CDCl_3$ except for compounds **3** and **6** which were measured in C_6D_6, downfield to TMS; Multiplicity is given as s, singlet;d, doublet; t, triplet; m, multiplet; [b] n.d. = not detected; [c] $^{3}J(^{119}Sn - H)$ Hz; [d] $^{2}J(^{119/117}Sn - CH_3)$ Hz.

Table 4.10 ^{1}H NMR chemical shifts (ppm) and coupling data (Hz) for **10-12**[a]

	10	11	12
H-1	5.03(s, 2H)	5.07	5.02(s, 2H)
H-2	9.35(s, 1H) [42][d]	9.38(s, 1H) [44][d]	9.41(s, 1H) [48][d]
H-5	6.96-6.93(d,1H)	6.96-6.94(d, 1H)	7.28-7.20(m,1H)
H-7	7.31-7.25(m,1H)	7.28-7.21(m,1H)	7.28-7.20(m,1H)
H-8,9	7.75-7.67(m,2H)	7.73-7.65(m,2H)	7.80-7.65(m,2H)
H-10	7.50-7.44(m, 1H)	7.50-7.42(m, 1H)	7.45-7.35(m,1H)
H-12	7.91-7.88(d, 1H)	7.89-7.86(d,1H)	7.88-7.85(d,1H)
H-α	0.89(s,6H) [73.5/70.5]	1.80-1.62(m, 4H)	-
H-β	-	1.55-1.46(m, 4H)	7.94-7.91(m,4H)
H-γ	-	1.42-1.32(m,4H)	7.45-7.35(m,4H)
H-δ	-	0.89(t, 6H)	7.45-7.35(m,2H)

[a] Spectra recorded in $CDCl_3$, downfield to TMS; Multiplicity is given as s, singlet; d, doublet; m, multiplet, t; triplet.

[b] Refer to the Fig. shown below for the numbering scheme in the ligand

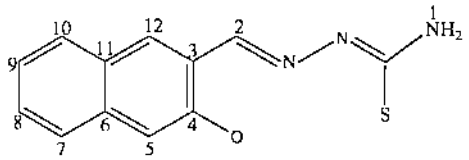

[c] Refer to Table 4.9 for numbering scheme in the Sn-R skeleton

[d] $^{3}J(^{119}\text{Sn-H})$ Hz ; [e] $^{2}J(^{119/117}\text{Sn-CH}_3)$ Hz.

Table 4.11 ^{13}C NMR chemical shifts (ppm) and coupling data (Hz) for **1-9**[a]

	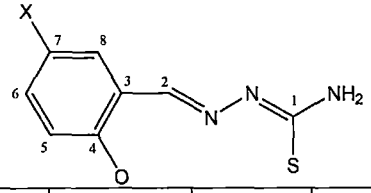								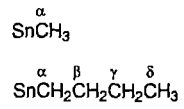		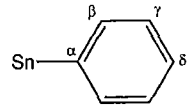	
	C-1	**C-2**	**C-3**	**C-4**	**C-5**	**C-6**	**C-7**	**C-8**	**C-α**	**C-β**	**C-γ**	**C-δ**
1	165.85	167.94	121.39	160.62 [20.17][g]	116.77	133.55	117.16	134.6	5.94 [595.90][b]	-	-	-
2	166.62	168.18	121.41	160.86 [16.80][g]	116.69	133.61	116.77	133.66	25.86 [562.50][b]	27.41 [30.80][c]	26.46 [90.0][d]	13.58
3	166.21	166.72	121.70	161.03 [20.4][g]	116.83	133.83	117.43	134.97	142.49 [865.3]	135.78 [56.32]	128.65 [82.35][d]	129.98 [16.72][e]
4	164.98	168.45	123.47	159.21 [20.12][g]	108.19	134.88	118.39	137.07	5.98 [593.10][b]	-	-	-
5	165.28	168.79	123.19	158.83 [16.82][g]	107.69	134.74	118.37	136.82	25.84 [557.60][b]	27.30 [30.75][c]	26.35 [64.50][d]	13.53
6	165.48	166.81	123.61	159.26 [18.6][g]	108.41	135.04	118.36	136.09	142.08 [843.75][b]	135.71 [57][c]	128.74 [82.5][d]	130.1 [16.87][e]
7	164.33	168.50	122.93	159.01 [20.25][g]	117.55	131.73	121.39	134.25	5.98 [592.90][b]	-	-	-
8	164.91	168.79	122.39	158.93 [16.88][g]	117.60	131.67	120.93	134.15	25.82 [558.1][b]	27.31 [30.63][c]	26.37 [81.0][d]	13.5
9	165.13	166.83	123.23	159.52 [20.25][g]	117.62	131.99	121.08	134.59	142.14 [807.69][b]	135.73 [56.4][c]	128.75 [82.65][d]	130.14 [16.57][e]

[a] Spectra recorded in $CDCl_3$ solution, downfield to TMS; [b] $^1J(^{119}Sn - ^{13}C)$ in Hz; [c] $^2J(^{119}Sn - ^{13}C)$ in Hz; [d] $^3J(^{119}Sn - ^{13}C)$ in Hz; [e] $^4J(^{119}Sn - ^{13}C)$ in Hz; [g] $^2J(^{119}Sn\text{-}O\text{-}^{13}C)$ in Hz.

Table 4.12 ^{13}C NMR chemical shifts (ppm) and coupling data (Hz) for **10-12**[a]

	10	**11**	**12**
C-1	166.63	166.61	164.77
C-2	168.02	168.10	168.88
C-3	123.07	123.12	123.18
C-4	156.62	156.84	156.92
C-5	107.35	107.30	107.54
C-6	133.47	133.35	133.52
C-7	124.03	124.09	124.14
C-8	127.94	127.09	128.03
C-9	127.25	127.31	127.39
C-10	129.08	129.10	129.15
C-11	119.36	119.32	119.28
C-12	136.17	136.25	136.68
C-α	5.35 [593.75][d]	25.83 [563]	141.96 [865.38][d]
C-β	-	27.42 [31]	135.85 [56.25][e]
C-γ	-	26.46 [89]	128.74 [81.75][f]
C-δ	-	13.54	130.08 [16.5][g]

[a] Spectra recorded in $CDCl_3$ solution, downfield to TMS.

[b] Refer to the Fig. shown below for the numbering scheme in the ligand

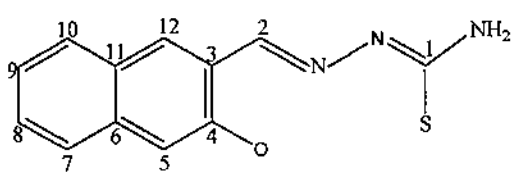

[c] Refer to Table 4.11 for numbering scheme in the Sn-R skeleton.
[d] $^1J(^{119}Sn - ^{13}C)$ in Hz.
[e] $^2J(^{119}Sn - ^{13}C)$ in Hz.
[f] $^3J(^{119}Sn - ^{13}C)$ in Hz.
[g] $^4J(^{119}Sn - ^{13}C)$ in Hz.

Important information relating to the structure of coordination polyhedron of dimethyltin and di-*n*-butyltin(IV) complexes are obtained from the values of coupling

constants $^{1}J(^{119}Sn-^{13}C)$ because they are directly linked to the size of the C-Sn-C angle (θ) according to the literature reports [177,178]. For **1**, using Lockhart-Manders' equation [177] a C-Sn-C angle of 129.02° was calculated (Table 4.13) which is in reasonable agreement with the angle observed in the solid state by X-ray study.

Table 4.13 C-Sn-C angles (°) calculated from NMR parameters

Complex	$^{1}J(^{119}Sn-^{13}C)$	C-Sn-C angles (°)
1	595.9	129.02
2	562.5	131.38
4	593.1	128.78
5	557.6	130.93
7	592.9	128.76
8	558.1	130.97
10	593.7	128.83

[a] C-Sn-C angles (°) calculated from $^{1}J(^{119}Sn-^{13}C)$.

The ^{119}Sn NMR data of **1-9** were recorded in $CDCl_3$ solution (Table 4.14). All of the spectrum displayed a sharp singlet. The number of signals observed and the value of chemical shifts $\delta(^{119}Sn)$ confirm the chemical composition of the investigated complexes. The observed ^{119}Sn shifts are indicative of penta-coordination [103, 176-178] around the tin atom in these complexes. A five-coordinated di-*n*-butyltin(IV) compound according to previous reports [178-180] can be characterized by chemical shifts $\delta(^{119}Sn)$ between -90 to -190 ppm .The chemical shift $\delta(^{119}Sn)$ values of -120.2 ppm and -116.4 ppm for **2** and **5** respectively are thus, indicative of five-coordinated di-*n*-butyltin(IV) compounds. In the diphenyltin derivatives (**3**, **6** and **9**), the ^{119}Sn signal lies as usual [181] at lower frequencies than the respective dimethyltin derivatives.

Table 4.14 ^{119}Sn NMR chemical shifts (ppm) for **1-9**[a]

Complex	^{119}Sn
1	–102.5
2	-120.2
3	–232.4
4	–98.0
5	-116.4
6	–229.4
7	-98.1
8	n.m.[b]
9	–229.3

[a] Spectra recorded in $CDCl_3$ solution.

[b] n.m. = not measured.

4.4.3.1.3 Electronic Spectra

Visible spectra of selected compounds are recorded in Table 4.15. As expected in the visible region the electronic spectra showed one broad absorption of medium intensity.

4.4.3.1.4 Study of Fluorescence properties

Fluorescent spectra of selected compounds are recorded in Table 4.16. The yellow colour is due to the n-π* transition of the thiosemicarbazide chromophore. Interestingly, the compounds are fluorescent under ordinary conditions of visible light. At this time it is difficult to conclusively indicate what the origin of this property is. However, in future, detailed studies would be undertaken.

Table 4.15 Electronic absorption spectra of organotin(IV) compounds recorded in methanol solution

Complex	λ_{max} (nm)
1	392
2	393
3	390
4	405
5	407
6	403
7	397
9	398
10	409
11	410
12	412

Table 4.16 Fluorescence data of selected compounds recorded in methanol solution

	Excitation (nm)	Emission (nm)
1	451.4	489.5
2	357.0, 451.4	491.3
3	308.0, 357.0, 445.9	487.7
4	373.3, 455.0	494.7
6	318.2, 366.1, 455.0	498.6
7	373.2, 459.6	490.3
9	311.6, 366.1, 453.2	493.1

4.4.3.1.5 X-ray Crystal Structures

This section deals with the X-ray crystallographic studies of diorganotin(IV) complexes of the type R_2SnL (R=Me and Ph) where L is the dianion derived from salicylaldehyde/ substituted salicylaldehyde thiosemicarbazones (L^1HH'-L^3HH'). In the present study efforts were undertaken to obtain single crystals for the X-ray analysis of the diorganotin derivatives of the ligands described above in Scheme 4.3. Compounds **1**, **3**, **4**, **6** and **9** provided single crystals suitable for the X-ray crystal structure determination .The crystal structures of all these complexes are described below.

It should be noted that during the progress of this work the author became aware of a few reports of closely related studies [102,103,161] where some organotin(IV) complexes of semi- and thiosemicarbazones, along with the compounds **1-3** (Scheme 4.3), were described as well as their molecular structures [102,103]. The author has included her data on the same compounds herein to allow comparison of their biocidal properties with the corresponding Cl/Br-substituted ligands. Further, those compounds were synthesized via a different route as reported here, requiring shorter reaction times and giving higher yields. In addition, full details of their supramolecular structures (which were not reported earlier in [102,103]) are reported as well as a correlation of geometric parameters with those of halide congeners.

4.4.3.1.5.1 Crystal structure of [Me_2SnL^1] (1)

The author could successfully isolate X-ray quality single crystal of **1** from the benzene solution of the compound. The molecular structure of **1** along with the crystallographic numbering scheme is given in Fig. 4.24. The crystal data and structural refinement parameters are presented in section 4.3 (Table 4.1).The selected bond lengths and bond angles are given in Table 4.17. The compound **1** crystallizes into a monoclinic lattice with $P2_1/n$ space group. The structure of **1** features a five-coordinate tin atom coordinated by the S1, O1 and N3 atoms of the tridentate ligand as well as two methyl groups.

The overall coordination geometry is based on a trigonal bipyramid with the S1 and O1 defining the axial positions. Distortions from the ideal geometry may be traced to the restraints imposed by the chelate rings. An examination of the geometric parameters indicates that the structure conforms to the generic structure shown in Scheme 4.3, with no evidence of tautomerism. The molecular geometries of the remaining structures of **3**, **4**, **6** and **9** are in essential agreement with that just described and are in agreement with previous literature reports of **1** and **3** [103], but have been determined to a higher level of precision.

Table 4.17 Selected bond distances (Å) and angles (°) for $[Me_2SnL^1]$ **(1)**

	1
Sn–S1	2.540(1)
Sn–O1	2.105(2)
Sn–N3	2.196(2)
C1–S1	1.729(2)
C1–N1	1.334(3)
C1–N2	1.315(3)
N2–N3	1.388(3)
S1–Sn–O1	158.44(5)
S1–Sn–N3	77.01(5)
O1–Sn–N3	81.74(7)
C9–Sn–C10	127.3(1)
C9–Sn–C15	-

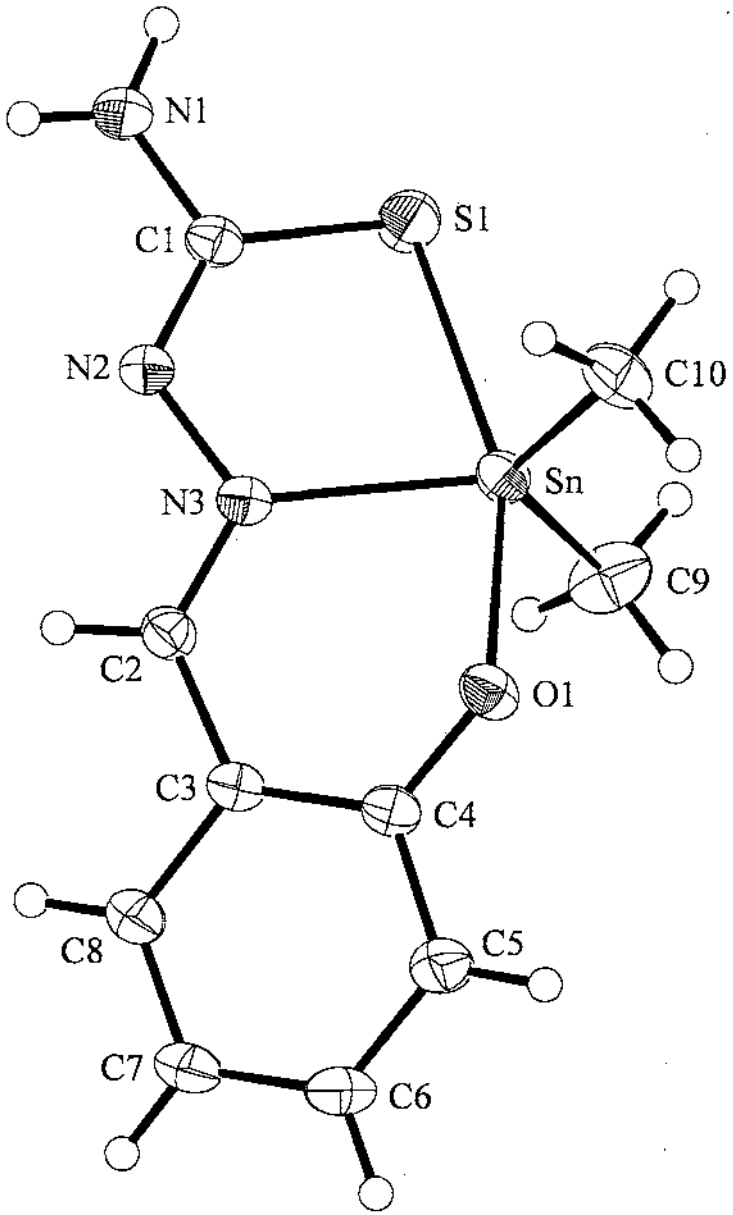

Fig.4.24 Molecular structure and crystallographic numbering scheme for $[Me_2SnL^1]$ (**1**).

In the crystal structure of $[Me_2SnL^1]$ (**1**), N–H...O hydrogen bonding interactions lead to a chain along the *b*-axis and these were connected to neighbouring chains by N–H...N hydrogen bonds via eight-membered $\{N–C–N–H\}_2$ synthons to form a 2D array that had a zig-zag topology as highlighted in Fig. 4.25. The geometric parameters defining these interactions and those found in the remaining structures are listed in Table 4.22.

(a)

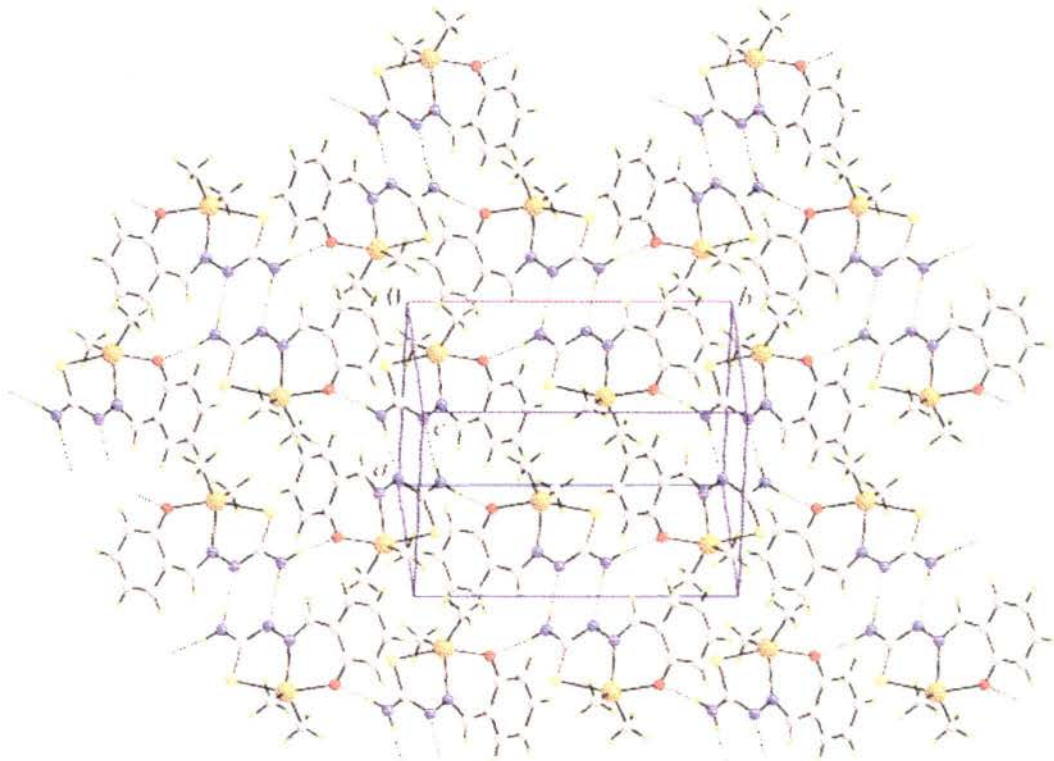

(a)

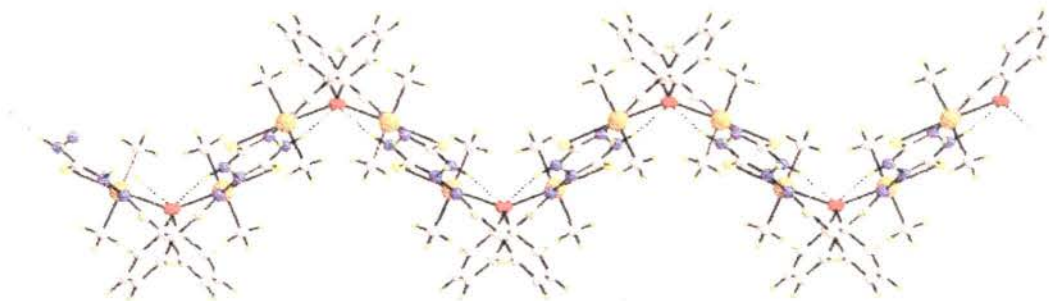

(b)

Fig. 4.25 Crystal packing in $[Me_2SnL^1]$ (**1**): (a) unit cell contents showing hydrogen bonding as dashed lines and (b) the zig- zag topology for the two-dimensional array.

4.4.3.1.5.2 Crystal structure of [Ph_2SnL^1] (3)

The author could successfully isolate X-ray quality single crystal of **3** from the petroleum ether (b.p. 60-80 °C) solution of the compound. The compound **3** crystallizes into a monoclinic lattice with $P2_1/c$ space group. The molecular structure of **3** along with the crystallographic numbering scheme is given in Fig. 4.26. The crystal data and structural refinement parameters are presented in section 4.3 (Table 4.2).The selected bond lengths and bond angles are given in Table 4.18.

The structure of **3** also features a five-coordinate tin atom surrounded by S1, O1 and N3 atoms of the tridentate ligand as well as two phenyl groups. As stated above, the molecular geometry of **3** is in essential agreement with previous literature report of the molecular structure of **3** [103], but has been determined to a higher degree of precision.

Table 4.18 Selected bond distances (Å) and angles (°) for [Ph_2SnL^1] **(3)**

	3
Sn–S1	2.546(1)
Sn–O1	2.067(2)
Sn–N3	2.191(2)
C1–S1	1.738(3)
C1–N1	1.349(3)
C1–N2	1.298(3)
N2–N3	1.387(3)
S1–Sn–O1	161.31(6)
S1–Sn–N3	77.94(5)
O1–Sn–N3	84.22(7)
C9–Sn–C10	-
C9–Sn–C15	127.24(9)

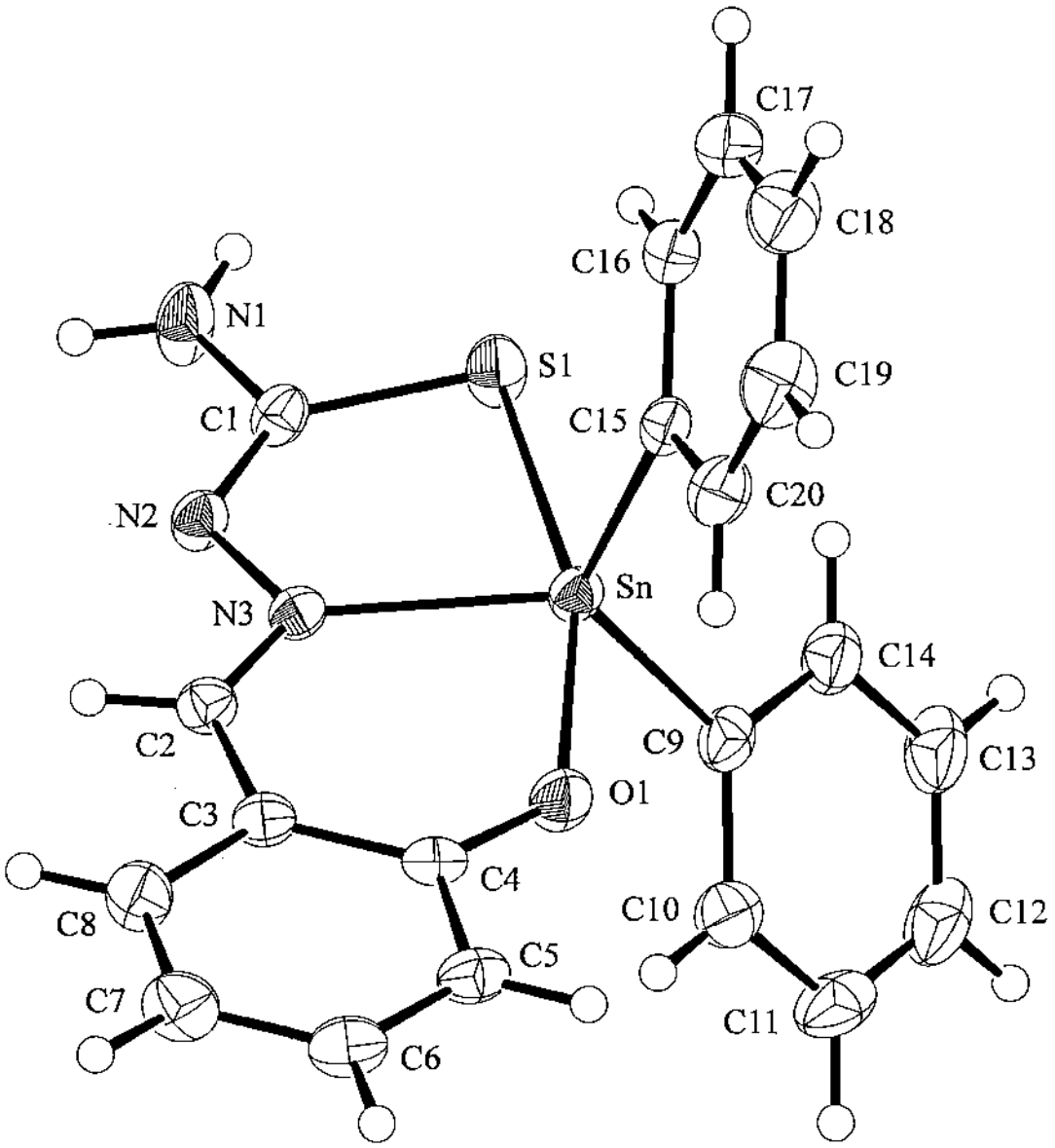

Fig. 4.26 Molecular structure and crystallographic numbering scheme for $[Ph_2SnL^1]$ (**3**).

The presence of tin-bound phenyl rings in $[Ph_2SnL^1]$ (**3**) had a profound influence upon the supramolecular aggregation pattern as the oxygen atom now formed an intramolecular C–H...O interaction that precluded its further association in the crystal structure. The global crystal packing may be described as being comprised of double layers of molecules that are connected via $\{S–C–N–H\}_2$ synthons as shown in

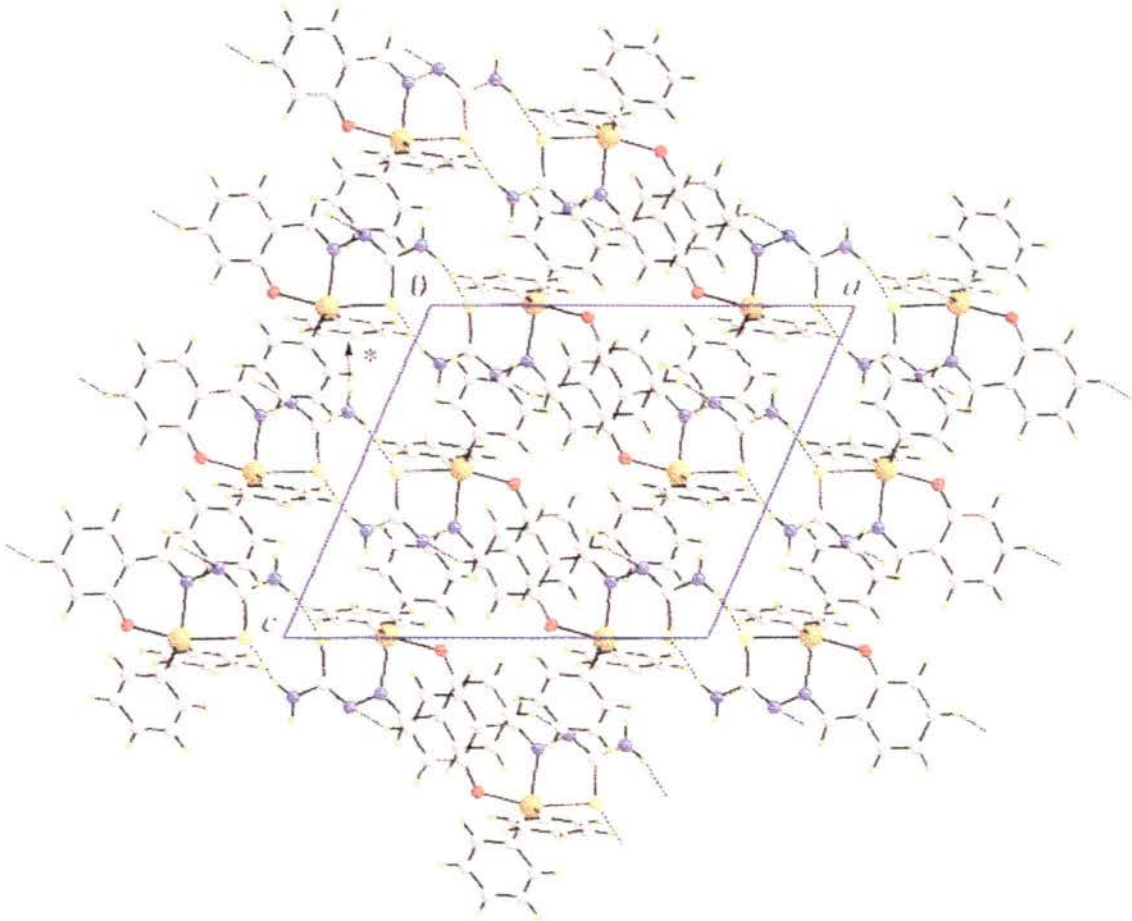

Fig. 4.27 View of the unit cell content of $[Ph_2SnL^1]$ (**3**) along the *b*-axis.

Fig. 4.27. The remaining N–H atom participates in N–H...π interactions with tin-bound phenyl groups: an example is marked with an asterisk in Figure 4.27. Finally, the imine-N2 atom participates in a C–H...N interaction and thereby contributes to the stability of the aforementioned double layer.

4.4.3.1.5.3 Crystal structure of $[Me_2SnL^2].H_2O$ (4)

Single crystals suitable for X-ray diffraction of the compound $[Me_2SnL^2].H_2O$ were grown by slow evaporation of the petroleum ether (b.p. 60-80 °C) solution of the compound. The structure of the molecule with atom numbering scheme is given in Fig. 4.28. The structural refinement parameters are described in section 4.3 and the selected bond distances and bond angles are given in Table 4.19. The compound **4** crystallizes into a monoclinic lattice with *C*2/c space group. The structure of $[Me_2SnL^2]$ (**4**) was isolated as a monohydrate and the water molecule plays a pivotal role in the crystal packing.

Table 4.19 Selected bond distances (Å) and angles (°) for $[Me_2SnL^2].H_2O$ (**4**)

	4
Sn–S1	2.510(1)
Sn–O1	2.103(2)
Sn–N3	2.250(3)
C1–S1	1.731(4)
C1–N1	1.339(4)
C1–N2	1.311(4)
N2–N3	1.382(3)
S1–Sn–O1	147.91(7)
S1–Sn–N3	76.92(7)
O1–Sn–N3	80.98(9)
C9–Sn–C10	118.5(2)
C9–Sn–C15	-

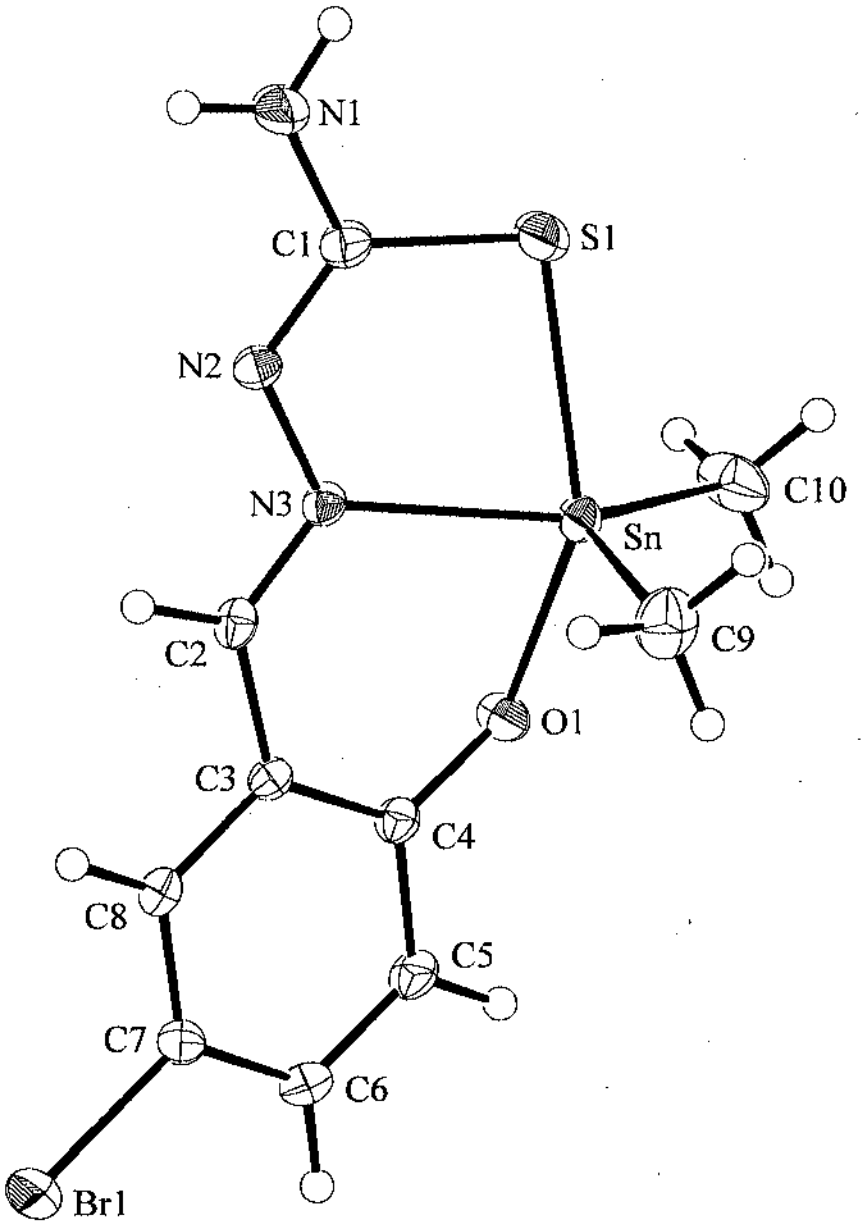

Fig. 4.28 Molecular structure and crystallographic numbering scheme for $[Me_2SnL^2].H_2O$ (**4**). Water molecule of crystallization is omitted.

Centrosymmetric molecules of **4** associate via the eight-membered $\{N–C–N–H\}_2$ synthon seen in compound **1**. These dimers are then linked into chains via a N1–H1b...O2–H1w...O1 sequence of hydrogen bonds and these chains are finally linked via weaker O–H...O hydrogen bonds involving the water molecules exclusively. As seen from the view in Figure 4.29, this arrangement resulted in the formation of narrow channels aligned along the *c*-axis.

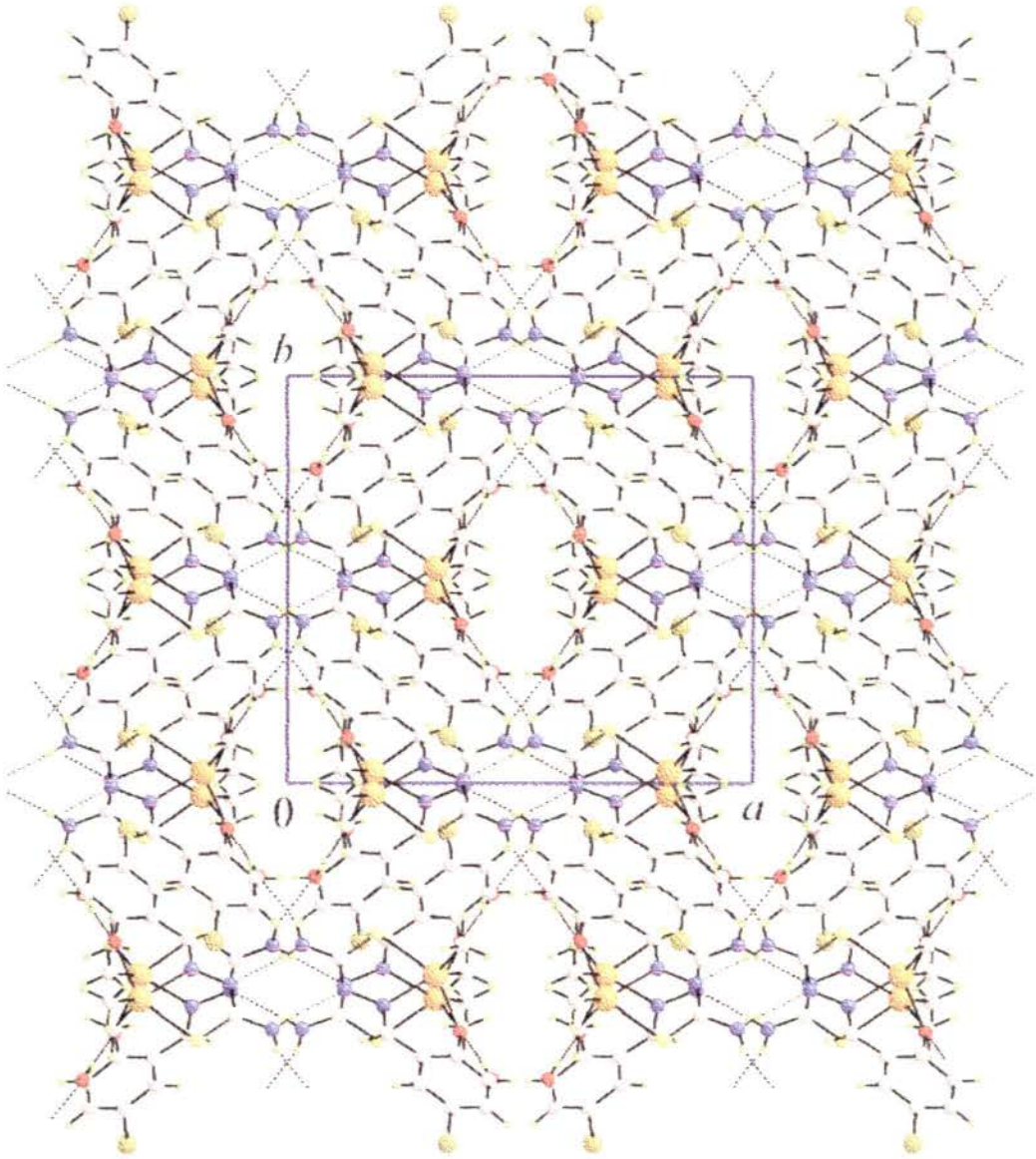

Fig. 4.29 View of the unit cell content of $[Me_2SnL^2].H_2O$ (**4**) along the *c*-axis.

4.4.3.1.5.4 Crystal structure of $[Ph_2SnL^2]$ 6 and $[Ph_2SnL^3]$ 9

Suitable X-ray quality single crystals of diphenyl tin derivatives of 5-bromosalicylaldehyde thiosemicarbazone $[Ph_2SnL^2]$ **6** and 5-chlorosalicylaldehyde thiosemicarbazone $[Ph_2SnL^3]$ **9**, were obtained from petroleum ether (b.p. 60-80 °C) solution of **6** and **9** respectively, by slow evaporation of the solvent at room temperature. The molecular structure of **6** and **9** along with their crystallographic numbering scheme are given in Fig. 4.30 and Fig.4.32 respectively. The crystal data and structural refinement parameters of **6** and **9** are presented in Table 4.4 and 4.5 respectively (section 4.3). The selected bond lengths and bond angles of **6** and **9** are given in Table 4.20 and 4.21 respectively. Both the complexes crystallize into triclinic lattice with *P*-1 space group.

Table 4.20 Selected bond distances (Å) and angles (°) for $[Ph_2SnL^2]$ **(6)**

	6 (a, b)
Sn–S1	2.494(1), 2.510(1)
Sn–O1	2.061(3), 2.071(3)
Sn–N3	2.265(3), 2.250(3)
C1–S1	1.740(4), 1.740(5)
C1–N1	1.350(5), 1.335(6)
C1–N2	1.313(5), 1.320(5)
N2–N3	1.388(5), 1.381(5)
S1–Sn–O1	150.1(1), 155.3(1)
S1–Sn–N3	77.11(9), 77.22(9)
O1–Sn–N3	80.8(1), 81.4(1)
C9–Sn–C10	-

Two independent molecules comprise the crystallographic asymmetric unit of **6** that differ from each other only in terms of minor conformational changes and the way they interact in the crystal structure (see below). The availability of a series of structures allows for the discernment of a number of trends in geometric parameters. From Table 4.20, it is evident that the inclusion of a halide substituent, i.e. chloride or

bromide, at the C7 position results in significant stronger Sn-S bonds with concomitant weakening of the Sn-N3 bonds and greater deviation of the axial angle from 180°. A systematic variation in the Sn-O1 bond is also apparent in that this bond is shorter in the dimethyltin derivatives compared with the diphenyltin species. The presence of hydrogen bond donors and acceptors in each of the structures lead to a variety of supramolecular arrays and these are discussed in turn below.

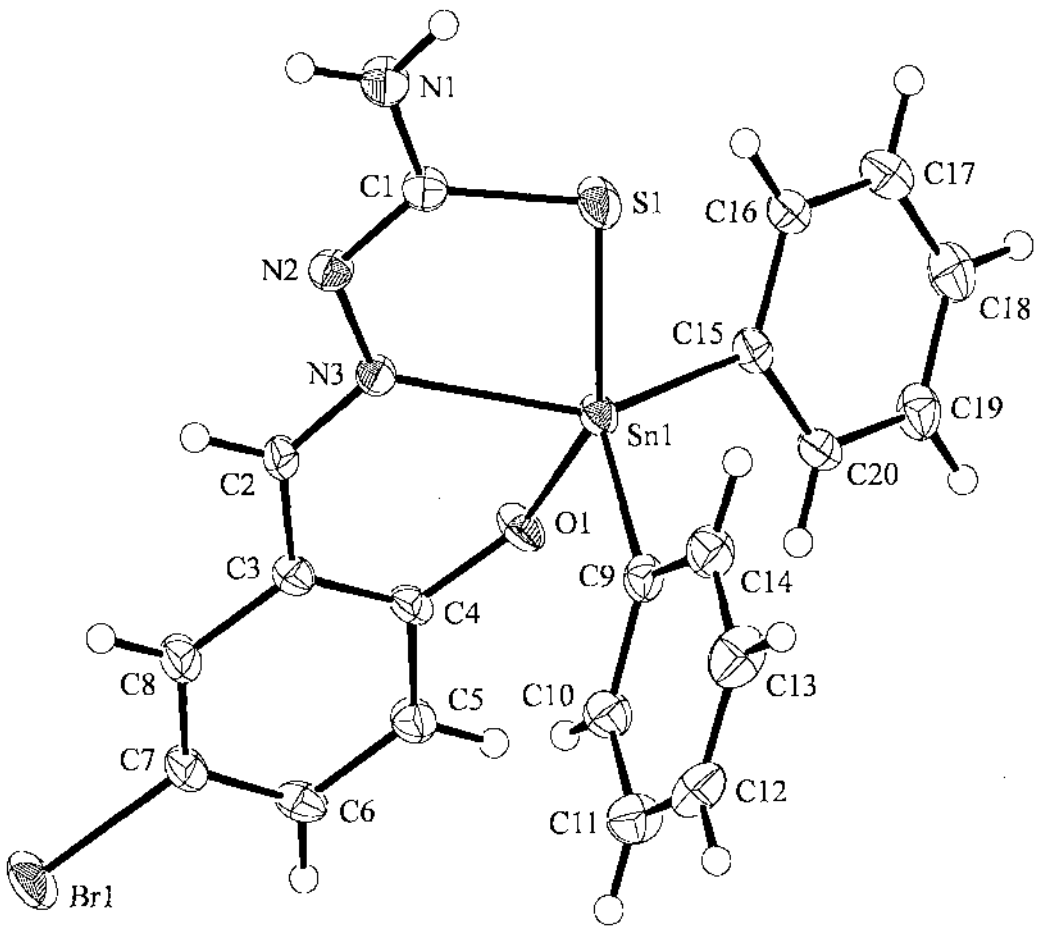

(a)

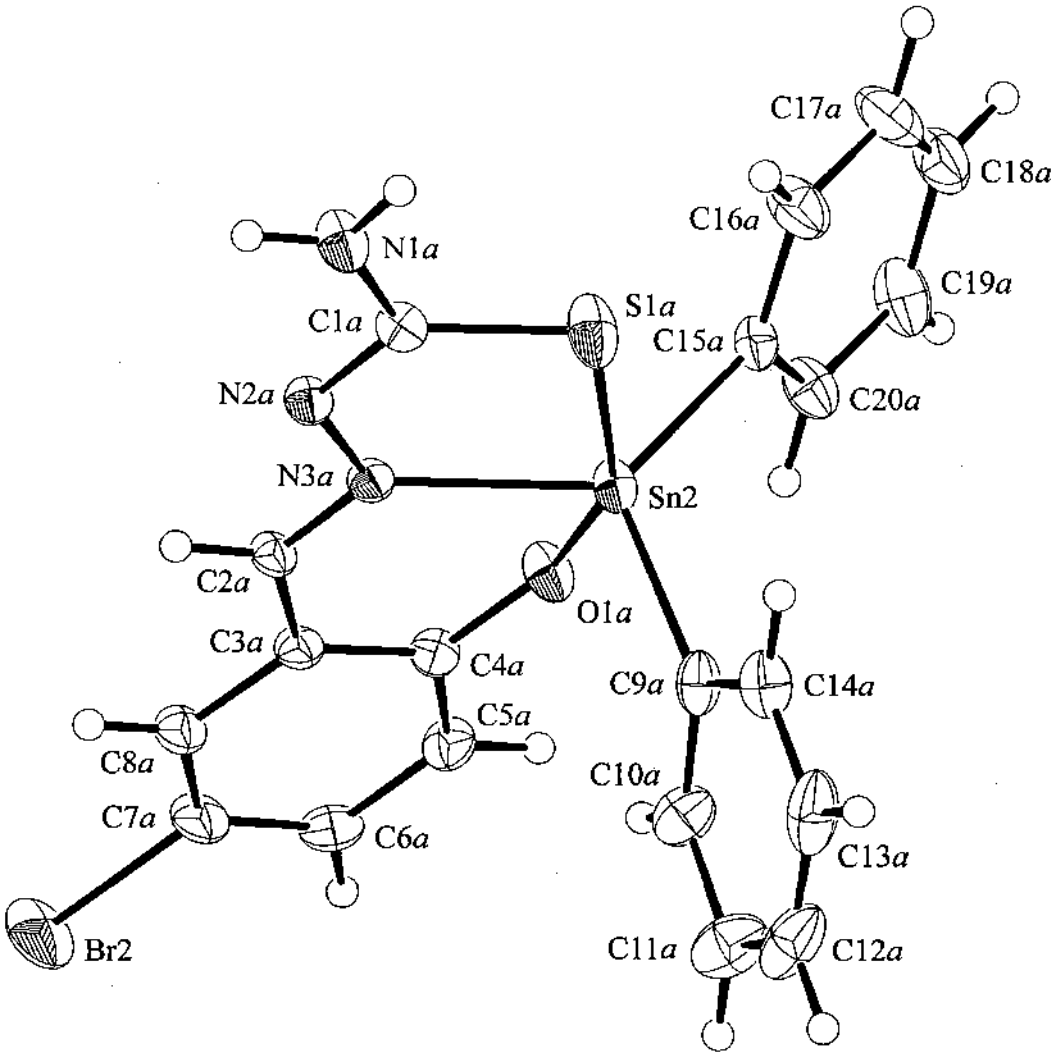

(b)

Fig. 4.30 Molecular structure and crystallographic numbering scheme for the two independent molecules comprising the asymmetric unit of $[Ph_2SnL^2]$ (**6**).

Eight-membered $\{N–C–N–H\}_2$ synthons are the dominant intermolecular interactions found in the crystal structure of $[Ph_2SnL^2]$ (**6**) and these occur between the two independent molecules comprising the asymmetric unit; these interactions are emphasized in Fig. 4.31. Each of the remaining amine-H atoms is involved in an N–H...π interaction but rather than interacting with a ring system, each was orientated towards the C19–C20 bond of the other molecule comprising the dimer. Again, the oxygen atoms are shielded from forming intermolecular interactions owing

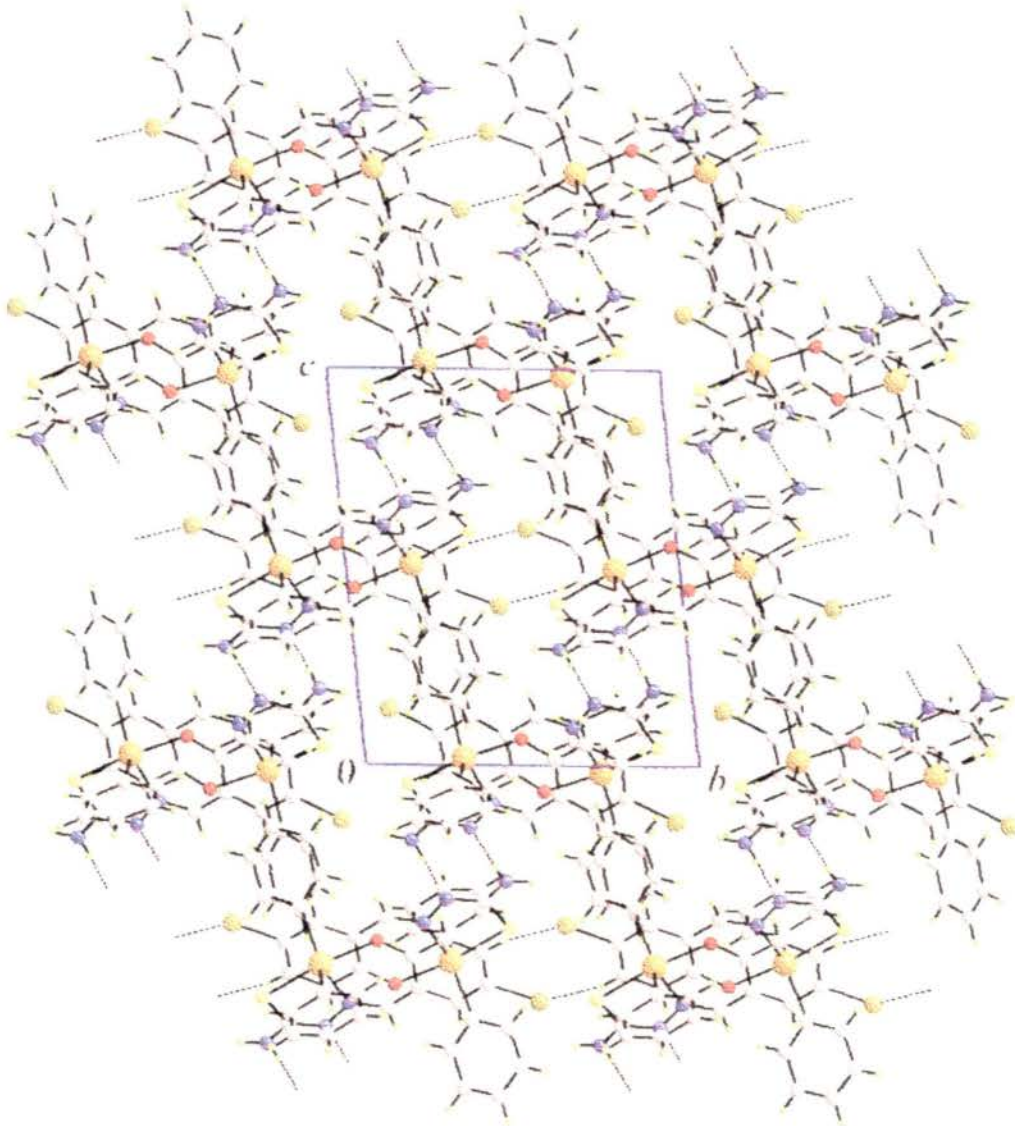

Fig. 4.31 View of the unit cell content of $[Ph_2SnL^2]$ (**6**) down the *a*-axis.

to the presence of intramolecular C–H...O interactions. The remaining interactions of note are of the type C–H...Br, with the closest of these involving each independent bromide atom listed in Table 4.22; those involving the Br2 atom are shown in Fig. 4.31. Finally, C–H...π contacts involving phenyl rings is noted.

Although not isomorphous, the crystal packing found in $[Ph_2SnL^3]$ (**9**) is similar to that just described for **6**. Hence, the $\{N–C–N–H\}_2$ synthon is present and these are connected to neighbouring molecules via N1–H1b...πC19–C20 interactions. In this way, chains are formed which are linked via C–H...Cl interactions. Two rows of chloride atoms align along the *a*-axis and interdigitate with each other, forming two C–H...Cl contacts with molecules of the opposite row and resulting in the formation of a double zig-zag ribbon.

Table 4.21 Selected bond distances (Å) and angles (°) for $[Ph_2SnL^3]$ (**9**)

	170 A
Sn–S1	2.500(1)
Sn–O1	2.065(2)
Sn–N3	2.250(3)
C1–S1	1.732(4)
C1–N1	1.340(4)
C1–N2	1.312(4)
N2–N3	1.394(3)
S1–Sn–O1	152.28(8)
S1–Sn–N3	77.40(7)
O1–Sn–N3	80.92(9)
C9–Sn–C10	-
C9–Sn–C15	118.7(1)

The geometric parameters defining intermolecular interactions operating in the crystal structure of **6** and **9** are presented in Table 4.22.

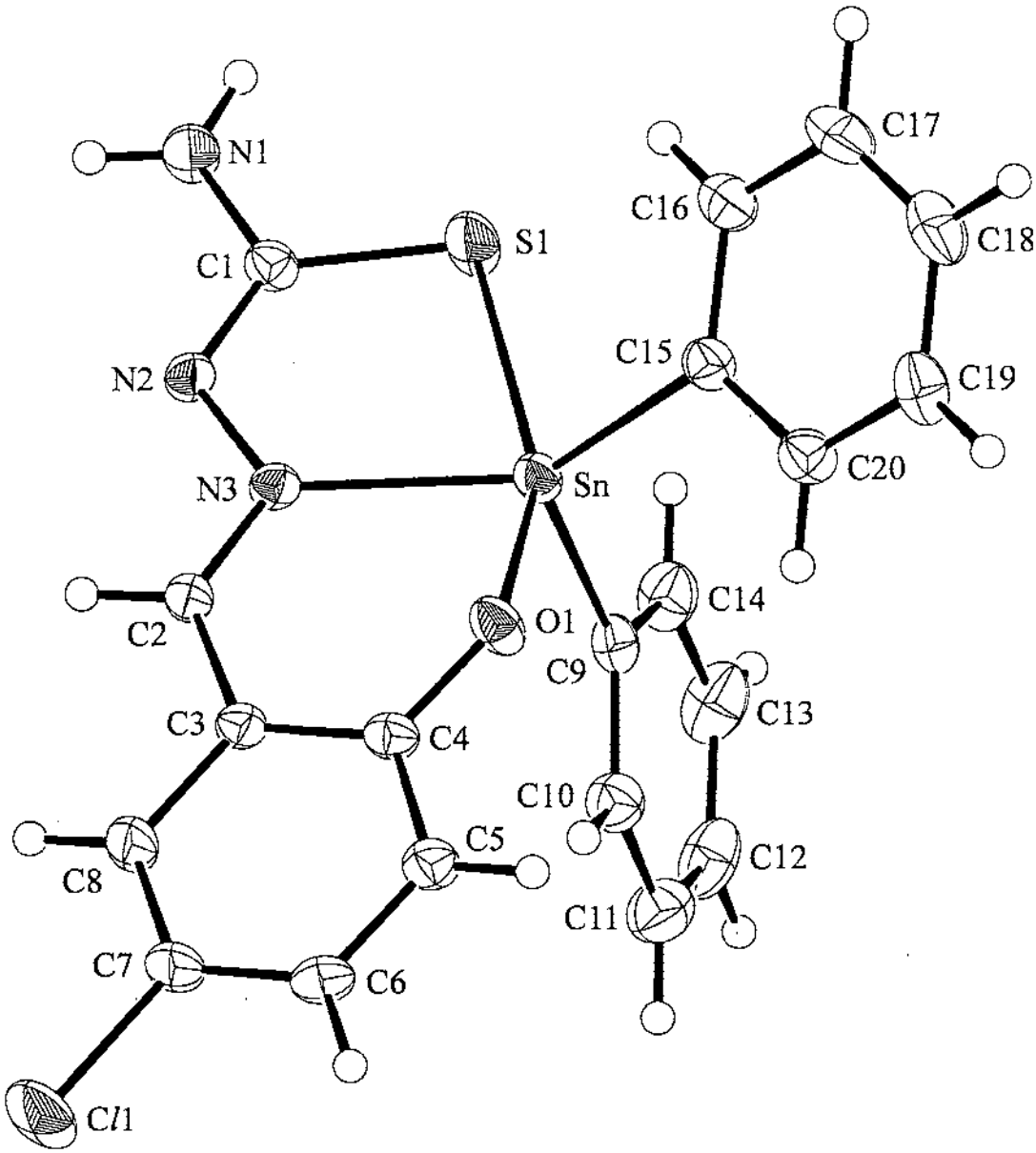

Fig. 4.32 Molecular structure and crystallographic numbering scheme for [Ph_2SnL^3] (**9**).

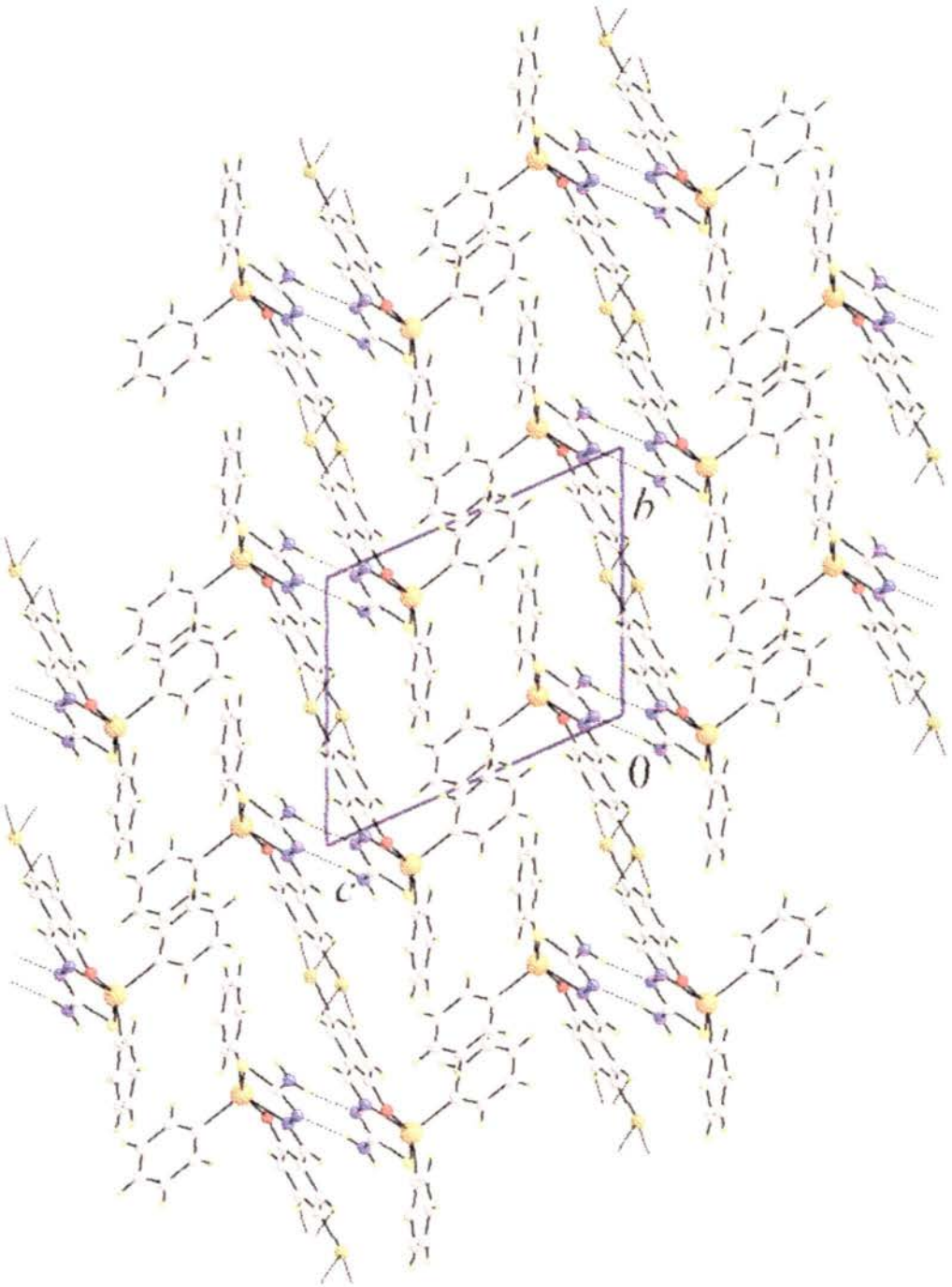

Fig. 4.33 View of the unit cell content of $[Ph_2SnL^3]$ (**9**) down the *a*-axis.

Table 4.22 Summary of intermolecular interactions (A–H...B; Å, °) operating in the crystal structures of $[Me_2SnL^1]$ (**1**), $[Ph_2SnL^1]$ (**3**), $[Me_2SnL^2].H_2O$ (**4**), $[Ph_2SnL^2]$ (**6**) and $[Ph_2SnL^3]$ (**9**)

	A	H	B	H...B	A...B	A–H...B	Symmetry operation
1	N1	H1b	O1	2.03	2.866(3)	162	½–*x*, –½+*y*,
	N1	H1a	N2	2.11	2.982(3)	176	1–*x*, –*y*, 1–*z*
3	N1	H1b	S1	2.77	3.507(3)	143	–*x*,–*y*,–*z*
	N1	H1a	Cg(C15–C20)[a]	2.59	3.445(3)	167	*x*, ½–*y*, ½+*z*
	C6	H6	N2	2.55	3.345(4)	143	1–*x*, ½+*y*, ½–*z*
4	N1	H1a	N2	2.23	3.102(4)	177	1–*x*, –*y*, –*z*
	N1	H1b	O2	2.18	2.979(4)	152	½+*x*, ½+*y*, *z*
	O2	H1w	O1	1.97	2.805(4)	177	*x*, *y*, *z*
	O2	H2w	O2	2.51	2.809(4)	102	–*x*, *y*, ½–*z*
6	N1	H1a	N2a	2.24	3.099(6)	168	–1–*x*, –*y*, –*z*
	N1a	H1a	N2	2.29	3.161(6)	174	–1–*x*, –*y*, –*z*
	C8	H8	Br1	3.03	3.628(5)	123	–*x*, 1–*y*, –*z*
	C6	H6	Br2	2.95	3.858(4)	163	–*x*, 1–*y*, 1–*z*
	C17	H17	Cg(C3a–C8a)[a]	2.88	3.576(7)	132	*x*, *y*, *z*
9	N1	H1a	N2	2.25	3.112(5)	173	1–*x*, –*y*, –*z*
	C8	H8	Cl	2.93	3.618(5)	131	–*x* 1–*y*, –*z*
	C6	H6	Cl	2.95	3.883(4)	169	1–*x* 1–*y*, –*z*

[a] Cg = centroid of indicated aromatic ring

4.4.4 Synthesis, spectroscopic characterization and X-ray crystallography of dibenzyltin(IV) derivatives of salicylaldehyde thiosemicarbazones

4.4.4.1 Synthesis and spectroscopic characterization of dibenzyltin(IV) derivatives of salicylaldehyde thiosemicarbazones *($L=L^1$ and L^3)*

The dibenzyltin derivatives (**13** and **14**) of salicylaldehyde thiosemicarbazones ($L = L^1$ and L^3) were obtained in 30-40% yields by the reaction of sodium salt of the respective salicylaldehyde thiosemicarbazone ligands with Bz_2SnCl_2.The products obtained were poorly soluble in the common organic solvents. This led to the technical difficulty of recording the NMR spectra of these compounds. The ^1H NMR spectral data were recorded and these provided some information about the chemical shifts of the different protons present indicating the binding of the ligand to the dibenzyltin moieties. Due to very poor signal-to-noise ratio in the ^{13}C NMR spectra of these complexes no substantial information could be obtained from these. IR spectra were recorded for these compounds.

4.4.4.1.1 Dibenzyltin(IV) salicylaldehyde thiosemicarbazonate (13)

Yellow crystals of **13** were isolated from benzene and dried in vacuo. Yield : 35%, M.p. 118-120 °C, IR (cm^{-1}): $\nu(NH_2)_{asym}$, 3400-3280 (b,w); $\nu(NH_2)_{sym}$, 3162 (w); ν(C=N-N=C), 1650 (m); $\nu(C=N)_{thio}$, 1600 (s); ν(C-O), 1209 (m); ν(C-S), 1035(m); ν(S-C-N), 761 (w). ^1H NMR: Ligand skeleton (see Table 4.9 for numbering scheme in the ligand skeleton): H-1, 5.17 (s, 2H); H-2 , 8.46 (s, 1H); H-5, 6.85-6.77 (d, 1H); H-6, 7.25 (m, 1H); H-7, 6.56 (m, 1H); H-8, 7.14-7.08 (d, 1H); Sn-benzyl skeleton: Sn-CH_2 , 2.17 (s, 4H); Ring protons, 7.25 (m, 10H).

4.4.4.1.2 Dibenzyltin(IV) derivative of 5-chlorosalicylaldehyde thiosemicarbazone Bz_2SnL^1 (14)

Yellow prism-shaped crystals of **14** were obtained from repeated recrystallization from methanol solution [36]. Yield: 30%, M.p. 144-146 °C, IR(cm^{-1}): $\nu(NH_2)_{sym}$,

3285(m); ν(C=N-N=C), 1619 (s); $\nu(C=N)_{thio}$, 1596 (s); ν(C-O), 1184 (m); ν(C-S), 996 (w); ν(C-S-N), 754 (w).). ^{1}H NMR: Ligand skeleton (see Table 4.9 for numbering scheme in the ligand skeleton): H-1, 5.10 (s,2H); H-2 , 8.45 (s,1H); H-5,6, 7.05-6.75 (m, 2H) H-8, 7.21 (s,1H); Sn-benzyl skeleton: Sn-CH_2 , 1.63 (s, 4H), Sn-OCH_3 (see Fig. 4.34), 3.48 (s, 6H); Ring protons, 7.30 (m, 8H).

Both the NMR and TGA analysis indicates the presence of OMe group in **14.14** was obtained as a result of debenzylation of an authenticated sample of $(PhCH_2)_2SnL^3$, where L^3H_2 is *p*-chlorosalicylaldehyde thiosemicarbazone, from a methanol solution. Debenzylation reactions are well documented in literature [182-184].It should be noted that in all the debenzylation reactions the final product still contains one benzyl group on tin [182], as is observed in this case too.Heterolytic cleavage of a Sn-C bond has been reported to occur with basic nucleophilic agents [185]. Sometimes, solvent may be the strongest nucleophile present [186]. In presence of polar nucleophilic solvents such as methanol or acetic acid the nucleophilic assistance is rendered by coordination of the solvent to the tin atom thereby increasing the polarity of Sn-C bonds [187] and hence facilitating debenzylation.

The debenzylation reaction observed in this case is remarkably facile taking place even during recrystallization. This is presumably mediated by traces of water in the solvents [188] or may be due to methanol which is rendering nucleophilc assistance at tin.

*4.4.4.2 Crystal Structure of di-μ_2-methoxo-bis[benzyl{5-chloro-2-oxido-benzaldehyde -thiosemicarbazonato}tin(IV)] [$Sn(Bz)_2(C_8H_6ClN_3OS)_2(CH_3O)_2$] **(14)***

Di-μ_2-methoxo-bis[benzyl{5-chloro-2-oxido-benzaldehydethiosemicarbazonato} tin(IV)] was isolated as yellow prisms from the attempted recrystallization of an authenticated sample of $(PhCH_2)_2SnL^3$ where L^3H_2 is *p*-chlorosalicylaldehyde thiosemicarbazone, from a methanol solution.

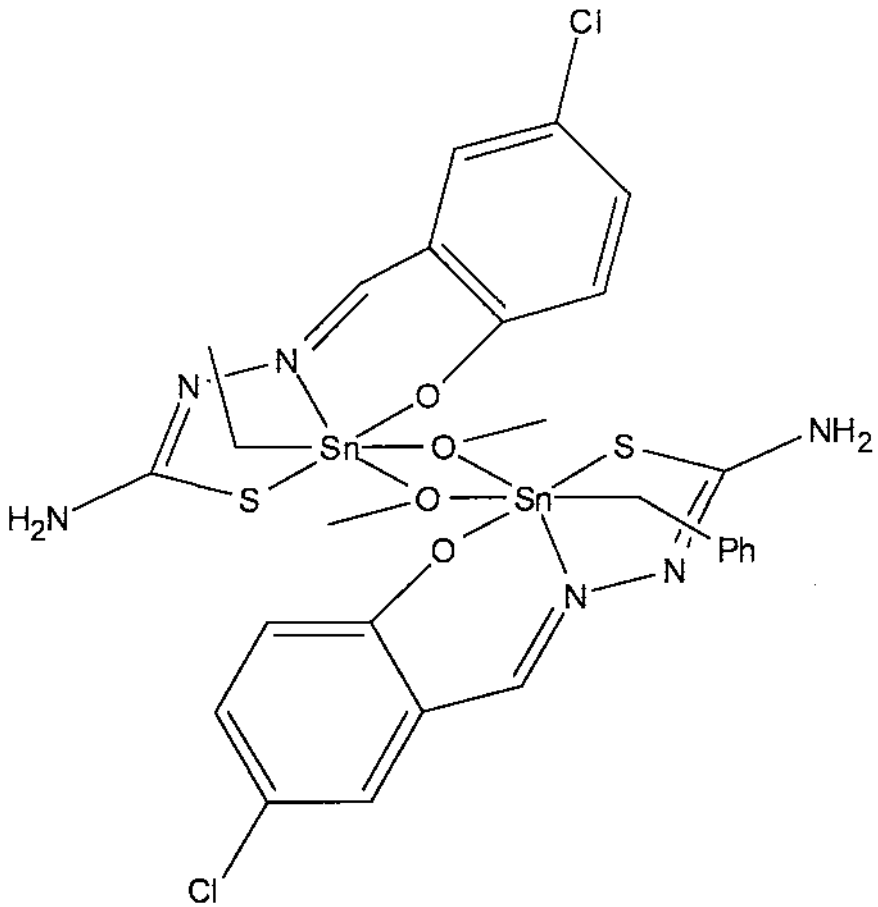

(14)

The crystal structure analysis showed a centrosymmetric molecule (Fig. 4.34) in which two $(PhCH_2)Sn$ entities were symmetrically bridged by two methoxide ligands (Table 4.23). The distorted octahedral coordination geometry for tin was completed by N-, O- and S-donor atoms derived from the dinegative and tridentate L^{2-} ligand. Distortions from ideal geometry may be traced to the strain found in the centrosymmetric Sn_2O_2 core and chelate rings [36].

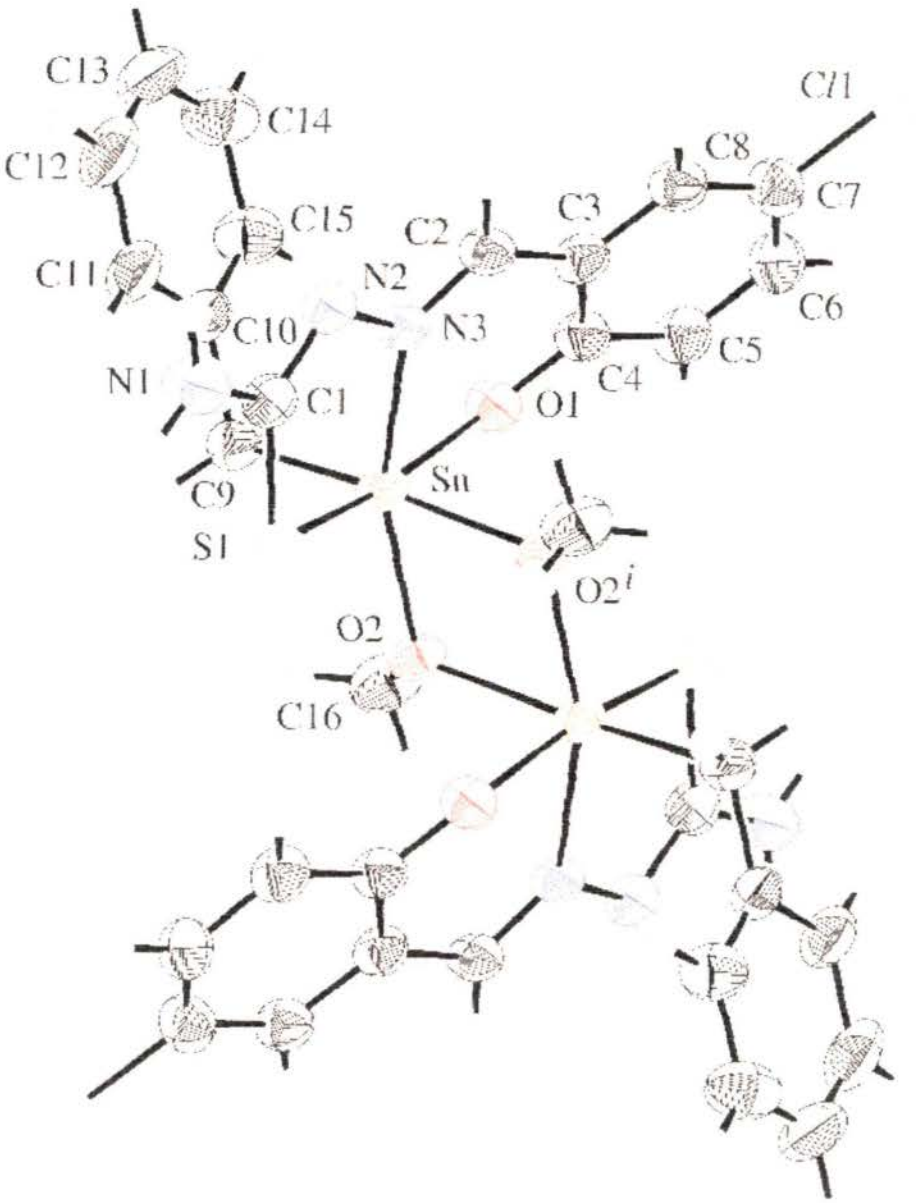

Fig.4.34 The molecular structure and atom-labelling scheme for **14**, showing 50% probability displacement ellipsoids [Symmetry code : (i) x , y , z].

Table 4.23 Selected geometric parameters (Å, ^{0}) of **14**

Sn-S1	2.1915(16)	O1-C1	1.326(6)
Sn-N3	2.221(4)	O2-C16	1.430(6)
Sn-O1	2.015(3)	N1-C1	1.343(6)
Sn-O2	2.108(3)	N2-N3	1.388(5)
Sn-O9	2.168(5)	N2-C1	1.317(6)
Sn-O2	2.161(3)	N3-C2	1.289(6)
S1-C1	1.753(5)		
S1-Sn-O1	162.51(9)	O2-Sn-O2	72.16(13)
S1-Sn-O2	99.97(10)	O9-Sn-O2	167.90(16)
S1-Sn-N3	78.35(10)	O9-Sn-N3	103.09(16)
S1-Sn-O9	99.11(15)	N3-Sn-O2	86.36(13)
S1-Sn-O2	89.82(10)	Sn-S1-C1	94.97(18)
O1-Sn-O2	93.59(13)	Sn-O1-C1	126.4(3)
O1-Sn-N3	85.00(13)	Sn-O2-C16	118.9(3)
O1-Sn-C9	89.49(17)	Sn-O2-C16	123.0(3)
O1-Sn-O2	83.75(14)	Sn-O2-Sn	107.54(13)
O2-Sn-N3	158.79(14)	Sn-N3-N2	119.9(3)
O2-Sn-O9	98.05(15)	Sn-N3-C2	124.3(3)

Symmetry code : (i)) $-x, -y, -z$.

Molecules were held in a three-dimensional array by a combination of N–H….N, N–H….π and C–H….π interactions. The hydrogen bonding between N1….H1*A* and N2^{ii} [symmetry code : (ii) $1-x, -y, 1-z$] lead to the formation of chain along [101] (see Fig. 4.35).The parameters associated with these interactions were N1–H1*A*….N2^{ii} – 2.26 Å and N1….N2^{ii} – 3.126 (6) Å with an angle of 169^{o} at H1*A*. While not involved in a conventional hydrogen bonding interaction , the amine

atom H1*B* formed an N-H....π interaction with the ring centroid of the aromatic proton of a tin-bound benzyl residue so that the N1–H1*B*.....ring centroid (C10-C15)^{iii} distance was 2.81 Å with an angle of 176° at H1*B* [symmetry code : (iii) $1-x$, $-1/2+y$, $1/2-z$] : some of these intearactions are highlighted with an '(a)' in Fig. 4.36. The methoxide –bound methyl - H atoms formed C–H....π interactions with the six-membered aromatic ring (C3-C8)^{iv} so that the H....ring centroid distance was 2.66 Å and the angle at H was 1.22° [symmetry code : (iv) x, $1/2-y$, $-1/2+z$], shown as '(b)' in Fig.4.36.

4.5 Biological Properties of diorganotin(IV) complexes of salicylaldehyde thiosemicarbazones

4.5.1 Antibacterial activity

The antibacterial properties of the diorganotin(IV) complexes of salicylaldehyde thiosemicarbazones were evaluated and results are summarized in Table 4.24. It was observed that all the test compounds inhibited bacterial growth to varying extent.

Compound **1** was found to be least potent among the four compounds tested. With the exception of *S. aureus* it had no effect on the different Gram-negative bacteria chosen for the study. However, it inhibited the growth of Gram-positive bacteria *B. subtilis* and *L. rhamnosus* when tested at high concentrations. It was found to be most sensitive to *S. aureus* (ED_{50} = 22.48 μg/ml).

It is evident from Table 4.24, that the dibutyltin compound **2** exhibited very powerful antibacterial properties. Different doses of the compound when used against both Gram-positive and Gram-negative bacteria could effectively kill these organisms. Even when present at low concentrations it brought about 50% inhibition of bacterial growth. It was noted that **2** was more potent against Gram-positive bacteria than Gram-negative bacteria. The compound **2** had a very low ED_{50} dose against *L. rhamnosus* and S. *aureus*. Interestingly, this compound had no effect on *B. Subtilis*. It would be interesting to study why **2** is ineffective against this bacterium [13].

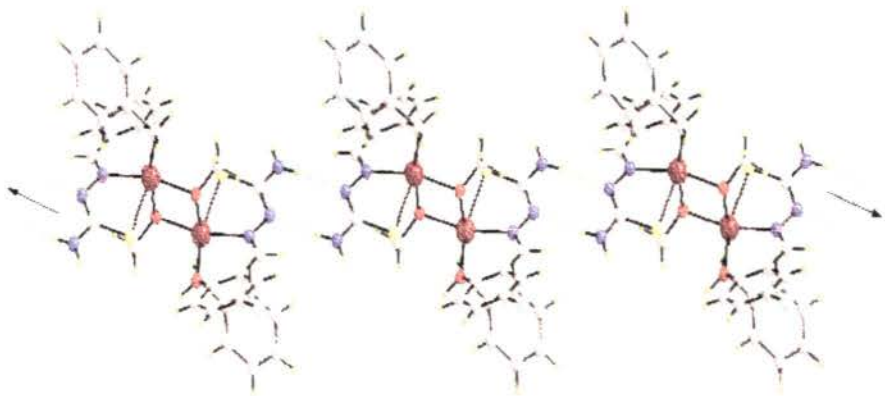

Fig. 4.35 Chains mediated by N–H....H hydrogen bonding interactions, shown as golden dashed lines, in (**14**) (Crystal Impact, 2006). Colour code: Sn (brown), Cl (cyan), S (yellow) O (red), N (blue), C (grey) and H (green).

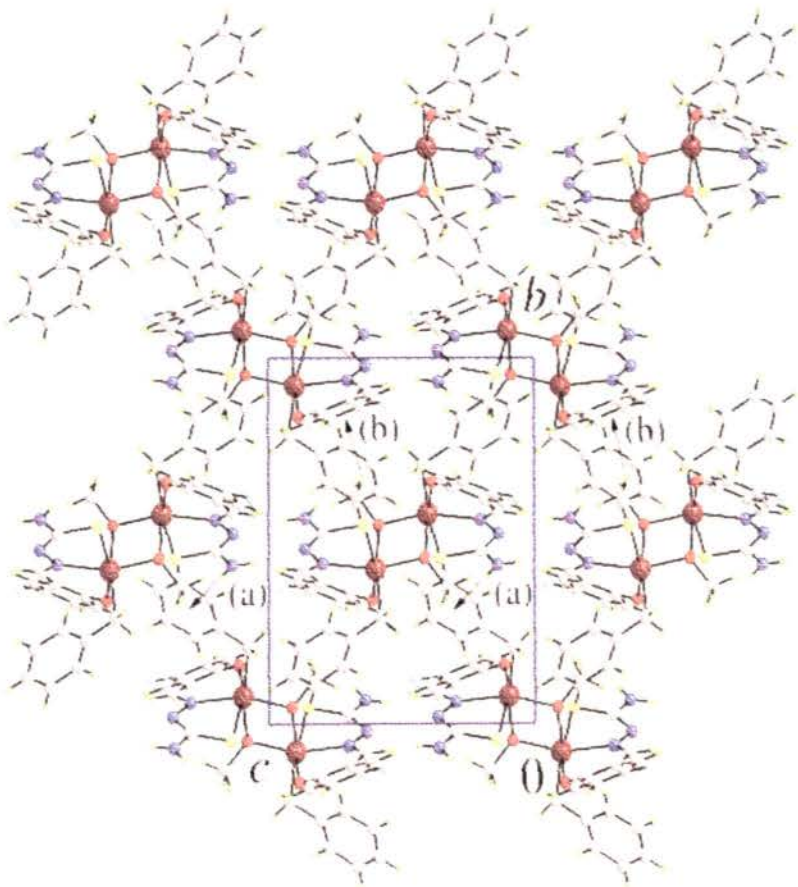

Fig. 4.36 The packing of (**14**), viewed down the *a* axis (Crystal Impact, 2006). Colour code as in Fig. 4.35.

On calculating the effect of **4** on bacterial growth it was noted that the compound was active only against gram negative bacteria like *S. typhi*, *A. hydrophila* and *E. coli*. The compound had no effect on *S. flexnri* and *S. typhimurium* as well as on any of the gram positive bacteria used in this study except *S. aureus*.

The compounds **3** and **6** appeared to have an almost similar antibacterial profile.

Table 4.24 Effect of different organotin compounds on bacterial growth[a] [ED_{50}=Effective Dose ($\mu g\ ml^{-1}$)]

	a	**b**	**c**	**d**	**e**	**f**	**g**	**h**
1	n.e.	n.e.	n.e.	n.e.	n.e.	32.58	22.28	45.00
2	7.3	3.4	n.e.	n.e.	38.01	n.e.	3.2	2.05
3	5.50	20.12	26.38	40.53	30.28	6.50	n.e.	2.02
4	28.88	35.55	17.07	13.35	37.20	40.00	n.e.	6.05
6	12.50	26.40	32.40	32.96	17.52	40.70	n.e.	23.10

[a] The doses mentioned represent the minimum effective dose needed to inhibit 50% growth of bacteria. MIC values above 50 $\mu g\ ml^{-1}$ were not considered significant.

n.e. = no effect. The values represent mean of three experiments.

[b] **a**, *A. hydrophila*; **b**, *S. typhi*; **c**, *S. typhimurium*; **d** ,*S. flexnri*; **e**, *E. coli*; **f**, *B. subtilis*; **g**, *S. aureus*; **h**, *L. rhamnosus*.

4.5.2 Effect of n-Bu_2SnL^1 (2) on bacterial disease

Since it was observed that **2** could effectively control the growth of different gram negative bacteria, an attempt was made to see whether the compound could control the progression of a disease caused by any of the pathogenic bacteria used in the study. *Aeromonas hydrophila*, a Gram-negative bacterium, is one of the etiologic agents responsible for EUS (Epizootic Ulcerative Syndrome) in fish. *A. hydrophila* were incubated with **2** for 6-8 hours and then injected into fish via intra-muscular route. Control fish were injected with untreated *A. hydrophila.* It was found that **2** treated bacteria failed to produce the redness and lesion characteristic of EUS, but the control fish exhibited all the characteristic features of EUS.

It was observed that, when **2** was injected locally into preformed bacterial lesions it effectively prevented the spread of this disease in infected fish. It was also noted that if **2** was dissolved in the tank it significantly reduced the bacterial load in water.

EUS is a fish disease affecting different parts of the globe. With the advent of multi-drug resistant strains it has become difficult to control the spread of this disease. Organotin compounds as mentioned before have been reported to have potent bactericidal properties [91].The experimental results obtained from this study also confirm the previous reports of high bactericidal activity of organotin compounds. Moreover, the compound **2** was effective even at very low concentrations.

4.5.3 Antifungal activity

The antifungal activity of the diorganotin(IV) complexes of salicylaldehyde thiosemicarbazones were investigated and the results are summarized in Table 4.25.When the antifungal properties of the compounds were evaluated it was observed that compound **4** was effective against all the four fungi selected in the study with the minimum MIC values obtained for *A. porri* and *M. phaseolina* (MIC 1.78 μg ml^{-1}). Compound **6** was effective against all the pathogenic fungi except *D. oryzae*, while **1** was effective against *A. porri* and *M. phaseolina* (MIC 3.76 μg ml^{-1}) and **3** was

effective only against *A. porri* (MIC 4.4 μg ml^{-1}). The study indicated that the alkyltin derivatives are more active than the aryltin compounds for both bacteria and fungi in accord with the literature conclusions [187].

It is not possible from this study to determine the structure activity relationship between the anti-microbial activity and structure of organotins used or suggest any specific mode of action of the organotins on the bacteria or fungi selected. However, earlier studies have suggested that charged metabolites of the organotins could play a role in their anti-microbial activities [189]. Moreover, the chelating potential of organotins could also be responsible for the enhanced anti-microbial activity observed [190,191]. The variation in the anti-microbial properties against different organisms observed probably depends on the impermeability of the cell or differences in ribosomes to the organotins used [192]. Also, the activity of any compound is a complex combination of steric, electronic and pharmacokinetic factors. A possible explanation for the toxicity of the complexes can be explained in the light of the chelation theory [193] which suggests that chelation reduces considerably the charge of the metal ion mainly because of the partial sharing of its positive charge with the donor groups and possible π-electron delocalization over the whole chelate ring. This increases the lipophilic character of the metal chelate which favours its permeation through lipid layers of fungus membranes. Furthermore, the mode of action of the compound may involve the formation of a hydrogen bond through the –N=C group of the chelate or the ligand with the active centres of the fungal cell constituents resulting in interference with the normal cell process. Further studies with bacteria and fungi are in progress to determine the mode of action of these compounds.

4.5.4 Phytotoxic Properties

The phytotoxic effects of selected organotin compounds were studied on three economically important crops namely *Oryzae sativa* (IR-8), *Lens culinaris,* and *Cicer aurantinum* (Table 4.26). It is evident from Table 4.26, that none of the compounds used in the study had any phytotoxic effect on seed germination.They did not affect the seed germination potency of *Oryzae sativa* , *Lens culinaris,* and *Cicer aurantinum.*

Table 4.25 Fungicidal activity of selected compounds against different fungi species - effects on spore germination[a]

Spore	Complex	Minimum Inhibitory concentration [MIC] (μg/ml)
Curvularia eragrostidis	**1**	37.6
	2	6.4
	3	440
	4	17.8
	6	18.4
	7	25
	9	20
Alternaria porri	**1**	3.76
	2	0.64
	3	4.4
	4	1.78
	6	1.84
	7	2.5
	9	2
Dreschlerea oryzae	**1**	376
	2	64
	3	440
	4	17.8
	6	184
	7	25
	9	200
Macrophomina phaseolina	**1**	3.76
	2	6.9
	3	44
	4	1.78
	6	18.4
	7	2.5
	9	20

[a] The reported values represent the mean determined from three experiments. MIC values above 30 μg ml^{-1} were not considered significant.

Table 4.26 Phytotxic effect (µg/ml) of selected organotin compounds[a,b,c]

Compound	Concentration (µg/ml)	Percentage germination following treatment with organotin compounds								
		Duration of treatment (**hrs**)								
		1			4			12		
		a	**b**	**c**	**a**	**b**	**c**	**a**	**b**	**c**
1	100	92	82	96	92	82	94	93	80	93
	50	95	83	95	94	85	94	94	80	92
	25	92	81	95	92	80	95	95	81	91
2	100	91	84	95	93	86	93	93	81	94
	50	93	85	96	94	86	94	95	83	94
	25	95	83	94	97	88	96	95	84	95
3	100	94	86	96	94	87	95	95	85	96
	50	94	88	94	95	87	96	95	85	98
	25	96	83	96	96	81	95	96	84	97
4	100	96	80	94	96	81	95	96	80	95
	50	94	82	93	94	81	93	94	83	93
	25	95	80	92	94	80	92	94	79	92
6	100	94	90	97	93	91	95	91	90	95
	50	93	92	96	94	90	94	93	91	94
	25	92	90	97	92	90	95	90	91	96
Control [d]		96	81	98	94	80	97	95	80	96

[a] The phytotoxicity of the compounds was checked by seed germination assays. Seeds were incubated with different concentrations of the compounds for 1, 4 and 12 h, washed to remove the excess unbound compounds and the percentage germination checked following incubation for 72 h. Control seeds exhibited 95-100 % germination efficacy. Values represent mean of three experiments.

[b] **a** *Cicer aurantinum*; **b** *Lens culinaris*; **c** *Oryzae sativa.*

[c] The control seeds were incubated in DMSO/water for the indicated time period.

References

1. E.S. Rasper, Coord. Chem. Rev. **61** (1985) 115.
2. M. Kemmer, H. Dalil, M. Biesemans, J.C. Martins, B. Mahieu, J. Organomet. Chem. **608** (2000) 63.
3. S.J. de Mora, in: S.J. de Mora (Ed.), Tributyltin:Case Study of an Environmental Contaminant, Cambridge University Press, London, 1996, pp. 1-20.
4. K.C. Molloy, K. Quill, I.W. Nowell, J. Chem. Soc., Dalton Trans. **5** (1986) 85.
5. K.C. Molloy, K. Quill, I.W. Nowell, J. Chem. Soc., Dalton Trans. (1987) 101.
6. J.A. Zubeita, J.J. Zuckerman, Inorg. Chem. **24** (1987) 251.
7. L. Pellerito, L. Nagy, Coord. Chem. Rev. **224** (2002) 111.
8. S. Mishra, M. Goyal, A. Singh, Main Group Met. Chem. **25** (2002) 437.
9. A. Saxena, J.P. Tandon, A.J. Crowe, Polyhedron **4** (1985) 1085.
10. H.L. Singh, S. Varshney, A.K. Varshney, Appl. Organomet. Chem. **13** (1999) 637.
11. I. Belsky, D. Gerther, A. Zilkla, J. Med. Chem. **1** (1968) 92.
12. K.C. Joshi, V. N. Pathak, P. Panwar, Agric. Biol. Chem. **41** (1977) 543.
13. M. Sen Sarma, S. Mazumder, D. Ghosh, A. Roy, A. Duthie, E.R.T. Tiekink, Appl. Organomet. Chem. (2007), DOI: 10.1002/aoc.1301.
14. K. Orita, Y. Sakamoto, K. Hamada, A. Mitsutome, J. Otera, Tetrahedron **55** (1999) 2899.
15. R.S. Collinson, D.E. Ferton, Coord. Chem. Rev. **148** (1996)19.
16. A.K. Saxena, F. Huber, Coord. Chem. Rev. **95** (1989) 109.
17. M. Gielen, Coord. Chem. Rev. **151** (1996) 41.
18. A.J. Crowe, P.J. Smith, C.J. Cardin, H.E. Parge, F.E. Smith, Cancer Lett. **24** (1984) 45.
19. A.J. Crowe, P.J. Smith, J. Organomet. Chem. **244** (1982) 223.
20. M. Gielen, Metal-Based Drugs. **1** (1994) 213.
21. A.J. Crowe, Drugs Future **2** (1987) 40.
22. M. Nath, S. Pokharia, R. Yadav, Coord. Chem. Rev. **215** (2001) 99.
23. D.K. Dey, M.K. Saha, M.K. Das, N. Bhartiya, R.K. Bansal, G. Rosair, S. Mitra, Polyhedron **18** (1999) 2687.
24. G.Y. Yeap, N. Ishizawa, Y. Nakamura, J. Coord. Chem. **44** (1998) 325.

25. B.S. Kawakami, M. Miya-Uchi, T. Tanaka, J. Inorg. Nucl. Chem. **42** (1980) 805.

26. H. Schiff, Ann. Chim. **131** (1864) 118.

27. S. Dayagi, Y. Degani, in: S. Patai (Ed.), The Chemistry of the Carbon-Nitrogen Double Bond, Wiley- Interscience, New York , 1970, pp.71.

28. N.S. Biradar, V.H. Kulkarni, J. Inorg. Nucl. Chem. **33** (1971) 2451.

29. B.N. Ghose, Synth. React. Inorg. Met. –Org. Chem. **12** (1982) 835.

30. B. S. Saraswat, G. Srivastava and R. C. Mehrotra, J. Organomet. Chem. **137** (1977) 301.

31. B. S. Saraswat, G. Srivastava and R. C. Mehrotra, J. Organomet. Chem. **164** (1979) 153.

32. R. Tiwari, G. Srivastava, R.C. Mehrotra, A.J. Crowe , Inorg. Chim. Acta **111** (1986) 167.

33. D. Cunningham, J.F. Gallanger, T. Higgins, P. McArdle, I. McGinley, M. Ogara, J. Chem. Soc., Dalton Trans. (1993) 2473.

34. R.C. Mehrotra, G. Srivastava, B.S. Saraswat, Rev. Silicon, Germanium, Tin and Lead Compounds **6** (1982) 171.

35. S. Gopinathan, M.P. Degaonkar, A.M. Hundekar, C. Gopinathan, Appl. Organomet. Chem. **7** (1993) 63.

36. M. Sen Sarma, C.A. Ellis, N. Moitra, A. Roy, E.R.T. Tiekink, Acta Cryst. **E62** (2006) m2067.

37. M. Nath, R.Yadav, M.Gielen, H. Dalil, D. de Vos, G. Eng, Appl. Organomet. Chem. **11** (1997) 727.

38. S.-G. Teoh, G.-Y. Yeap, C.-C. Loh, L.-W. Foong, S.-B. Teo, H.-K. Fun, Polyhedron **16** (1997) 2213.

39. L. Tian, Z. Shang, X. Zheng, Y. Sun, Y. Yu, B. Qian, X. Liu, Appl. Organomet. Chem. **20** (2006) 74.

40. H.P.S. Chauhan, A. Bhargava, R.J. Rao, Ind. J. Chem. **32A** (1993) 157.

41. J. Wang, Y. Zhang, Y. Xu, Z. Wang, H. Youji, Heteroatom Chem. **13** (1993) 289.

42. A.Saxena, J.P. Tandon, K.C. Molloy, J.J. Zuckerman, Inorg. Chim. Acta **63** (1982) 71.

43. S. Gopinathan, M.P. Degaonkar, C. Gopinathan, Appl. Organomet.Chem. **6** (1992) 69.

44. F.Q. Liu, J.T. Wang, R.J. Wang, H.G. Wang , X.K. Yao, J. Organomet. Chem. **371** (1989) 35.

45. Z. -K. Yu, S.-H. Wang, Z.-Y. Yang, X.-M. Liu, N.-H. Hu, J.Organomet.Chem. **447** (1993) 189.

46. N.K. Singh, U. Sharma, S.K. Kulshreshtha, J.Organomet. Chem. **382** (1990) 375.

47. S. Ianelli, P. Mazza, M. Orcesi, C. Pelizzi, G. Pelizzi, F. Zani, J. Inorg. Biochem. **60** (1995) 89.

48. A. Bergamschi, A. Bonardi, E. Leporati, P. Mazza, P. Pelagatti, C. Pelizzi , G. Pelizzi, M. C. Rodriguez Argüelles , F. Zani, J. Inorg. Biochem. **68** (1997) 295.

49. A. Bacchi, A. Bonardi, M. Carcelli, P. Mazza, P. Pelagatti, C. Pelizzi, G. Pelizzi, C. Solinas , F. Zani , J. Inorg. Biochem. **69** (1998) 110.

50. T. M. Aminabhavi, N. S. Biradar, S. B. Patil . D. E. Hoffman V. N. Biradar. Inorg. Chim. Acta **135** (1987) 139.

51. N.K. Goh, L .E. Khoo, T.C.W. Mak, Polyhedron **8** (1993) 925.

52. S .G. Teoh, S.-B. Teo, G.-Y. Yeap, J.-P. Declercq, Polyhedron **10** (1991) 2683.

53. J.-P. Charland, F.L. Lee, E.J. Gabe, L.E. Khoo, F.E. Smith, Inorg. Chim. Acta **130** (1987) 55.

54. T.A.K. Al-Allaf, L.J. Rashan, A. Stelzner, D.R. Powell, Appl. Organomet. Chem. **17** (2003) 891.

55. H.D. Yin, S.W. Chen, Inorg. Chim. Acta **359** (2006) 3330.

56. B.K. Dwivedi, K. Bhatnagar , A.K. Srivastava, Synth. React. Inorg. Met.-Org. Chem. **16** (1986) 715.

57. M.R. Maurya, M.N. Jayaswal, V.G. Puranik, P. Chakrabarti, S. Gopinathan, G. Gopinathan, Polyhedron **16** (1997) 3977.

58. J.N.R. Ruddick, J.R. Sams, J. Organomet. Chem. **60** (1973) 233.

59. N.S. Biradar, V.K. Kulkarni, J. Inorg. Nucl. Chem. **33** (1971) 3781.

60. D.L. Evans, B.R. Penfold, J. Cryst. Mol. Struct. **5** (1975) 93.

61. A.A. Diamantis, J.M. Gulbis, M.Manikas, E.R.T. Tiekink, Phosph., Sulf., Silicon **151** (1999) 251.

62. A.vander Bergen, J.D. Cashion, G.D. Fallon, B.O. West, Aust. J. Chem. **43** (1990) 1559.

63. C. Pettinari, F. Marchetti, R. Pettinari, D. Martini, A. Drozdov, S. Troyanov, Inorg. Chim. Acta **325** (2001) 103.

64. B. Yearwood, S. Parkin, D.A. Atwood, Inorg. Chim. Acta **333** (2002) 124.

65. M. Boyce, B. Clarke, D. Cunningham, J.F. Gallanger, T. Higgins, P. McArdle, N. Cholchuin, M. Ogara, J. Organomet. Chem. **498** (1995) 241.

66. B. Clarke, N. Clarke, D. Cunningham, T. Higgins, P. McArdle, N. Cholchuin, M. Ogara, J. Organomet. Chem. **559** (1998) 55.

67. M. Carcelli, G. Corazzari, S. Ianelli, G. Pelizzi, C. Solinas, Inorg. Chim. Acta **353** (2003) 310.

68. T. Sedaghat, S. Menati, Inorg. Chem. Commun. **7** (2004) 760.

69. S. Bhattacharyya, S. Mukhopadhyay, S. Samanta, T.J.R. Weakly, M. Chaudhury, Inorg. Chem. **41** (2002) 2433.

70. E. Pereira, L. Gomes, B. Decastra, Inorg. Chim. Acta **271** (1998) 83.

71. J.M. Rivera, D. Guzmán, M. Rodriguez, J.F. Lamère, K. Nakatani, R. Santillan, P.G. Lacroix, N. Farfán, J. Organomet. Chem. **691** (2006) 1722.

72. H. -X. Yu, J. -F. Ma, G.-H. Xu, S.-Li Li, J.Yang, Y.-Y. Liu, Y.-X.Cheng, J.Organomet. Chem. **691** (2006) 3531.

73. M.J.M. Campbell, Coord. Chem. Rev. **15** (1975) 279.

74. S. Padhye, G.B. Kauffmann, Coord. Chem. Rev. **63** (1985) 127.

75. D.X. West, S.B. Padhye, P.B. Sonawane, Struct. Bond. **76** (1991) 1.

76. D.X. West, A.E. Liberta, S.B. Padhye, R.C. Chikate, P.B. Sonawane, A.S. Kumbhar, R.G. Yerande, Coord. Chem. Rev. **123** (1993) 49.

77. J.S. Casas, M.S. Garcia-Tasende, J.Sordo, Coord. Chem. Rev. **209** (2000) 197.

78. M.C. Miller III, C.N. Stineman, J.R. Vance, D.X. West, I.H. Hall, Appl. Organomet. Chem. **13** (1999) 9.

79. D. Singh, R.V. Singh, R.B. Goyal, Appl. Organomet. Chem. **5** (1991) 45.

80. J. Eugênio J.C. Graúdo, N.L. Spezialli, A. Abras, M. Hörner, C.A.L. Filgueiras, Polyhedron **18** (1999) 2483.

81. P. Sengupta, R. Dinda, S. Ghosh, Trans. Met. Chem. **27** (2002) 665.

82. G.J. Palenik, R.F. Rendle, R.S. Carter, Acta Crystallogr. Sect. B **30** (1974) 2390.

83. S. Chandra, X. Sangeetika, Spectrochim. Acta (A) **60** (2004) 147.

84. N.K. Singh, A. Srivastava, A. Sodhi, P. Ranjan, Trans. Met. Chem.**25** (2000) 133.

85. N.V. Gerbeleu, V.B. Arion, J. Burgess, Template Synthesis of Macrocyclic Compounds, Wiley- VCH, Weinheim, 1999.

86. A.P. Koley, S. Purohit, S. Ghosh, L.S. Prasad, P.T. Manoharan, J. Chem. Soc., Dalton Trans. (1988) 2607.

87. S. Purohit, A.P. Koley, L.S. Prasad, P.T. Manoharan, S. Ghosh, Inorg. Chem. **28** (1989) 3735.

88. U. Knof, T. Weyhermuller,T. Wolter, K. Weighardt, J. Chem. Soc. Chem. Commun. (1993) 726.

89. M.R. Bermejo, R. Pedrido, M.I. Fernández, A.M. González-Noya, M. Maneiro, M.J. Rodríguez, M.J. Romero, M. Vázquez, Inorg. Chem. Commun. **7** (2004) 4.

90. V. Arion, K. Weighhardt, T. Weyhermuller, E. Bill, V.M. Leovac, A. Rufinska, Inorg. Chem. **36** (1997) 661.

91. S. Belwal, R.V. Singh, Appl. Organomet. Chem. **12** (1998) 39.

92. A.P. Rebolledo, G.M. de Lima, L.N. Gambi, N.L. Speziali, D.F. Maia, C.B. Pinheiro, J.D. Ardisson, M.E. Cortes, H. Beraldo, Appl. Organomet. Chem. **17** (2003) 945.

93. A.P. Rebolledo, G.M. de Lima, N.L. Speziali, O. E. Piro, E. E. Castellano, J. D. Ardisson , H. Beraldo, J. Organomet. Chem. **691** (2006) 3919.

94. R.S. Barbieri, H.O. Beraldo, C.A.L. Filgueiras, A. Abras, J.F. Nixon, P.B. Hitchcock, Inorg. Chim. Acta **206** (1993) 169.

95. L. Labib,T.E. Khalil, M.F. Iskander, L.S. Refaat, Polyhedron **15** (1996) 349.

96. T.T. Bamgboye, O.A. Bamgboye, Inorg. Chim. Acta **144** (1988) 249.

97. J.S. Casas, M.S. García-Tasende, C. Maichle-Mössmer, M.C. Rodríguez-Argüelles, A. Sánchez, J. Sordo, A. Vázquez-López, S. Pinelli, P. Lunghi, R.Albertini , J. Inorg. Biochem. **62** (1996) 41.

98. S.O. Sommerer, G.J. Palenik, Inorg. Chim. Acta **183** (1991) 217.

99. G.F.de Sousa, C.A.L. Filgueiras, A. Abras, S.S. Al-Juaid, P.B. Hitchcock, J.F. Nixon, Inorg. Chim. Acta **218** (1994) 139.

100. J. S. Casas, A. Castifieiras, A. Sánchez, J. Sordo, A. Vázquez-López, M. C. Rodriguez-Argüelles, U. Russo, Inorg. Chim. Acta **221** (1994) 61.

101. P.C. Moreno, R.H.P. Francisco, M.T. do, P. Gambardella, G.F. de Sousa, A. Abras, Acta Crystallogr. Sect. **C 53** (1997) 1411.

102. S.W. Ng, V.G. Kumar Das, B.S. Luo, T.C.W. Mak, Z. Kristallogr. **209** (1994) 961.

103. J. S. Casas, A. Sánchez, J. Sordo, A. Vázquez- López, E. E. Castellano, J. Zukerman-Schpector, M.C. Rodriguez-Arguelles, U. Russo, Inorg. Chim. Acta **216** (1994) 169.

104. S. W. Ng, V.G. Kumar Das, B.W. Skelton, A.H. White, J. Organomet. Chem. **377** (1989) 211.

105. S.-G. Teoh, S.-H. Ang, S.-B. Teo, H.-K. Fun, K.-L. Khew, C.-Wi Ong, J. Chem. Soc., Dalton Trans. (1997) 465.

106. M. Carcelli, D. Delledonne, A. Fochi, G, Pelizzi, M.C. Rodríguez-Argüelles, U. Russo, J. Organomet. Chem. **544** (1997) 29.

107. E. L -Torres, M. A. Mendiola, C. J. Pastor, J. R. Procopio, Eur. J. Inorg. Chem. (2003) 2711.

108. G.F.de Sousa, D.X. West, C.A. Brown, J.K. Swearingen, J.V. Martínez, R.A. Toscano, S.H. Ortega, M. Hörner, A.J. Bortoluzzi, Polyhedron **19** (2000) 841.

109. B.A. Gingras, R.W. Hornal, C.H. Baylay, Canad. J. Chem. **38** (1960) 712.

110. J.P. Scovill, D.L. Klayman, C.F. Franchino, J. Med. Chem. **25** (1982) 1261.

111. G. Domagk, R. Behinsch, F. Mietzsch, H. Schmidt, Naturwissenschaften **33** (1946) 315.

112. D.L. Klayman, J.E. Bartosevich, T.S. Griffith, C.J. Mason, J.P. Scovill, J. Med. Chem. **22** (1979) 855.

113. H. Beraldo, D. Gambino, Mini-Rev. Med. Chem. **4** (2004) 31.

114. N.C. Kasuga, K. Onodera, S. Nakano, K. Hayashi, K. Nomiya, J. Inorg. Biochem. **100** (2006) 1176.

115. H.A. Tang, L.F. Wang, R.D. Yang, Trans. Met. Chem. **28** (2003) 395.

116. F. Gialdi, R. Ponci, Farmaco **6** (1951) 332.

117. M.C. Cardia, M. Begala, A. Delogu, E. Maccioni, A. Plumitallo, Farmaco **55** (2000) 93.

118. N.C. Kasuga, K. Sekino, C. Koumo, N. Shimada, M. Ishikawa, K. Nomiya, J. Inorg. Biochem. **84** (2001) 55.

119. M.C. Rodriguez Arguelles, E.C. Lopez-Silva, J. Sanmartin, P. Pelagatti, F.Zani, J. Inorg. Biochem. **99** (2005) 2239.

120.M.T. Cocco, C. Congiu, V. Onnis, M.L. Pellerano, A. De Logu, Bioorg. Med. Chem. **10** (2002) 501.

121. S.M. Rida, I.M. Labouta, H.M. Salama, Y.S. Ghany, E. El-Ghazzaui, M.T. Cocco, A. Plumitallo, M.L. Schivo, A. De Logu, Farmaco **45** (1990) 1101.

122.O.E. Offlong, S. Martelli, Farmaco **49** (1994) 513.

123. Z.H. Chohan, H. Pervez, K.M. Khan, C.T. Supuran, J. Enzyme Inhib. Med. Chem. **20** (2005) 81.

124. O.E. Offlong, S. Martelli, Farmaco **48** (1993) 777.

125. A. Walcourt, M. Loyevsky, D.B. Lovejoy, V.R. Gordeuk, D.R. Richardson, Internat. J. Biochem. Cell Biol. **36** (2004) 401.

126. L. Heinisch, D.Tresselt, Pharmazie **32** (1977) 582.

127. A.M. Omar, N.H. Eshba, H.M. Salama, Arch. Pharm. **317** (1984) 701.

128. J. Shipman, S.H. Smith, J.C. Drach, D.L. Klayman, Antiviral Res. **6** (1986) 197.

129. T. Varadinova, D. Kovala-Demertzi, M. Rupelieva, M. Demertzis, P. Genova, Acta Virol. **45** (2001) 87.

130. N. Bharti, S.S. Sharma, F. Naqvi, A. Azam, Bioorg. Med. Chem. **11** (2003)2923.

131. E.W. Ainscough, A.M. Brodie, W.A. Denny, G.J. Finlay, J.D. Ranford, J. Inorg. Biochem. **70** (1998) 175.

132.A.R. Jalilian, M. Sadeghi, Y.Y. Kamrani, Radiochim Acta **94** (2006) 865.

133. V. Mishra, S.N. Pandeya, C. Pannecouque, M. Witvrouw, E. De Clercq, Arch. Pharm. **335** (2002) 183.

134. T.R. Bal, B. Anand, P. Yogeeswari, D. Sriram, Bioorg. Med. Chem. Lett. **15** (2005) 4451.

135. N.N. Orlova, V.A. Aksensova, D.A. Selidovkin, N.S. Bogdanova, G.N. Pershin, Russ. Pharmacol. Toxicol. **348** (1968).

136.D.J. Bauer, L.S. Vincent, C.H. Kempe, A.W. Downe, Lancet. **2** (1963) 494.

137.P. Genova, T. Varadinova, A.I. Matesanz, D. Marinova, P. Souza, Toxic. Appl. Pharmacol. **197** (2004) 107.

138.H.W. Gausman, C.L. Rhykerd, H.R. Hinderliter, E.S. Scott, L.F. Audrieth, Botan. Gaz. **114** (1953) 292.

139.M. Joseph, V. Suni, M.R.P. Kurup, M. Nethaji, A. Kishore, S.G. Bhat, Polyhedron **23** (2004) 3069.

140. R.K. Agarwal, L. Singh, D.K. Sharma, Bioinorg. Chem. and Appl. 2006, DOI 10.1155/BCA/2006/59509.

141. P. Bindu, M.R.P. Kurup, T.R. Satyakeerty, Polyhedron **18** (1999) 321.

142. R.S. Srivastava, Inorg. Chim. Acta **56** (1981) L65.

143. A.K. Srivastava, C.B. Suresh, J. Indian Chem. Soc. **53** (1976) 841.

144. V.K. Sharma, S. Srivastava, A. Srivastava, Bioinorg. Chem. and Appl., 2007, DOI: 10.1155/2007/68374.

145.A. Albert, R.J. Goldcre, Nature **161** (1948) 95.

146.A. Albert, S.D. Rubbo, R.J. Goldcre, B.G. Balfour, Brit. J. Exptl. Path. **28** (1947) 69.

147.S.D. Rubbo, A. Albert, N.I. Gibson, Brit. J. Exptl. Path. **31** (1960) 425.

148.A.Y. Louie, T.J. Meadle, Chem. Rev. **99** (1999) 2711.

149.F.M. Collins, D.L. Klayman, N.E. Morrison, J. Gen. Microbiol. **128** (1982) 1349.

150.R. Brown, R. Fischer, J. Blunk, K.D. Berlin, K. Ramalingam, N.N. Durham, Proc. Okla. Acad. Sci. **56** (1976) 15.

151.A.P. Koley, S. Purohit, L.S. Prasad, S. Ghosh, P.T. Manoharan, Inorg. Chem. **31** (1992) 305.

152. L.J. Laughlin, C.G. Young, Inorg. Chem. **35** (1996) 1050.

153. R. H. Holm, Coord. Chem. Rev. **100** (1990) 183.

154. F. Basuli, S.M. Peng, S. Bhattacharya, Inorg. Chem. **36** (1997) 5645.

155. F. Basuli, M. Ruf, C.G. Pierpont, S. Bhattacharya, Inorg. Chem. **37** (1998) 6113.

156. I. Haiduc, C. Silvestru, Coord. Chem. Rev. **99** (1990) 253.

157. G.A. Ayoko, J.J. Bonire, S.S. Abdulkadir, P.F. Olurinola, J.O. Ehinmidu, S.Kokot, S. Yiasel, Appl. Organomet. Chem. **17** (2003) 749.

158. M. Nath, R. Yadav, G. Eng, T.T. Nguyen, A. Kumar, J. Organomet. Chem. **577** (1999) 1.

159. V.J. Moebus, R. Stein, D.G. Kieback, I.B. Runnebaum, G. Sass, R. Kreienberg, Anticancer Res. **17** (1997) 815.

160. M. Gielen, E.R.T. Tiekikink, in: Metallotherapeutic Drugs and Metal-Based Diagnostic Agents: The Use of Metals in Medicine', M. Gielen, E.R.T. Tiekink (Eds.), John Wiley & Sons Ltd. 2005, Chapter **22,** pp.421.

161. A. Saxena, J.P. Tandon, Polyhedron **3** (1984) 681.

162. K. Sisido, Y. Takeda, Z. Kinugawa, J. Am. Chem. Soc. **83** (1961) 538.

163. P.T. Beurskens, G. Admiraal, G. Beurskens, W.P. Bosman, S. García-Granda, R.O. Gould, J.M.M. Smits, C. Smykalla, in : The DIRDIF Program System, Technical Report of the Crystallography Laboratory', University of Nijmegen, The Netherlands, 1992.

164. G.M. Sheldrick, SHELXL-97, Program for the Crystal Structure Refinement, University of Göttingen, Germany, 1997.

165. C.K. Johnson, ORTEP. Report ORNL-5138; Oak Ridge National Laboratory, TN, 1976.

166. DIAMOND, Visual Crystal Structure Information System, Version 3.1d, Crystal Impact, Postfach 1251, D-53002 Bonn, Germany, 2006.

167. T. Majumdar, S. Ghosh, J. Pal, S. Mazumder, Aquaculture **256** (2006) 95.

168. T. Rouxel, A. Sarniget, A. Kollmann, J.F. Bousquet, Physiol. Mol. Plant Pathol. **34** (1989) 507.

169. S.K. Kamruddin, Ph.D.Thesis, University of North Bengal, West Bengal, India, 1996.

170. R.M. Silverstein, G.C. Bassler, T.C. Morrill, Spectrometric Identification of Organic Compounds, 5th Ed., John Wiley & Sons Inc. Canada, 1991.

171. L. Labib, T.E. Khalil, M.F. Iskander, L.S. Refaat, Polyhedron **21** (1996)3697.

172. T.S. Basu Baul , S. Dutta , E. Rivarola , M. Scopelliti , S. Choudhuri, Appl. Organomet Chem. **15** (2001) 947.

173. E.G. Martinez, A. Sanchez Gonzalez, J.S. Casas, J. Sordo, J.Organomet. Chem. **47** (1993) 453.

174. M.F. Iskander, L. Labib, M.M.Z. Nour El Din, M. Tawfik, Polyhedron **8** (1989) 2755.

175. H.V. Pham, B. Rusterholz, E. Pretsch, W. Simon, J. Organomet. Chem. **403** (1991) 311.

176. F. Ahmad, S. Ali, M. Parvez, A. Munir, M. Mazahar, K.M. Khan,T.A. Shah, Heteroatom Chem. **13** (2002) 638.

177. T.P. Lockhart, W.F. Manders, Inorg. Chem. **25** (1986) 892.

178. J. Holecek, A. Lyčka, Inorg. Chim. Acta **118** (1986) L17.

179. J. Otera, J. Organomet. Chem. **221** (1981) 57.

180. S. Roelins, M. Taddei, J. Chem. Soc., Perkin Trans. **2** (1985) 799.

181. A.P. Tupciauskas, Annu. Rep. NMR Spectrosc. **8** (1978) 291.

182. V. Chandrasekhar, K. Gopal, P. Sasikumar, R. Thirumoortii, Coord. Chem. Rev. **249** (2005) 1745 and references therein.

183. H. Yin, C. Wang, Y. Wang, Ind. J. Chem. **43B** (2004) 1493.

184. R.K. Ingham, S.D. Rosenberg, H. Gilman, Chem. Rev. **60** (1960) 459.

185. X. Song, G. Zhong, Q. Xie, G. Eng, Inorg. Chem. Commun. **8** (2005) 725.

186. L.F. McGahey, F.R. Gensen, J. Am. Chem. Soc. **101** (1979) 4397.

187. R.C. Poller, The Chemistry of Organotin Compounds, Logos Press, London, 1970, pp.274.

188. T.S. Basu Baul, K.S. Singh, A. Lycka, M. Holcapek, A. Linden, J. Organomet. Chem. **690** (2005) 1581.

189. K.A. Winship, Adverse Drug React. Acute Poisoning Rev. **7** (1988) 19.

190. J.J. Cooney, S. Wuertz, J. Ind. Microbiol. Biotechnol. **4** (1989) 375.

191. S. Rehman, S. Ali, M. Mazhar, A. Badshah, M. Parvez, Heteroat. Chem. **17** (2006) 420.

192. H.L. Singh, A.K. Varshney, Bioionorg. Chem. Appl. DOI: 10.1155/ BCA/ 2006/ 23245.

193. E. Sinn, Inorg. Chem. **15** (1976) 366.